AN INVESTIGATION INTO THE ROLE OF ENDOTHELIAL-DERIVED MICROPARTICLES IN AN *IN VITRO* MODEL OF VASCULAR HEALTH AND DISEASE

DANIEL MORENO MARTINEZ

A thesis submitted in partial fulfilment
of the requirements of the
Manchester Metropolitan University
for the degree of Doctor of Philosophy

Healthcare Science Research Institute
Faculty of Science and Engineering

2017

List of Figures

List of Tables

List of Abbreviations

± SEM	Standard Error Mean
ALP	Alkaline Phosphatase
ANOVA	One-Way Analysis of Variance
AoEMPs	Aortic Endothelial Microparticles
APC	Allophycocyanin
BCA	Bicinchoninic Acid
βGP	B-glycerophosphate
BMP-2	Bone Morphogenetic Protein 2
BMP-4	Bone Morphogenetic Protein 4
BSA	Bovine Serum Albumin
Cbfa1	Core-binding Factor Subunit alpha-1
CCL20	Chemokine (C-C motif) Ligand 20
CHD	Coronary Heart Disease
CVD	Cardiovascular Disease
cDNA	Complementary DNA
CXCL1	Chemokine (C-X-C motif) Ligand 1
DAPI	Diamidino-2-Phenylindole
DGCR8	DiGeorge Syndrome Chromosomal Region 8
DMSO	Dimethylsulphoxide
DNA	Deoxyribonucleic Acid
dNTP	Deoxynucleotides
DTT	Dithiothreitol
EC	Endothelial Cell
ECGS	Endothelial Cell Growth Supplement
ECL	Enhanced Chemiluminescence
EDTA	Ethylenediaminetetra-Acetic Acid
ELISA	Enzyme-Linked Immunosorbent Assay

EMP	Endothelial Microparticle
eNOS	Endothelial Nitric Oxide Synthase
EPB41L3	Erythrocyte Membrane Protein Band 4.1 like 3
FBS	Fetal Bovine Serum
FGF-1	Fibroblast Growth Factor-1
FGF-2	Fibroblast Growth Factor -2
FMD	Flow Mediated Dilatation
FITC	Fluorescein Isothiocyanate
HAoEC	Human Aortic Endothelial Cell
HCMEC	Human Microvascular Endothelial Cell
HCoASMC	Human Coronary Artery Smooth Muscle Cell
HGF	Hepatocyte Growth Factor
HRP	Horseradish Peroxidase
HUVEC	Human Umbilical Vein Endothelial Cell
ICAM-1	Intercellular Adhesion Molecule-1
IF	Inmunofluorescence
IκB	Inhibitor-kB
IκB	Inhibitor-kB alpha
IL-1	Interleukin-1
IL-6	Interleukin-6
IL-8	Interleukin-8
INPP5D	Inositol Polyphosphate-5-Phosphatase
IL-32	Interleukin-32
LDL	Low Density Lipoprotein
MAPK	Mitogen-Activated Protein Kinase
MEJ	Myoendothelial Junction
MGP	Matrix Gla Protein
MIF	Macrophage Migration Inhibitory Factor

miRNA	MicroRNA
MMP	Matrix Metalloproteinase
MMP-2	Matrix Metalloproteinase-2
MMP-10	Matrix Metalloproteinase-10
MP	Microparticle
NFκB	Nuclear Factor-kB
NOX4	Nicotinamide Adenine Dinucleotide Phosphate Oxidase 4
NZB/W	New Zealand Black and White
OCN	Osteocalcin
OPG	Osteoprotegerin
OPN	Osteopontin
PAGE	Polyacrylamide Gel Electrophoresis
PARP	Poly (ADP-ribose) Polymerase
PBS	Phosphate Buffered Saline
PBST	Phosphate Buffered Saline Tween
PCR	Polymerase Chain Reaction
PE	Phycoerythrin
PFA	Paraformaldehyde
PS	Phosphatidylserine
PU.1	Transcription Factor PU.1
RANK	Receptor Activator of Nuclear Factor Kappa-B
RANKL	Receptor Activator of Nuclear Factor Kappa-B Ligand
RGS16	Regulator of G-protein Signalling 16
RIPA	Radioimmunoprecipitation Assay Buffer
RISC	RNA-induced Silencing Complex
RMVEC	Rat Renal Microvascular Endothelial Cell
RNA	Ribonucleic Acid
ROCK II	Rho-Associated Protein Kinase 2

RT	Reverse Transcriptase
RT-qPCR	Reverse Transcription Quantitative Polymerase Chain Reaction
SD	Standard Deviation
SDS	Sodium Dodecyl Sulfate
SEM	Scanning Electron Microscopy
sEMPs	Stimulated Endothelial Microparticles
Sirt-1	Silent Mating Type Information Regulation 2 Homolog 1
SLE	Systemic Lupus Erythematosus
SMC	Smooth Muscle Cell
SOST	Sclerostin
SPRED1	Sprouty Related EVH1 Domain Containing 1
SPRY1	Sprouty RTK Signalling Antagonist 1
TF	Tissue Factor
TNFα	Tumor Necrosis Factor-alpha
TNFR	Tumor Necrosis Factor Receptor
TRAF	TNF Receptor Associated Factor
TRAIL	TNF-Related Apoptosis-Inducing Ligand
TRPC6	Transient Receptor Potential Cation Channel Subfamily C Member 6
TSG101	Tumor Susceptibility Gene 101
uEMPs	Unstimulated Endothelial Microparticles
VCAM-1	Vascular Cell Adhesion Molecule-1
VE-Cadherin	Vascular Endothelial Cadherin
VEGF-A	Vascular Endothelial Growth Factor-A
VEGF-C	Vascular Endothelial Growth Factor-C
VSMC	Vascular Smooth Muscle Cell
v/v	Volume / Volume
w/v	Weight / Volume
ZO.1	Zonula Occludens-1

ABSTRACT

Endothelial microparticles (EMPs) are complex structures with pleiotropic properties and are emerging as an index of endothelial damage. Increased circulating levels of EMPs have been identified in several inflammatory disorders and are reduced following anti-inflammatory treatment. Since they are cell-to-cell communicators, this study aimed to identify specific effects on both endothelial and vascular smooth muscle cell (VSMC) function. We hypothesise that EMPs have a dual role, depending on the stimuli involved in their release, potentially playing a role in vascular homeostasis, but also in exacerbating vascular damage under disease conditions and this can be executed via activating the endothelium, and also in the cross-talk to the smooth muscle layer, in terms of depositing a calcified matrix.

The study is presented in two sections: first, to investigate the effect of EMPs on endothelial cells, by studying EMP release, endothelial cell activation and migration, and second, to investigate whether they modulate osteogenic differentiation of VSMCs *in vitro,* focusing on the mechanistic pathways involved using a microRNA and proteomic screening. To achieve these aims, three different sets of extracellular vesicles were generated (probably containing EMPs and exosomes): i) uEMPs, which were generated from healthy growing untreated human umbilical vein endothelial cells (HUVECs), ii) sEMPs, from Tumor Necrosis Factor alpha (TNFα)-stimulated HUVECs and iii) AoEMPs, from TNFα-stimulated human aortic endothelial cells. In the first study, HUVECs were treated with either uEMPs or sEMPs for 24 hours to investigate their effects on endothelial cell function, while in the second study, VSMCs were treated with AoEMPs for 3 weeks in osteogenic media to assess their effects on vascular calcification.

The study confirmed that EMP content, which depends on their cellular origin and the stimuli involved in their release, defines their properties. Both uEMPs and sEMPs increase vascular cell adhesion protein (VCAM-1) and intercellular adhesion molecule 1 (ICAM-1) and cell migration. However, sEMPs increase EMP release and carry elevated Chemokine (C-C motif) Ligand 20 (CCL20), identified in the proteomic screening and validated by flow cytometry, in comparison to uEMPs, thus contributing to the elevated EMP levels and disease pathogenesis via CCL20 and dysregulated inflammatory pathways. In addition, Alizarin Red S and calcium deposition assays demonstrated that VSMCs treated with AoEMPs in osteogenic media for 3 weeks show enhanced calcification *in vitro*, using Alizarin Red staining and calcium deposition assays. These findings may be in part, linked with miRNA-3148/osteoprotegerin signalling pathway, as miRNA-3148 was identified in the microRNA screening and using transfection studies, we identified its relationship with its target osteoprotegerin RNA. This study provides improved understanding of the mechanisms in which EMPs affect endothelial function and VSMC calcification *in vitro.* Further research will help understanding the ultimate role of EMPs on the vessel wall.

Acknowledgements

I would like to express my most sincere gratitude to Professor Yvonne Alexander and Dr Fiona Wilkinson for their endless support, guidance, help and direction throughout this journey. Their feedback, comments and attitude towards helping me achieving this goal is invaluable. I consider myself really fortunate to have had the opportunity to complete this work in such great company, under the best supervision I could have possibly had. My thanks to Dr Benjamin Parker for his extremely valuable and necessary clinical insights when these were most needed. My gratitude also to Genzyme and Manchester Metropolitan University, who have contributed to the experimental funding of this work.

My thanks go to every colleague in the laboratory; Dr Ayman Moawad and Dr Eoghan McCarthy for not only putting a smile on my face every day during the difficult first months in research, but also for their technical help in every experiment. A huge thanks to Dr Gary Sidgwick, Dr Alex Langford-Smith and Dr Ria Weston for their relentless support, professionally and personally, when it was most needed. And of course, Mr Ahmad Najib, who made of hard times good memories and who always listened to me and endeavoured to understand my feelings. Wherever I am, you will all have a friend.

Most importantly, I am thankful and blessed to have such a wonderful family and friends. To all my childhood and university friends, who have always welcomed me with a warm smile and tons of laughs, like I never departed. To my lovely wife Marga, who did this journey by my hand from the beginning to the end, believing in me more than anyone else has ever done and keeping me on my feet when difficulties arose. I will never be able to thank her enough for what she has done. To my wonderful mother, father, brother and grandmother, because despite the distance and that you would rather have me closer, you always encouraged me to pursue my dreams. I promise you one day I will be back. And finally to my grandfather, who I wish one day I will be able to thank by myself.

Novelty statement

The findings arising from this thesis demonstrate an association between the distinct role of endothelial microparticles and their different origin and mechanism of generation, which has an important impact on their molecular components, as well as their role in the regulation of endothelial function. To our knowledge, this is the first study to describe that endothelial microparticles enhance vascular calcification *in vitro* partially via the transmission of microRNA-3148, which selectively targets the calcification inhibitor osteoprotegerin.

List of Publications Arising from this Thesis

Published

1. McCarthy E, **Moreno-Martinez D**, Wilkinson FL, McHugh NJ, Bruce IN, Pauling JD, Alexander MY, Parker B. *Microparticle subpopulations are potential markers of disease progression and vascular dysfunction across a spectrum of Connective Tissue Disease*. BBA Clinical. 2016 Nov 10; 7:16-22

2. **Moreno-Martinez D**, Wilkinson F, McCarthy E, Mahmoud A, Alexander M. *Endothelial microparticles: novel regulators of vascular calcification in vitro.* Heart. 2016;102(Suppl 6): A122-A123. British Society for Cardiovascular Research Spring 2016 meeting, Manchester, UK (conference abstract)

3. **Moreno-Martinez D**, Wilkinson F, Parker B, McCarthy E, Mahmoud A, Bruce I, Alexander Y. *Endothelial microparticles as biomarkers of endothelial function in inflammation*. Keystone Symposia: Exosomes/ Microvesicles: Novel Mechanisms of Cell-Cell Communication 2016, Colorado, USA (conference abstract)

4. **Moreno-Martinez D**, Wilkinson F, McCarthy E, Mahmoud A, Alexander M. *Endothelial microparticles: investigating their role on endothelial cells in vitro*. Heart. 2015;101(Suppl 6): A12. British Society for Cardiovascular Research Autumn 2015 meeting, Glasgow, UK (conference abstract)

5. **Moreno-Martinez D**, Wilkinson F, Parker B, Pieri M, Barraclough M, Bruce I, Alexander M. *Endothelial microparticles: complex structures that have potential to attenuate osteogenic differentiation of human smooth muscle cells*. Heart. 2014;100 (Suppl 4): A2-A3. British Society for Cardiovascular Research Autumn 2014 meeting, Reading, UK (conference abstract)

Submitted

6. Mahmoud AM, Wilkinson FL, E McCarthy, **Moreno-Martinez D**, Langford-Smith A, Romero M, Duarte J, Alexander MY. *Endothelial microparticles prevent lipid-induced endothelial dysfunction through activation of AKT/ENOS signalling pathway and attenuation of oxidative stress*. Hypertension.

List of Scientific Meetings Attended

2016

1. Keystone Symposia. 2016, Colorado, USA. Poster presentation
2. British Society for Cardiovascular Research Spring Meeting. 2016, Manchester. Poster presentation
3. 19th Scottish Cardiovascular Forum. 2016, Queen's University Belfast. Oral presentation

2015

4. Northern Vascular Biology Forum 2015. University of Leeds. Oral presentation
5. British Society for Cardiovascular Research Autumn Meeting. 2015, University of Glasgow. Poster presentation
6. British Society for Cardiovascular Research Spring Meeting. 2015, Manchester

2014

7. Northern Vascular Biology Forum 2014. MMU. Co-organiser
8. Postgraduate Researchers conference 2014. MMU. Poster presentation
9. Science & Engineering symposium 2014. MMU. Oral presentation
10. British Society for Cardiovascular Research Autumn Meeting. 2014, University of Reading. Poster presentation
11. British Society for Cardiovascular Research Spring Meeting. 2014, Manchester. Poster presentation

2013

12. Northern Vascular Biology Forum 2013. University of Sheffield

Prizes: nominations and awards

1. Finalist (1 of 5) for the Roger Wadsworth prize: oral presentation at the 19th Scottish Cardiovascular Forum. 2016, Queen's University Belfast.
2. Awarded a travel Bursary from the British Society of Cardiovascular Research to attend the Autumn Meeting in Glasgow in 2015.
3. 1st prize winner: oral presentation at the MMU Faculty of Science & Engineering symposium 2014.

CHAPTER 1:
INTRODUCTION

CHAPTER 1: INTRODUCTION

1.1. Clinical problem: vasculitis and inflammation in systemic lupus erythematosus

Vasculitis is an inflammatory condition with a wide range of clinical manifestations. It is known that patients suffering autoimmune disorders may develop vascular problems and therefore, may have a higher risk of suffering cardiovascular disease (CVD), which is a major cause of mortality (1). An example of this is systemic lupus erythematosus (SLE), which is the focus of this study.

SLE is a chronic multi-system inflammatory autoimmune disease that can affect most of the organs in the body, leading to a wide range of diverse clinical manifestations (1). It is characterised by an immune system dysfunction that leads to the loss of immunologic tolerance and the creation of antibodies targeting nuclear material (2). It has been reported that SLE patients have a higher probability of suffering coronary heart disease (CHD) as well as an increased chance of producing atherosclerosis plaques, thus a lower life expectancy compared to a healthy population is expected, due to the increased risk of CVD and accelerated vascular ageing (3). Despite mortality rate being reduced during the last decades, CVD remains a major cause of mortality worldwide, with SLE patients having more than 50 times the risk of general population (4).

SLE has been shown to have a higher influence in female rather than male individuals, predominantly in fertile age, with an impact ratio of 6-10:1. In the USA and Europe, SLE has a very similar incidence rate, ranging from 1.8 and 7.6 cases per 100.000 people a year respectively (2). SLE presents with a gradual progression over the years and some of its common clinical manifestations may include fatigue or weight loss; while others include malar rash, photosensitivity (cutaneous hypersensitivity), non-erosive polyarthritis, and often neurological and vascular problems. SLE is a disease characterised by alternate flare and remission periods that are associated with a decreased quality of life and a lower life expectancy mainly due to its activity, but also to organ damage and an increased risk of suffering CVD (3).

Due to the heterogeneity of SLE and its wide range of clinical manifestations, treatment options are not ideal and thus, the management of patients with SLE focuses on controlling the inflammatory activity in order to preserve organ function

and minimise side effects. Rituximab and standard immunosuppressive agents are common medications prescribed to manage the disorder (4).

1.1.1. Endothelial dysfunction and cardiovascular disease in SLE

The definition of endothelial dysfunction can be described from a physiological point of view, as a loss of response of the vascular endothelium to the stimuli promoting its vasodilation and contraction (5). In other words, endothelial dysfunction refers to the inability of the endothelium to vasodilate and contract, as well as to its incapacity to control inflammation, cell proliferation and thrombosis. This coincides with the cellular and molecular aspects of activation of adhesion molecule expression. The role of the endothelia in the maintenance of vascular homeostasis is widely known, e.g. the endothelium is known to control vascular inflammation, smooth muscle cell proliferation, platelet adhesion and fibrinolysis among others (6). A scheme of the structure of the vessel wall be found in Figure 1.

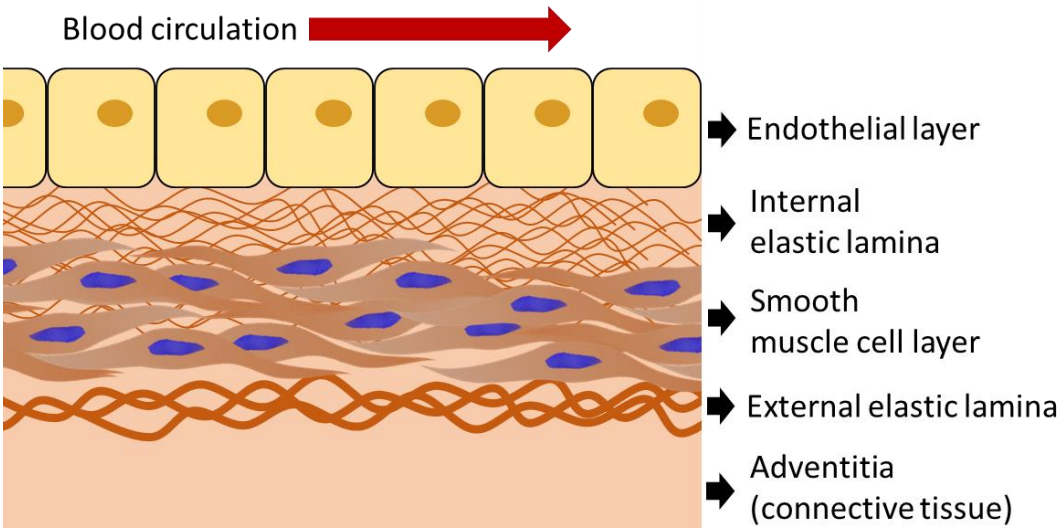

Figure 1. Schematic representation of the vessel wall. The vessel wall is composed of different elements: a single layer of endothelial cells, the internal elastic lamina, which separates the endothelium from the smooth muscle cell layer, followed by the external lamina and the adventitia, which is composed mostly of connective tissue. Adapted from Blausen (7)

It is important to evaluate endothelial function within the content of its cross-talk with smooth muscle cells. Along with endothelial dysfunction, SLE is an independent risk factor for CVD and is associated with a 5-fold increased risk in adults and a 50-fold increase in younger patients (8). In order to gain insight to develop improved and more individualised therapeutic approaches, this study has focused on understanding the basis of endothelial dysfunction observed in SLE patients (Figure 2) compared to the normal function of endothelial cells, and if any links can be made

on the inflammatory effects resulting from an activated endothelium and the response within the medial layer of smooth muscle cells (9).

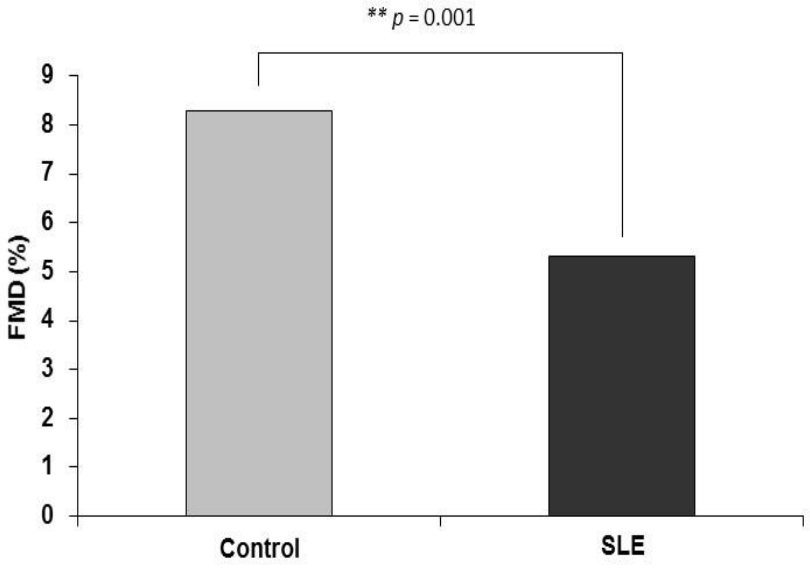

Figure 2. SLE patients have impaired endothelial function. Previous research has demonstrated that SLE patients show decreased flow-mediated dilatation (FMD) reflected in reduced endothelial function when compared to healthy controls. Adapted from Kerekes *et al* (9)

1.1.2. Tumor Necrosis Factor-alpha, a key cytokine in inflammation in SLE

Inflammation is a known stimulus for the development of vasculitis, and in particular, it is known to be elevated in SLE patients compared to age-matched controls (6).

It is generally accepted that several kinds of stimuli may result in an increased expression of adhesion molecules on the endothelial cell monolayer. Adhesion molecules allow endothelial cells to capture leukocytes (monocytes, etc.) which later will differentiate into macrophages and form foam cells, which will take part in the progression of the lesion. Ultimately causing migration and phenotypic switching of smooth muscle cells into a secretory cell depositing a matrix that will form a fibrous cap. Thin fibrous caps can lead to a rupture which in turn cause thrombosis (10).

Tumor Necrosis Factor-alpha (TNFα) is a cytokine produced predominantly by activated macrophages and T lymphocytes that has been shown to play a role in the course of several inflammatory diseases, but understanding how its pleiotropic properties affect inflammation is challenging (11). For example, TNFα can act as a growth factor in B cells, thereby inducing the production of Interleukin-1 (IL-1) or Interleukin-6 (IL-6) (12, 13), but it can also act as an inhibitor or as a promoter of

cell apoptosis and regulate the expression of anti-apoptotic or adhesion molecules, ultimately leading to inflammation (14).

The relevance of TNFα in the pathogenesis of SLE has been extensively reviewed (11, 14-16) and as such, anti-TNFα drugs are often used in the management of the disease, but it has been shown to be protective or detrimental depending on the mouse model of the disease investigated (17, 18). Previous findings have shown that serum concentration of TNFα is high in active SLE patients and that it correlates with disease activity (17). Other studies found that TNFα only produces a mild SLE-like phenotype in New Zealand black and white (NZB/W) mice, which are prone to autoimmune diseases (18).

Although TNFα receptors are expressed on different cell types, many of its inflammatory effects can be explained through its effects on vascular endothelium and leukocyte interactions in which endothelial cells promote inflammation by up-regulating the expression of adhesion molecules for leukocytes such as intercellular adhesion modelule-1 (ICAM-1) and vascular cell adhesion molecule-1 (VCAM-1), thereby facilitating extravasation (19, 20). Despite the fact that TNFα is considered not to be as relevant in SLE as in other vascular conditions, elevated circulating TNFα levels have been reported in patients with very active SLE (21, 22). Since endothelial damage is an early event prior to the development of inflammatory and cardiovascular conditions, it is necessary to assess the risk of CVD in SLE patients.

1.2. Microparticles in health and disease

Extracellular vesicles are membrane-bound vesicles released from cells that can transport nucleic acids and proteins. It is recognised that three main categories of extracellular vesicles exist: exosomes (< 100 nm), microparticles (MPs) (> 100 nm and < 1 μm) and apoptotic bodies (< 1 μm). Extracellular vesicles are often investigated together, albeit important differences have been reported in the literature with regards to their generation mechanisms and contents (23-25). A summary of the main characteristics and differences between exosomes, MPs and apoptotic bodies reported by the literature can be found on Table 1.

	Characteristics		
	Origin	**Size**	**Contents**
Exosomes	Multivesicular bodies	20 – 100 nm	Nucleic acids, proteins, membrane receptors
Microparticles	Cell surface, membrane blebbing	100 – 1000 nm	Nucleic acids, proteins, membrane receptors
Apoptotic bodies	Cell surface, apoptotic cells	Larger than 1000 nm	Nuclear fractions, organelles

Table 1. Differences between MPs, exosomes and apoptotic bodies. Based on their biogenesis and origin, three main classes of extracellular vesicles have been described: exosomes, microparticles and apoptotic bodies. Adapted from El Andaloussi *et al.* (25)

Vascular cells, just like many other cell types, participate in the release of microparticles. MPs are a heterogeneous submicron sized circulating population (< 1 μm) of vesicles present in the blood stream which contain cytosolic components generated usually from apoptotic or activated cells. They have shown to be involved in many different conditions including SLE, although they are also found in healthy individuals (26, 27). Although the mechanisms underpinning their generation are still poorly understood, several authors have reported that they might be a result of vesicles blebbing off from the plasma membranes in response to a certain stimulus such as TNFα, mainly due to cell activation or apoptosis (28). Also, their phenotypical characteristics can be distinguished from their cellular origin, as reviewed by Hugel *et al.* (29).

A correlation between the stage of some diseases and MP levels from a certain cellular origin has been reported in the literature including SLE (10, 11), making them a potential biomarker for predicting CVD risk and, since they have been reported to trigger an endothelial repair response (12). They may also act as a novel therapeutic approach (30). It has been widely reported that platelet derived microparticles (PMPs) levels are increased in many autoimmune diseases; however, few studies have investigated the differences in endothelial derived microparticle (EMP) levels in these conditions, probably due to the higher

concentration of PMPs compared to EMPs in the blood stream (13). Moreover, differences in storage, manipulation and processing of plasma samples (as well as activation, isolation and measurement method) have shown to have an important effect in MP detection in *in vitro* models (14-16); despite several attempts to standardise the variables (17) these differences still exist, providing the impetus for a standardised approach in detection and measurement (31, 32).

As it has been discussed previously, SLE patients are more likely to develop endothelial dysfunction increasing their predisposition to cardiovascular disorders. Our laboratory have previously demonstrated that MP circulating levels are modulated in different conditions, including SLE, and that their levels can be reduced by pharmacological treatment (33). MP research is of growing importance as evidenced by the numbers of EMP reports in the literature during the past 2 decades (Figure 3). Despite clinical trials have already investigated using MPs as biomarkers of disease prognosis in patients with cerebral infarction, heart failure, acute coronary syndrome or diabetes mellitus (34, 35), their mechanism of action has yet to be elucidated before they can be used as a biomarker of CVD and a potential therapeutic target (33, 36).

Our laboratory is particularly interested in investigating the role that MPs play in endothelial and smooth muscle cell signalling, with a focus on how these MPs modulate endothelial function and vascular calcification in inflammatory conditions such as SLE (27). The following points will discuss the different types of MPs, although of particular interest are EMPs. Furthermore, the different methods used to quantify MPs will be discussed, as well as their role in SLE, endothelial and smooth muscle cell signalling, and their potential diagnostic and therapeutic utility.

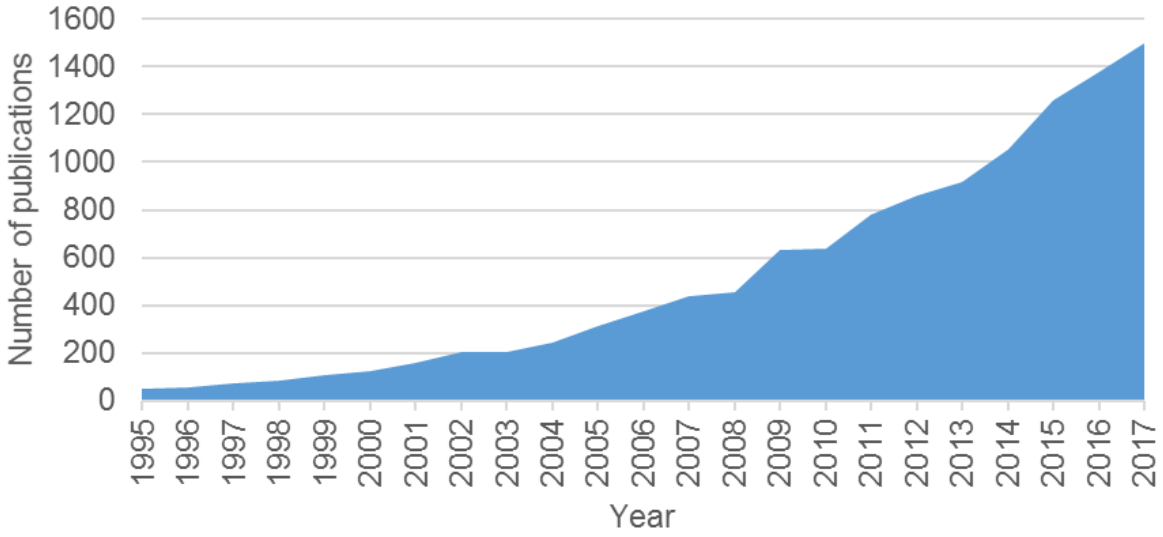

Figure 3. **Evidence of increased EMP publications in PubMed on an annual basis**. The number of publications in PubMed containing the words "endothelial microparticles" has increased year after year during the last 22 years.

1.2.1. Endothelial microparticles: origin, formation and composition

1.2.1.1. EMP origin and formation

MPs are derived from many different cell types and as such, they share characteristics with their cell of origin, such as surface markers (37). Platelet-derived microparticles (PMPs) are the most abundant type of MPs found in circulation, along with EMPs (38). However, MPs derived from megakaryocytes (39) and leukocytes (40) have also been found in circulation. Although it is possible to detect MPs in healthy individuals, several conditions such as inflammatory diseases exacerbate the generation and release of MPs as a result of membrane shedding due to apoptosis or cell activation (33). A common characteristic of all MP populations is their formation and shedding, which involves the reorganisation of the phospholipid membrane distribution, exposing phosphatidylserine (PS) on the outer membrane of the cell.

Most available knowledge of the molecular mechanisms leading to MP release has its origin in *in vitro* studies, in which a variety of stimuli (including TNFα) can induce the release of MPs by endothelial cells (21, 41). Other inflammatory cytokines, reactive oxygen species, thrombin, c-reactive protein, plasminogen activator inhibitor among others have also been shown to induce EMP release (42). In quiescent cells, the membrane is characterised by exposing neutral phospholipids such as phosphatidylcholine and sphingomyelin on its external layer, and

phosphatidylserine (PS) on its inner side; an equilibrium regulated by the three proteins flippase, floppase and scramblase. When cell activation or apoptosis processes occur, calpain is activated, allowing intracellular calcium to increase, which induces aminophospholipid movements from the inner to the outer leaflet, leading to membrane blebbing due to the disruption of the phospholipid membrane and cytoskeleton reorganisation ultimately leading to EMP formation (43-45) (Figure 4).

The mechanisms by which this process is regulated are still unclear and seem to be diverse. A study from Sapet *et al.* using siRNAs and pharmacological inhibitors of Rho-kinases first described an nuclear factor kappa B (NFκB)-dependent activation of Rho-associated protein kinase 2 (ROCK II) by caspase 2 as potentially responsible of EMP release in human microvascular endothelial cells (46). Another study by Curtis *et al.* described the role of the p38 MAPK pathway, and showed that the pharmacological inhibition of p38 in human aortic endothelial cells reduces TNFα-mediated EMP release (47).

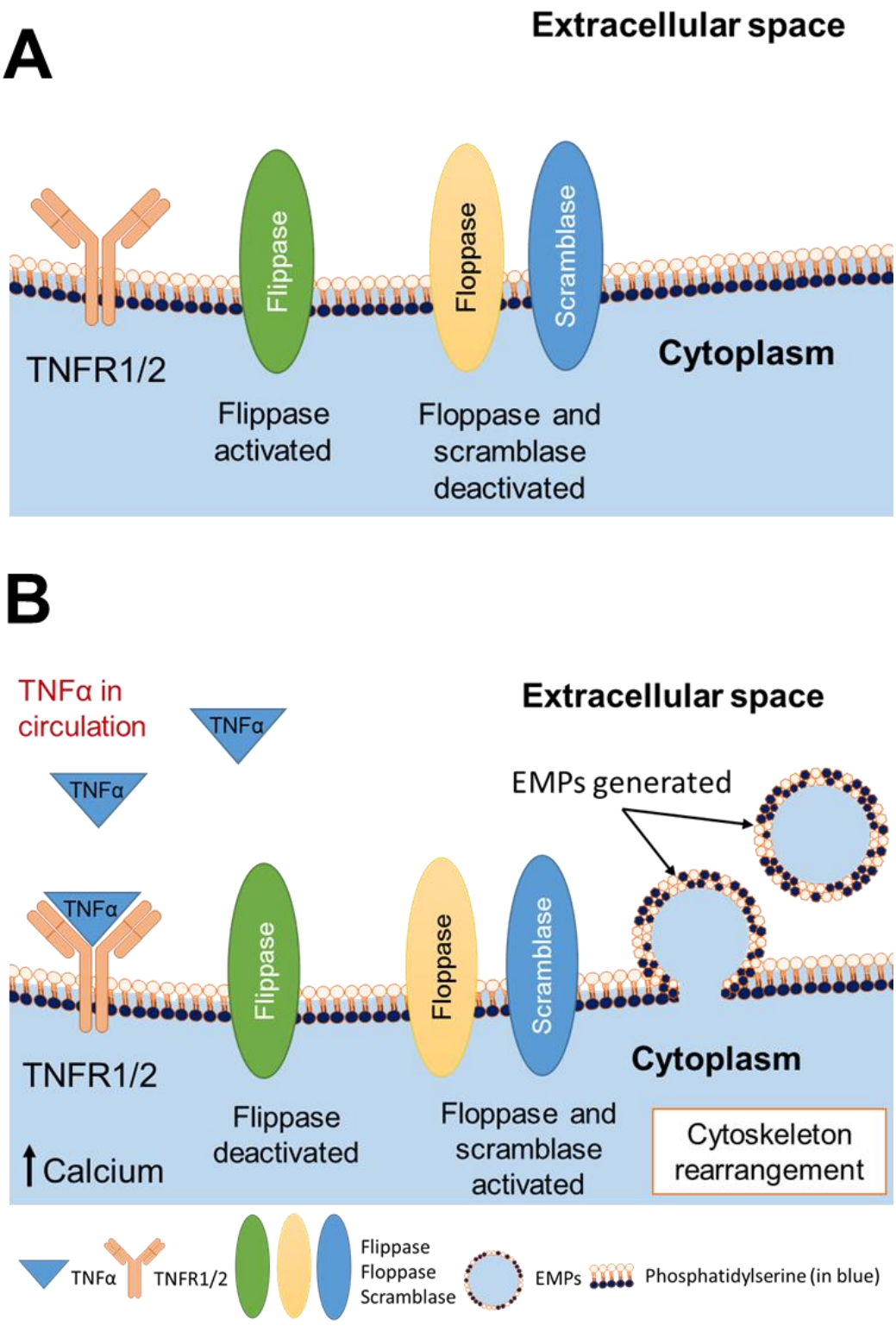

Figure 4. Schematic representation of the mechanisms of EMP formation. A) In quiescent cells, PS localisation in the inner leaflet is regulated by flippase activity. B) Upon TNFα to its receptor, floppase and scramblase activate upon increased intracellular Ca^{2+} leading to cytoskeleton reorganisation and the release of EMPs exposing PS in the outer membrane. TNFα: Tumor necrosis factor alpha; PS: Phosphatidylserine; EMPs: Endothelial microparticles. Adapted from Baron *et al.* (30)

1.2.1.2. TNFα-mediated EMP generation

It is well established that TNFα can induce MP generation in cell culture models (21, 41), but also other inflammatory cytokines and stimuli are able to generate MPs *in vitro*. On the one hand, pro-apoptotic stimuli such as high concentrations of TNFα, IL-6, IL-8 or even DNA damage can lead to caspase activation and cell death, which is accompanied by the generation of apoptotic bodies (> 1 μm), but on the other hand, inflammatory stimuli, low shear stresses, vascular damage or the presence of particular growth factors may lead to endothelial cell activation and the production of EMPs (48-52) (Figure 5). Finally, and as an example of the many TNFα roles, it is able to induce a concrete vesiculation pathway present in endothelial cells that involves NFκB and TNF-related apoptosis-inducing ligand (TRAIL), leading to ROCK II activation by caspase 2 (46).

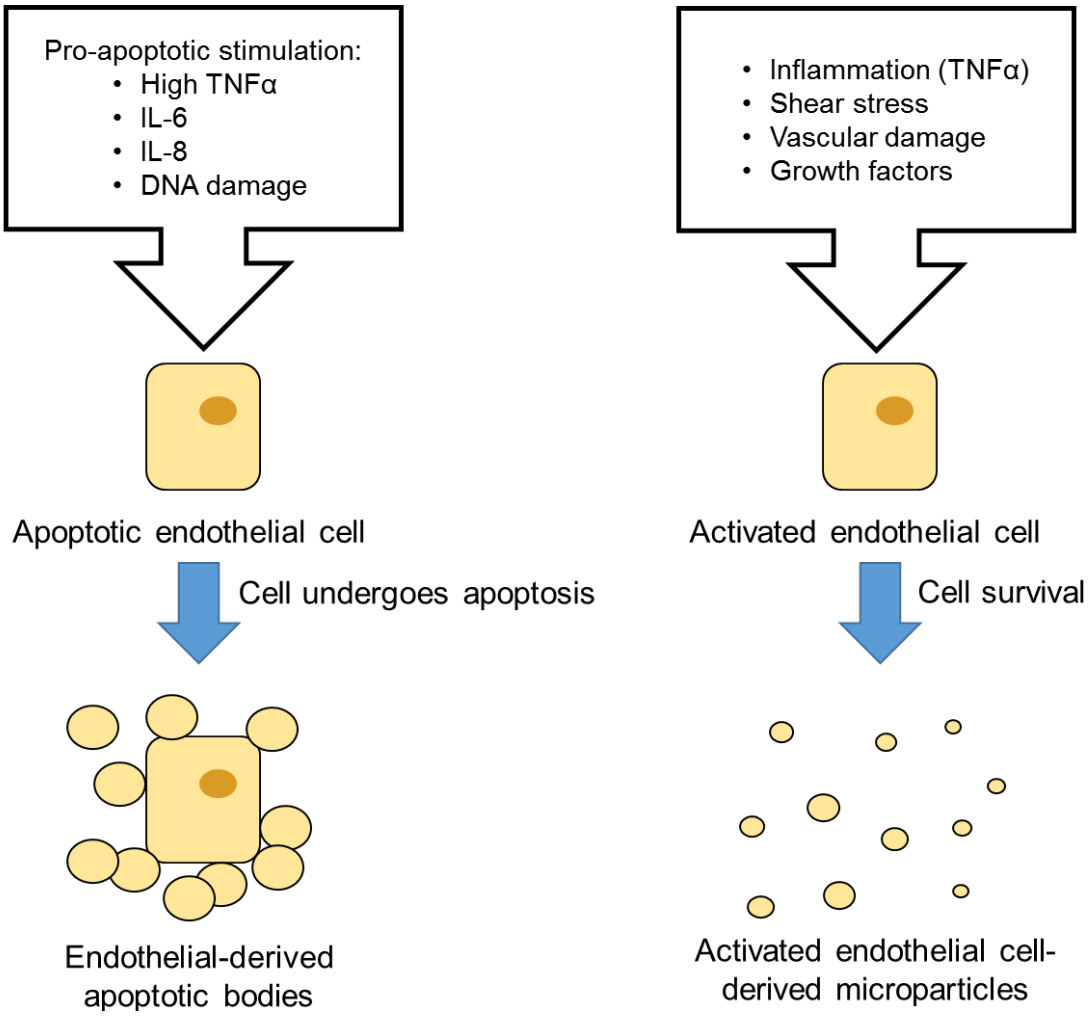

Figure 5. TNFα-mediated EMP formation. High TNFα concentrations initiate cell apoptosis and ultimately the release of apoptosis-derived bodies, whereas lower TNFα concentrations initiate inflammatory or endothelial damage ultimately leading to EMP release. TNFα: tumor necrosis factor alpha; IL-6: interleukin 6; IL-8: interleukin 8. Adapted from Curtis *et al.* (53)

TNFα can either bind the TNFR1 or TNFR2, initiating either the NFκB, mitogen-activated protein kinase (MAPK) or cell death signalling pathways (54, 55). The NFκB pathway, which is activated by a myriad of cytokines in addition to TNFα, is an important pathway that has been shown to be involved in many aspects of endothelial function, inflammation and homeostasis regulation (56). In the canonical NFκB pathway, the inhibitory protein IκBα binds to NFκB and retains it in the cell cytoplasm. Upon activation of the pathway due to TNFα, IκBα is phosphorylated and degraded, releasing NFκB which is then free to translocate to the nucleus, where it will act as a transcription factor of several proteins involved in inflammation, cell survival and cell proliferation (Figure 6).

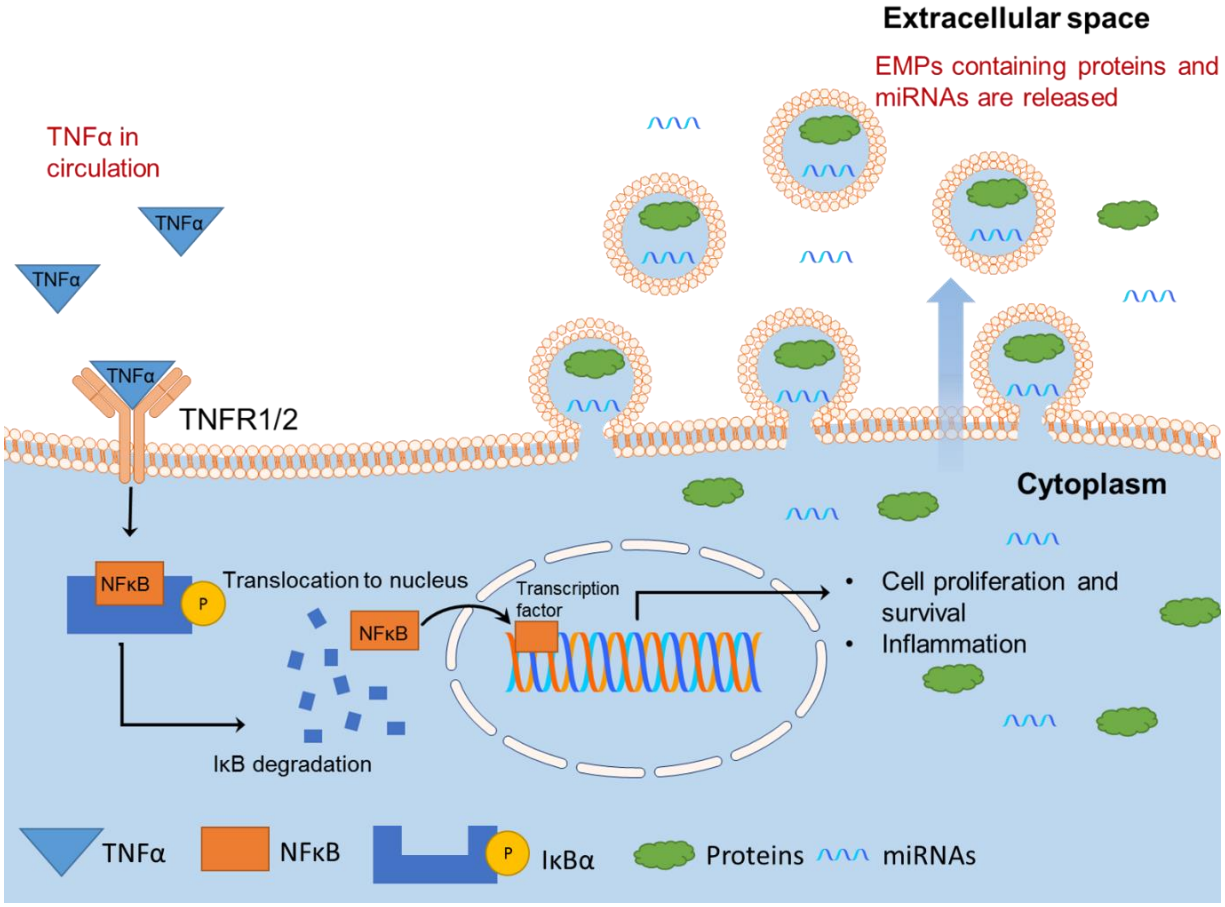

Figure 6. Proposed model of activation of the NFκB pathway and TNFα-mediated EMP release. Upon activation of the pathway due to TNFα, IκBα is phosphorylated and degraded, releasing NFκB which is then free to translocate to the nucleus, where it will act as a transcription factor of several proteins involved in inflammation, cell survival and cell proliferation. As a consequence, EMPs containing inflammatory-derived proteins and miRNAs are generated and will act as paracrine signalling molecules. TNFα: tumor necrosis factor alpha; TNFR1/2: tumor necrosis factor receptor 1/2; EMPs: endothelial microparticles; NFκB: nuclear factor kappa b; IκBα: inhibitor kappa b alpha

1.2.1.3. EMP composition

Microparticles are vehicles of biological information, which carry enzymes, bioactive lipids, proteins and/or RNAs, thus engaging in signalling pathways (10). As part of the research programme of work, we focused on MPs proteomic and microRNA (miRNA) content analysis.

1.2.1.3.1. Cytokine content of EMPs

Several research groups working with EMPs have shown that the proteomic content of these clearly depends not only on the cell lineage that generates the EMPs, but also on the sort of stimulus leading to vesiculation (57-59). For instance, Jimenez *et al.* demonstrated that endothelial cells release qualitatively and quantitatively distinct EMPs in response to TNFα (inflammatory model) and upon the induction of apoptosis by growth factor deprivation *in vitro* (60). Besides mediating exchange of intercellular information by their surface molecules, MPs have been shown to be carriers of important soluble mediators, such as cytokines (summarised in Table 2).

Cytokine	**Cell line origin**	**Reference**
Interleukin 1β (IL-1 β)	Leukemic cell line (THP-1)-derived MPs	(61, 62)
Interleukin 1α (IL-1 α)	HUVEC-derived EMPs	(63)
Interleukin 18 (IL-18)	Macrophage-derived MPs	(64)
Interleukin 32 (IL-32)	Epithelial-derived MPs	(65)
Membrane-bound tumour necrosis factor α (TNFα)	Synovial cell line (L929)-derived MPs	(66)
Interleukin 6 (IL-6)	Leukemic cell line (HMC-1)-derived MPs	(67)
Vascular endothelial growth factor (VEGF)	Carcinoma cell line (A2780)-derived MPs	(68)
Interleukin 8 (CXCL8)	HPC-4, A549 (tumor cell lines)-derived MPs	(69)
CCL2, CCL3, CCL4, CCL5 and CCL20	Dendritic-derived MPs	(70)

Table 2. Cytokines transported by MPs from different cell types. MPs have shown to be vehicles of biological information and to act as paracrine signalling molecules by participating in the transportation of cytokines. MPs: microparticles; EMPs: endothelial microparticles; CCL: chemokine (C-C motif) ligand.

With these observations in mind, this thesis describes the investigation of the molecular differences (proteomic and miRNAs) between two different vascular beds (HAoECs and HUVECs) and two different EMP populations generated from HUVECs, uEMPs and sEMPs, in which the first was generated from unstimulated while the second was from TNFα-activated cells.

1.2.1.3.2. microRNA signalling within EMPs

MicroRNAs (miRNAs) are small non-coding RNAs that function as critical repressors/silencers of gene expression. Previous studies have demonstrated that MPs carry miRNAs (71) which play an essential role regulating processes such as endothelial cell proliferation or angiogenesis (72), suggesting that partly, MPs role in SLE may be one of signalling (73).

miRNA production is a two stage process occurring in nucleus and in cytoplasm respectively. First, the enzymes DiGeorge syndrome chromosomal region 8 (DGCR8) and Drosha catalyse the conversion of the primary miRNA transcripts into pre-miRNAs (60-70 bp) in the nucleus (74). The pre-miRNAs leave the nucleus and once in the cytoplasm, their terminal loop is cleaved by RNAase III Dicer, generating a miRNA-miRNA duplex. After this, the RNA-induced silencing (RISC) complex incorporated the -5p end to the duplex, which makes the miRNA functional and able to bind the 3' UTR region of its target mRNA. There has been much discussion on the role of miRNAs and whether they silence/repress transcription or whether they degrade their target mRNA (75-77), but in either case, miRNAs will act as gene regulators by repressing the expression of their targets.

miRNAs have been implicated at various stages of endothelial and smooth muscle cell signalling. For instance, miRNA-146 targets the signalling molecule TNF receptor associated factor 6 (TRAF-6), which is up-stream of the NFκB signalling pathway and results in the modulation of NFκB translocation and in turn, the reduction of TNFα (78-80). A summary of some the miRNAs identified in EMPs to date can be found in Table 3.

miRNA	Extracellular Vesicles	Function	Target	References
miRNA-126	EMPs (patients) & PMPs	Promotes endothelial repair. Effects are impaired in hyperglycaemic conditions	SPRED1	(81, 82)
miRNA-26a	EMPs (patients)	Regulates insulin sensitivity and glucose metabolism. Reduced in EMPs in hyperglycaemia	TRPC6	(82)
miRNA-21	EMPs (HAoECs) & PMPs	Elevated in carotid artery disease	SPRY1	(83-85)
miRNA-155	EMPs (patients)	Modulates T-cell function and contributes to the development of myocarditis	PU.1	(86)
miRNA-223	PMPs (patients)	Promotes tumor progression in lung cancer	EPB41L3	(87, 88)
miRNA-423-5p	EMPs (patients)	Low levels are associated with poor long-term outcome in diabetic patients	Unknown	(82, 89)
miRNA-451	EMPs (epithelial cells)	Inhibits cell proliferation, migration and invasion through regulating macrophage inhibitory factor in renal cell carcinoma	MIF	(90)
miRNA-19	EMPs (HUVECs) & PMPs	Anti-thrombotic effect. Inhibits tissue factor on target endothelial cells	TF	(91-93)
miRNA-105	Exosomes from glioblastoma (patients)	Overexpression in non-metastatic cancer cells induces metastasis and vascular permeability	ZO-1	(94)
miRNA-155	Exosomes (bone marrow-derived dendritic cells)	Promotes endotoxin-induced inflammation in mice	INPP5D	(95)
microRNA-126	Endothelial derived apoptotic bodies (HUVECs)	Promotes the incorporation of Sca-1+ progenitor cells	RGS16	(96)

Table 3. miRNAs found in extracellular vesicles. Summary of the miRNAs carried by MPs which are reported to be associated with CVD. EMPs: endothelial microparticles; PMPs: platelet microparticles; miRNA: microRNA; HAoECs: human aortic endothelial cells; HUVECs: human umbilical vein endothelial cells; SPRED1: sprouty related EVH1 domain containing 1; TRPC6: Transient receptor potential cation channel, subfamily C, member 6; SPRY1: sprouty RTK signalling antagonist 1; PU.1: Transcription factor PU.1; EPB41L3: erythrocyte membrane protein band 4.1 like 3; MIF: macrophage migration inhibitory factor; TF: tissue factor; ZO-1: zonula occludens-1; INPP5D: inositol polyphosphate-5-phosphatase; RGS16: regulator of G-protein signalling 16.

It is important to remember that upon EMP formation/generation, cytoplasmic content is often encapsulated and released from the cell in the form of MPs. Therefore, it is during this process when pre-miRNAs or mature miRNAs are packaged in the MPs, which can then regulate gene expression and post-translational regulation of mRNA (97). Also, a single miRNA can modulate several genes, and a single gene can be modulated by several miRNAs, and of note, some studies have identified that miRNAs carried by MPs have significant relevance in immunological disorders (98). As such, it makes sense to understand MPs as key signalling molecules, with a huge potential to affect cell function possibly via horizontal transfer of miRNAs.

1.2.2. Identification and quantification of EMPs *in vivo* and *in vitro*

Flow cytometry is the gold-standard technique for quantifying MPs in plasma and in whole blood (32, 33, 99). Despite MPs having components from their cells of origin and their phospholipid and protein composition varying depending on their cell of origin and their releasing method, the exposure of PS is generally accepted regardless of the fact that several authors have reported to have found vesicles of the size of MPs not containing PS, as is often used for their characterisation (100). However, PS does not differentiate between different cellular origins and therefore, other surface markers specific to the cell of origin are used to differentiated between MPs.

As a common criteria for MP detection, PS positive particles (AnnexinV^{+}) smaller than 1 μm are considered as MPs; however, other criteria to assess their cell of origin or their nature as extracellular vesicle should be applied. For each cell type involved in MP generation, various surface markers can be used depending on the cell origin of interest. Apart from PS, EMPs may express adhesion molecules specific to mature endothelial cells such as CD54 (ICAM-1), CD62E (E-selectin) or CD31 (PECAM). However, CD31 is also detected on platelet microparticles (PMP), thus a usual labelling strategy for EMP detection would include labelling with positive and negative markers to eliminate other hematopoietic cells e.g. CD31^{+}/CD41^{-} or CD31^{+}/CD42b^{-}, since CD41 nor CD42b are expected to be present in EMPs (30). A summary of the most commonly used markers is shown in Table 4. Characterisation of the cell of origin is not a necessary requirement when working with *in vitro* generated EMPs, as a single pure population of one cell phenotype is being used,

and in this case, the sole use of AnnexinV^{+} (in combination with sizing beads to detect MPs) is commonly accepted (32, 101).

Vesicle type	Antigen
PMP	CD41 (102), CD42a (103), CD42b (104),CD61 (105),CD62P (73)
EMP	CD31* (106), CD62E (107), CD34 (108), CD51* (109), CD54 (110), CD105* (111), CD144 (102), CD146 (112)
Exosomes	CD63 (113), CD9 (114), TSG101 (113), CD81 (115)
Apoptotic bodies	Heavy phosphatidylserine externalisation (116), PI (117)

Table 4. Commonly used antigen markers in flow cytometry for PMP, EMP, exosome and apoptotic bodies quantification. CD31, CD51 and CD105 are not specific to endothelial-derived MPs and are often used in combination with other markers to identify EMPs. PMP: platelet microparticles; EMP: endothelial microparticles; TSG101: tumor susceptibility gene 101; PI: propidium iodide.

As mentioned before, a fraction of smaller sized particles (< 100 nm), named exosomes, has been extensively described in the literature and its generation mechanisms, contents and effects on target cells have often been studied alongside those of MPs (42, 118, 119). Together with apoptotic bodies (> 1 μm), exosomes pose a challenge in MP isolation as the lack of standardisation in EMP isolation techniques often means the exosomal and MP fractions are not separated. There are commercially available kits that use specific markers for exosomes (CD63, CD81 or others) in order to isolate populations, but their accuracy is debatable, as most of the markers are also found on MPs. Current MP isolation techniques include centrifugation at high speed for specific periods of time. However, it is important to mention that several groups have reported that differences in centrifugation speeds and timings can significantly affect MP quantification, suggesting the need for standardisation (30, 31). Centrifugation speed and length have been shown to be paramount in isolating MP populations avoiding the apoptotic fraction, therefore, it has been suggested that a consensus is needed to ensure consistency between laboratories when describing studies using MPs. A summary of some of the

currently described centrifugation techniques used by different laboratories to isolate EMPs can be found in Table 5.

Cell model used	Preparation of supernatant	Isolation of EMP pellet	Reference
Human umbilical vein endothelial cells (HUVECs)	4,300 x g 5 min	100,000 x g 90 min 10 °C	(41)
Rat renal microvascular endothelial cells (RMVECs)	5,000 x g 5 min	100,000 x g 120 min	(120)
HUVECs	4,000 x g 5 min	100,000 x g 90 min 10 °C	(121)
Human Jurkat T cells	1,500 x g 5 min	100,000 x g 20 min 20 °C	(52, 122)
Human microvascular endothelial cells (HCMECs)	4,300 x g 5 min	20,000 x g 120 min 4 °C	(123)
HUVECs	200 x g 4 min	100,000 x g 60 min 4 °C	(124)
T cells	800 x g 5 min then 4,500 x g 5 min	100,000 x g 60 min 4 °C	(125)
Human aortic endothelial cells (HAoECs)	4,300 x g 5 min	200,000 x g 120 min 20 °C	(126)
HAoECs, Human lung microvascular endothelial cells (HMVECs)	400 x g 15 min	3 x (21,000 x g x 45 min)	(127)
HUVECs	3890 x g 5 min	100,000 x g 90 min 4 °C	(21), (52), (128), (48), (50), (129)

Table 5. Summary of centrifugation methods used for isolating *in vitro* generated EMPs. Considerable variation in centrifugal speeds used to pellet EMPs is apparent between different laboratories, hence discrepancies can arise between publications regarding the signalling pathways activated since there could be MP preparations that also contain an exosomal fraction. The studies performed in this thesis used similar centrifugal speeds to those described in Heathfield *et al.* (21).

1.2.3. Mechanisms of EMP:cell interaction

It has been shown that the mechanisms in which exosomes and MPs interact with their targets cells are diverse and involve endocytic pathways and membrane fusion among others (130). A study by Valadi *et al.* demonstrated that exosomes act as signalling molecules and transfer functional mRNA and miRNAs from MC/9 mouse to HMC-1 human mast cells *in vitro*, as mouse proteins were found in the human cells (71). Another study by Alvarez-Erviti *et al*. showed that *in vitro* generated exosomes injected in mice can knockdown GAPDH gene expression by carrying and delivering siRNAs (131). Similarly, Montecalvo *et al.* used dendritic-derived exosomes loaded with luciferin to treat bone marrow derived dendritic cells that had been transfected with luciferase, thereby producing bioluminescence and confirming the transfer of functional material from the exosomes to the target cells (132).

MP uptake can be visualised directly using fluorescence microscopy. However, the mechanisms involved in such process are complex and diverse and have raised great debate in the literature (119, 130). Various mechanisms for MP:cell interaction have been suggested, including membrane fusion (133), ligand-receptor interaction (134), lipid-mediated endocytosis (135), caveolin-1/caveolae-mediated endocytosis (136), phagocytosis/macropinocytosis (137) and extracellular degradation. However, the question of whether or not MP uptake is a cell type-dependent process remains to be elucidated, as the majority of research in the literature investigating internalisation and cell interaction has been performed on exosomes rather than MPs. Whereas some studies have shown that internalisation and exosome:cell interaction is a highly specific process and requires the presence of the right combination of ligands and receptors either on the cells or on the exosomes, some others have shown that exosomes can be taken up by many cell types (135, 138).

The current lack of knowledge in MP:cell interaction probably accounts for the difficulty and lack of standardisation of MP isolation techniques. However, a summary of the most accepted mechanisms for MP:cell interaction can be found on Figure 7. In this study, Calcein-AM was used to demonstrate that EMPs enter their cells to deliver their contents, but the mechanisms by which EMPs interact with their target cells was beyond the scope of this thesis.

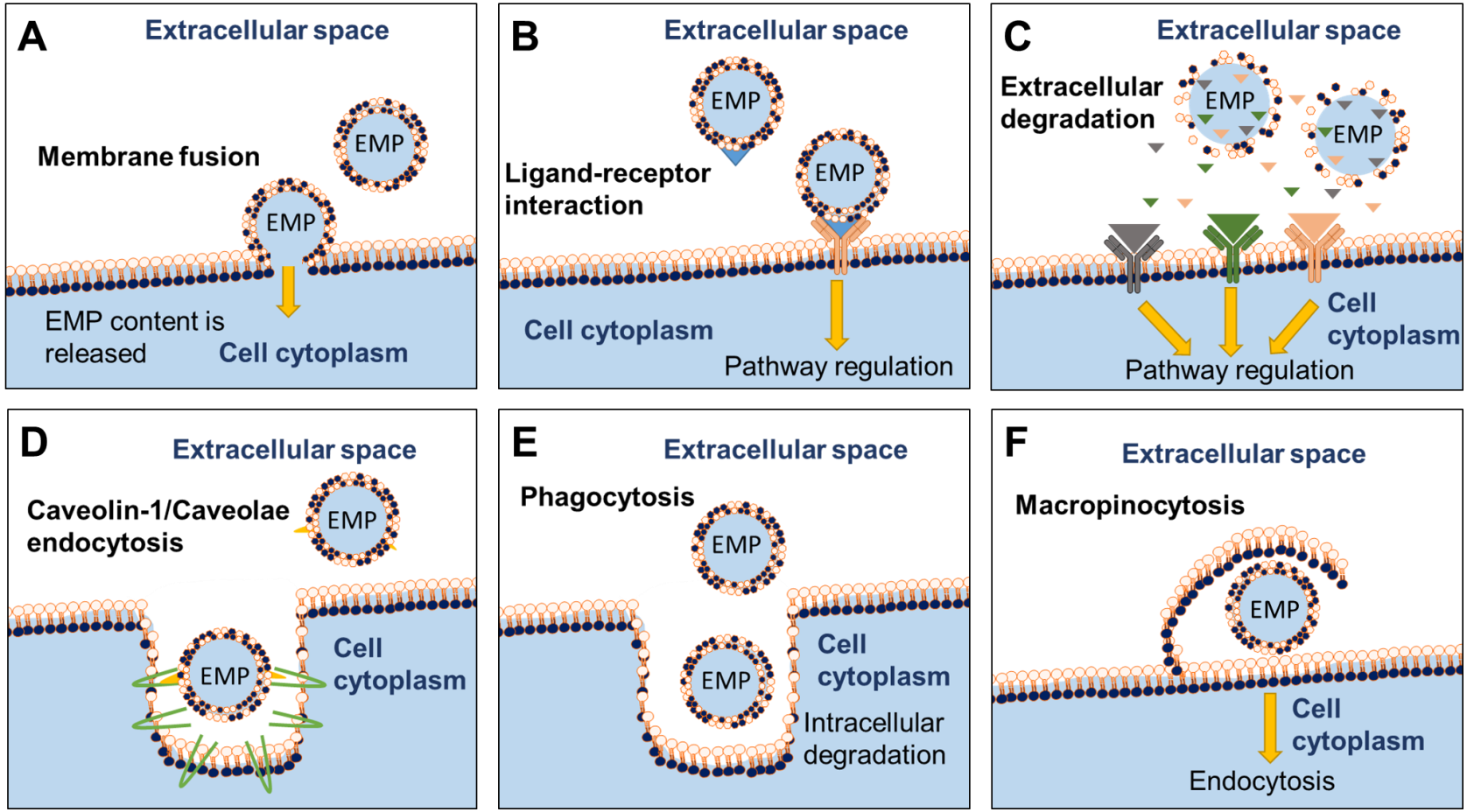

Figure 7. Proposed putative pathways/mechanisms of EMP:cell interaction. MPs act as cell to cell communicators as they carry proteins and RNAs from their cell of origin. However, the mechanisms by which MPs interact with their targets cells are still being investigated. A) Membrane fusion, B) ligand-receptor interactions, C) extracellular degradation, D) caveolin-1/caveolae endocytosis, E) phagocytosis, and F) macropinocytosis are some of the suggested mechanisms by which EMPs exert their effects on target cells. EMP: endothelial microparticle.

1.2.4. The role of EMPs in endothelial cell signalling

Increased microparticle concentrations of various cellular origins have been found in individuals under certain pathological conditions, which are usually associated with an increased thrombotic risk and endothelial dysfunction. Currently, endothelial function *ex vivo* is often measured using wire myography, a technique in which a blood vessel is cannulated and endothelial function and vasoconstrictor or vasodilator properties of the vessel in response to different pathophysiological stimuli are measured (139). Since elevated levels of EMPs compromise homeostasis of the vascular tone by decreasing nitric-oxide-dependent vasodilation, increasing arterial stiffness, promoting inflammation and initiating thrombotic events, they play a key role in the regulation of the different inflammatory and thrombotic diseases (140). Accumulating evidence strongly suggests that EMPs have pro-coagulant, pro-inflammatory and pro-angiogenic effects, indicating that they are not only an indicator of endothelial damage or CVD risk but also possible pathogenic factors (141). For instance, PS exposure in the outer membrane of EMPs (often accompanied by tissue factor) is associated with an increased thrombotic activity. Such pro-thrombotic and pro-coagulation activity of EMPs was studied in an investigation carried out by Abid Hussein *et al.*, which demonstrated that thrombin formation *in vitro* and thrombus formation *in vivo* is triggered by HUVEC-derived EMPs in a tissue factor-dependent manner (142), and another study by Leroyer *et al.* found EMPs in atherosclerotic plaques in patients undergoing carotid endarterectomy (143).

It has been demonstrated that MPs can be detected in plasma of healthy individuals at a level of 10^5 EMPs/mL (33). Under healthy conditions, vessel homeostasis is driven by the anti-inflammatory, anti-thrombotic and anti-atherogenic properties of the endothelial monolayer, and it is suggested that endothelial integrity is maintained by cell regeneration and the mobilisation of endothelial progenitor cells from the bone marrow (140). Some studies have found a protective function of EMPs too (144, 145), such as one from our laboratory in which we found that EMPs prevent lipid-induced endothelial damage via Akt/eNOS signalling *in vitro* (146). Another study by Hussein *et al.* showed that EMPs regulate pro-apoptotic activity and cell detachment by encapsulating caspase-3 away from the endothelial cells, and that inhibiting EMP release pharmacologically lead to the accumulation of caspase-3 and ultimately cell detachment and cell death, thus demonstrating their role in increasing cell survival (147). Moreover, a different study by Perez-Casal *et al.* found that EMPs

participate in the regulation of the coagulation cascade by exposing endothelial protein C receptor on their surface thus acting as anticoagulant molecules (144), much to the contrary of the pro-thrombotic activity effects reported also by Hussein *et al.* just a year before (142). To simplify this, a schematic representation of the role of EMPs on endothelial cell function and its associated proteins is illustrated in Figure 8.

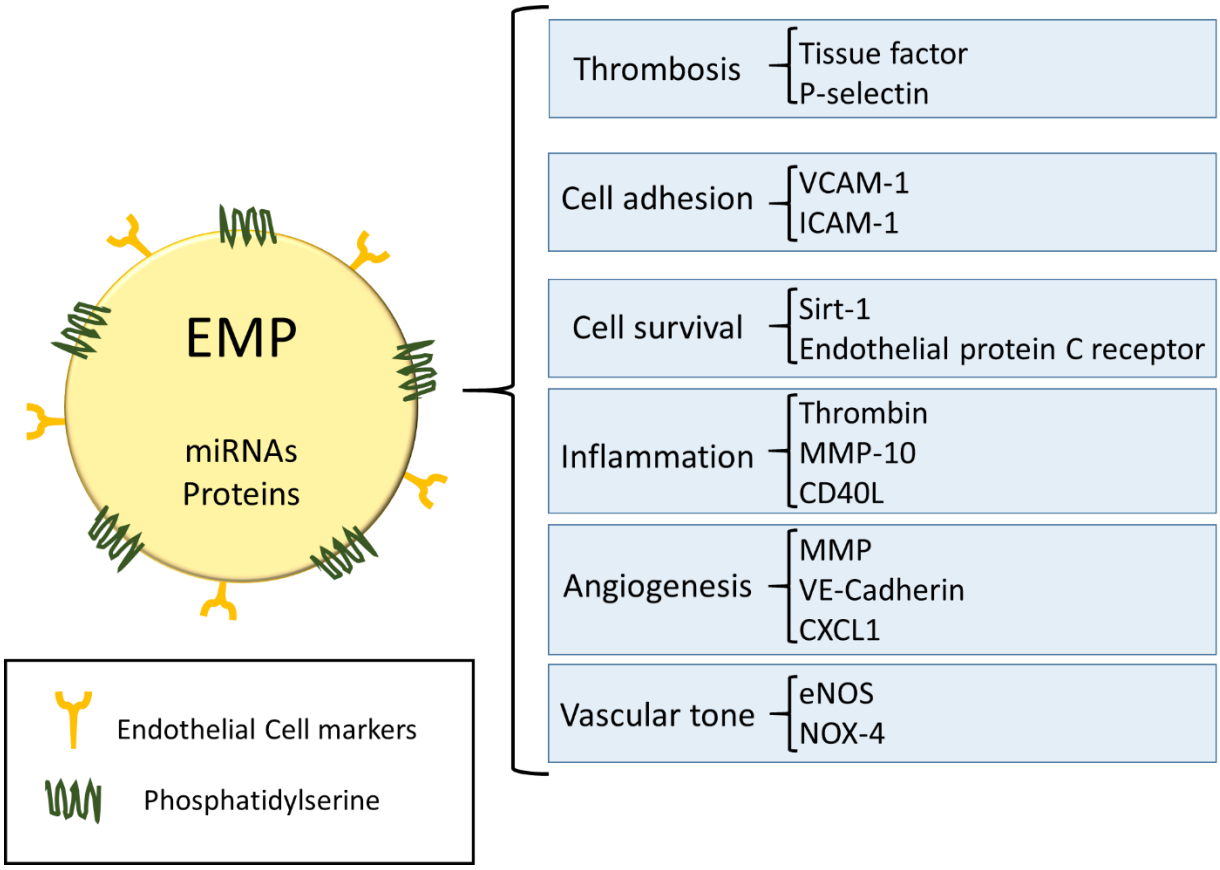

Figure 8. Schematic representation of the functional role of EMPs and their associated proteins. EMPs carry molecular components involved in different endothelial cell functions such as tissue factor, VCAM-1, ICAM-1 and eNOS and therefore, they are associated with both damage and repair mechanisms. EMP: endothelial microparticle; VCAM-1: vascular cell adhesion molecule-1; ICAM-1: intercellular adhesion molecule-1; Sirt-1: silent mating type information regulation 2 homolog 1; MMP-10: matrix metalloproteinase 10; MMP: matrix metalloproteinase; VE-Cadherin: vascular endothelial cadherin; CXCL1: chemokine (C-X-C motif) ligand 1; eNOS: endothelial nitric oxide synthase; NOX-4: Nicotinamide adenine dinucleotide phosphate oxidase 4. Adapted from Pieri *et al.* (148)

The literature suggests that EMPs could act as a potential biomarker of disease stage and CVD risk, as well as a potential therapeutic tool (36) or a signalling mechanism. Of note, since they may provide valuable information of hard to access tissue, distinct EMP levels may be representative of the progression of CVD or

endothelial dysfunction (149); for example, a recent study in our laboratory found that EMPs are elevated in patients with unstable asymptomatic carotid artery plaques (145). EMPs are biological effectors of cardiovascular pathophysiology and may not only play a role as disease biomarkers, but also as promoters of endothelial dysfunction and inflammation. Therefore, it is necessary to gain further understanding of the whole process, including their role in disease and their mechanism of action. New knowledge would provide the necessary insight to allow research into developing novel therapies.

1.2.5. The role of EMPs in vascular smooth muscle cell signalling

Endothelial dysfunction in rheumatic autoimmune diseases such as SLE involves innate immune responses, including macrophages and dendritic cells and expression of scavenger and toll-like receptors for low density lipoprotein (LDL), as well as the activation of complement and dysregulation of adaptive immune responses (150). As it has been demonstrated (151), EMPs may have a pro-inflammatory effect, thus they might lead to the production of cytokines that increase the expression of adhesion molecules. Adhesion molecules such as ICAM-1 and VCAM-1 when up-regulated, cause activation and adhesion of inflammatory circulating cells, which in turn triggers a response in the media layer, often resulting in the aberrant proliferation of smooth muscle cells (SMCs), which migrate to the intimal layer and in some cases cause the deposition of a fibrous matrix and thickening of the vessel wall, contributing to the formation of fibrous tissue and so leading to the development of CVD (152).

Smooth muscle cells are capable to undergo phenotypic changes during development, both *in vitro* and in association with diseases. In diseases such as SLE, a dysregulation in the molecular signals regulating the differentiation of smooth muscle cells (SMCs) can occur, which leads to inappropriate differentiation into cells with features of other mesenchymal lineages such as osteoblasts or chondrocytes, a process known as vascular calcification (153). Vascular calcification is a relevant clinical problem in many conditions (including SLE among others) and it is considered to be an independent predictor of CVD (10). It is characterised by the loss of contractility by the SMCs and the expression of lower levels of contractile proteins (SMC-actin and SMC-myosin heavy chain) (154), and the formation of calcium deposits in the arteries, ultimately reducing elastic compliance and

therefore, inducing an impaired circulation activity. It is well established that vascular calcification is a cell-regulated process with many similarities to bone formation; i.e. human vascular smooth muscle cells (hVSMCs) express osteogenic-related proteins, ultimately leading to matrix mineralisation (155-157).

It has been reported recently that microparticles are able to induce a senescent phenotype in endothelial cells (EC) (158). In that study, the authors demonstrated that MPs promoted EC senescence through nicotinamide adenine dinucleotide phosphatase oxidase and mitochondrial-derived reactive oxygen species. These findings form the basis for further studies involving different cell populations and pathobiologies. In a similar line, our study investigates the potential effects that EMP populations may exert in smooth muscle cells in an *in vitro* calcification model.

It has been increasingly recognised that hVSMCs generate matrix vesicles that deposit in the vessel wall, where they act as a nucleation and vascular medial calcification niche (159). Very much like endothelial-derived MPs, these membrane-bound vesicles carry proteins that are related to extracellular mineralisation, cellular stress and other proteins that regulate Ca^{2+} and phosphate trafficking. A study by Kapustin *et al.* demonstrated that elevated intracellular Ca^{2+} levels initiate the translocation of the cell membrane in hVSMCs, leading to the secretion of Ca^{2+} containing vesicles (160), suggesting that the generation mechanism of these vesicles is of similar nature to that of EMPs described in section 1.2.1.1, which makes us question whether EMPs are also playing an active role in the regulation of smooth muscle cell calcification.

The mechanisms by which endothelial and smooth muscle cells communicate are diverse, and as reviewed by Straub *et al*., myoendothelial junctions (MEJs) play an active role in this (161). MEJs are cellular extensions from an endothelial cell (and from smooth muscle cells to a lesser extent), of approximately 0.5 µM in width and depth, that allow either direct or indirect contact between the endothelial and the smooth muscle cell layer by protruding through the internal elastic lamina. MEJs have been cited as possible key elements in the control of several vascular pathologies (162) and therefore, they may not only be able to facilitate the transport of different vascular factors released from endothelial cells to smooth muscle cells, such as calcium and potassium (163, 164), but also possibly EMPs (Figure 9).

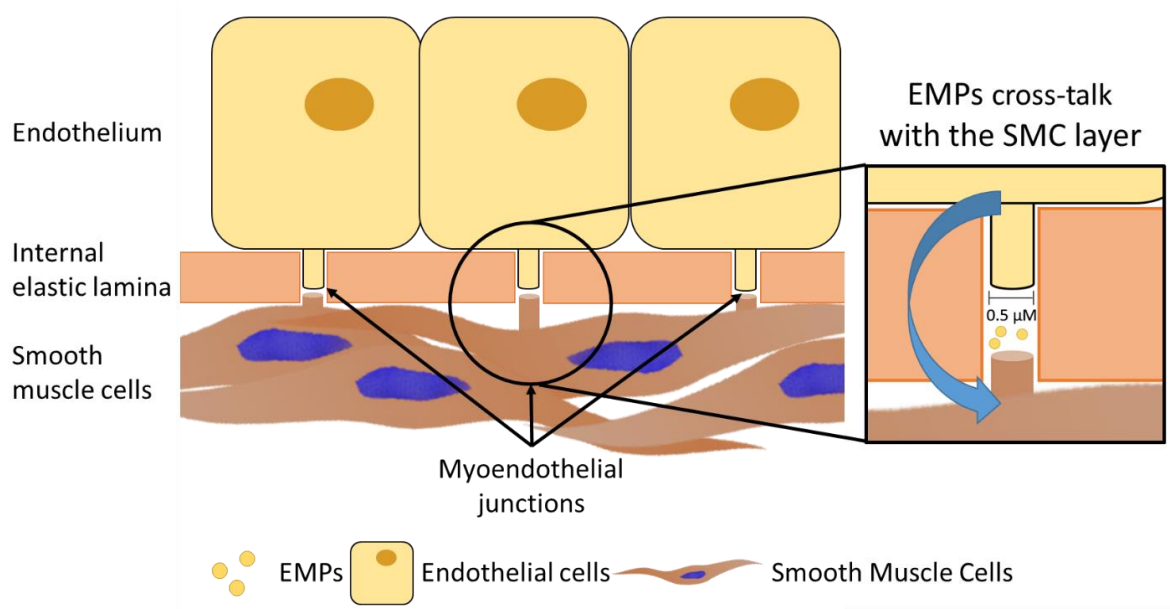

Figure 9. MEJs allow the cross-talk between endothelial and smooth muscle cells. MEJs are recognised as facilitators of the intercellular communication between endothelial and vascular smooth muscle cells of several vascular factors, and possibly, EMPs. EMPs: endothelial microparticles; SMC: smooth muscle cells. Adapted from Gladwin *et al.* (165)

1.2.5.1. Regulatory molecules involved in vascular calcification

Vascular calcification is a regulated process with similarities to osteogenesis which has been extensively investigated during recent years and as such, a variety of osteogenic regulatory molecules have been identified contributing to this pathological process (157), and it is the imbalance between such molecules that leads to pathogenic vascular calcification. Osteocalcin (OCN), C-met and hepatocyte growth factor (HGF) among others have been identified as promoters (166) whereas osteoprotegerin (OPG) is known to be a regulator of the receptor activator of nuclear factor kappa-B (RANK) pathway, where it acts as a scavenger for receptor activator of nuclear factor kappa-B ligand (RANKL), a calcification initiator, thereby inhibiting calcification (167).

Alterations to the expression of calcification promoters and inhibitors heavily influences the development of calcification (168, 169). For instance, the inhibition of the calcification inhibitors Matrix Gla Protein (MGP) (170) and Fetuin-A leads to soft tissue and intravascular calcification in mice (171), whereas Alkaline Phosphatase (ALP) has been shown to be up-regulated in human vessels as they calcify (172). Many studies have found that regulatory proteins involved in calcification are also present in the calcification sites, such as the transcription factor Cbfa1/Osf2, which regulates the expression of both OCN (a calcification promoter with mineral binding

capacity) (173) and osteopontin (OPN) (a calcification inhibitor) (174), therefore, an imbalance in Cbfa1/Osf2 could have a great impact in osteogenic differentiation (175).

Bone morphogenetic protein 2 (BMP-2), another protein that has been shown to be implicated in the osteoblastic differentiation of mesenchymal progenitor cells by inducing Msx2 gene expression via Notch *in vitro* (176), and bone morphogenetic protein 4 (BMP-4), which is an active mediator in RANKL mediated-calcification and like Cbfa1/Osf2, have been found to be localised in calcified areas (177). Furthermore, inflammatory cytokines such as IL-8 or TNFα have also been shown to promote osteogenic differentiation (178), and may also participate in the generation of calcium-rich osteoblast/chondrocyte-derived MPs, which are known to act as nucleation sites for calcium phosphate crystal formation (157, 179).

As part of this study, we investigated whether EMPs also play a role in the regulation of the calcification process. A summary of some of the mechanisms regulating vascular calcification can be found in Figure 10.

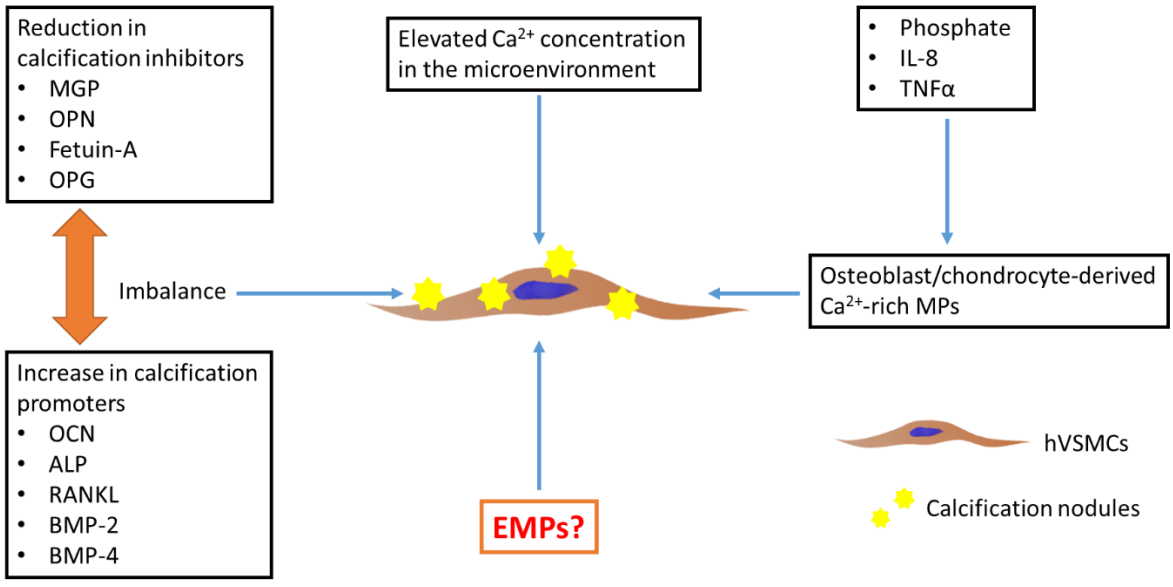

Figure 10. Proposed schematic summary of the mechanisms regulating vascular calcification. The imbalance between calcification inhibitors and promoters is known to play an important role in the regulation of smooth muscle cell calcification. However, elevated Ca^{2+} and phosphate concentrations in the microenvironment are also known to be important effectors. In addition, inflammatory cytokines may promote the generation of osteoblast/chondrocyte-derived Ca^{2+}-rich MPs. MGP: matrix Gla protein; OPN: osteopontin; OPG: osteoprotegerin; IL-8: interleukin 8; TNFα: tumor necrosis factor alpha; OCN: osteocalcin; ALP: alkaline phosphatase; RANKL: receptor activator nuclear factor kappa B ligand; BMP-2: bone morphogenic protein 2; BMP-4: bone morphogenic protein 4; EMPs: endothelial microparticles; hVSMCs: human vascular smooth muscle cells.

As previously described, TNFα activates endothelial cells, elevating the expression of adhesion markers such as ICAM-1 or VCAM-1 leading to the secretion of inflammatory molecules which ultimately induces smooth muscle cell reprogramming and EMP release. As reviewed by Bruce *et al.* (180), EMP levels are found to be increased in autoimmune and vasculitis disease patients and therefore, it is possible that they play a role not only in endothelial dysfunction but also in vascular calcification. However, the mechanisms for the phenotypic reprogramming of VSMCs into osteoblast-like cells is still only partly understood and accumulating studies indicate that an imbalance between calcification promoters and inhibitors is the most relevant mechanism underlying vascular calcification (169), therefore, EMPs may play a significant role as signalling molecules. This study will investigate whether EMPs may play a role in the phenotypic switching of smooth muscle cells into osteoblast-like cells, contributing to vascular calcification.

1.3. Remodelling the vasculature: inflammation and vascular calcification

1.3.1. An *in vitro* model of inflammation

In vitro models of inflammation are diverse, but provide valuable insight into mechanisms underpinning vascular inflammation, as they remove the complexity of interactive physiology associated with animal or patient studies. The culturing of endothelial cells from different vascular beds in combination with inflammatory stimuli (such as TNFα) has been used extensively to investigate the molecular mechanisms involved in the regulation of endothelial function and homeostasis. In this thesis, this model is used to investigate the effects of EMPs (and their proteomic and miRNA content) in endothelial cell function.

The literature is extensive in reporting the effects of different inflammatory cytokines on endothelial function. For instance, when endothelial cells are cultured in the presence of TNFα, the pathways activated and in turn, its effects on endothelial cell function strongly depend on the concentration of TNFα used (181-183). It is known that lower concentrations of TNFα activate canonical pathways, such as the NFκB pathway described in section 1.2.1.2 which will lead to inflammation and the expression of adhesion molecules VCAM-1 and ICAM-1 (182, 184, 185). However, higher concentrations TNFα will lead to caspase-3 activation and ultimately cell apoptosis and death (186).

In this study, a concentration of 10 ng/mL of TNFα, which has been proven not to activate apoptotic pathways after 24 hours (21), was used on HUVECs to simulate an inflammatory environment, in combination with healthy and inflammatory-derived EMPs (uEMPs and sEMPs respectively) generated from HUVECs, in order to study their effects on endothelial function in disease (Figure 11). HUVECs were chosen to generate EMPs and to perform functional assays due to their well described culture conditions and ease of access.

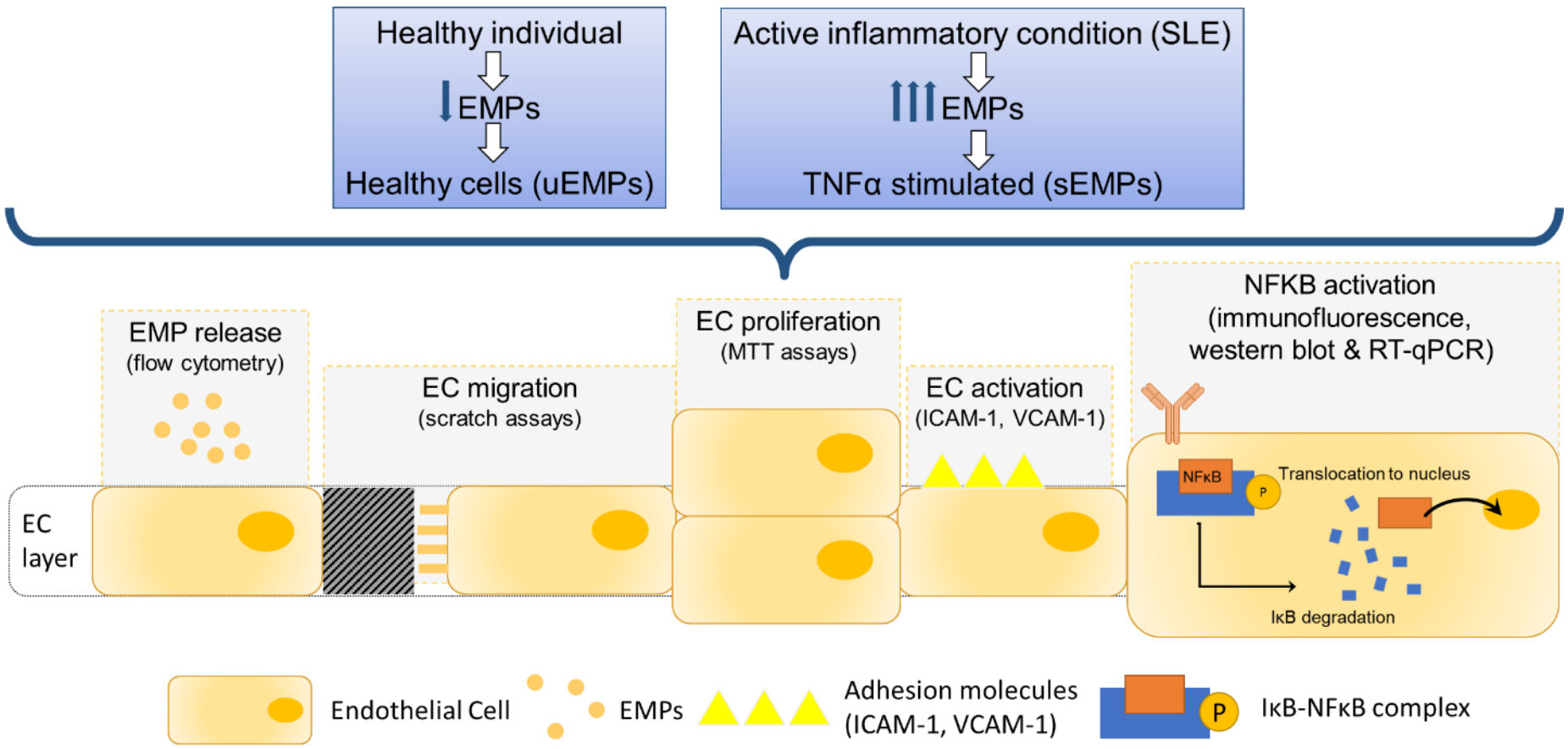

Figure 11. Proposed *in vitro* model of inflammation. HUVECs were treated with uEMPs or sEMPs and with or without TNFα (10 ng/mL) to investigate their effects on EMP release, activation, migration, proliferation, and activation of NFκB. EMPs: endothelial microparticles; EC: endothelial cell; ICAM-1: intercellular adhesion molecule 1; VCAM-1: vascular cell adhesion molecules 1; NFκB: nuclear factor kappa B.

1.3.2. An *in vitro* model of vascular calcification

In vitro models of calcification have been used extensively and involve culturing vascular smooth muscle cells and their ability to deposit a mineralised matrix. *In vitro* calcification models provide an excellent tool to investigate the molecular mechanisms underlying osteogenic differentiation of smooth muscle cells (187, 188). In this thesis, this model was used to investigate the effects of EMPs (and their proteomic and miRNA content) in vascular smooth muscle calcification.

When cultured in the presence of βGP (β-glycerophosphate) and increased calcium levels (> 2.6 mM), vascular smooth muscle cells deposit a mineralised matrix (189). Such deposition is often accompanied by the loss of characteristic hVSMC markers, such as alpha smooth muscle actin (accompanied by the loss of contractility), the dysregulation of calcification inhibitors such as OPG, OPN or MGP, and the gain of osteogenic markers, such as ALP or OCN (190). In this thesis, human coronary artery smooth muscle cells (HCoASMCs) were obtained from Caltag, cultured in osteogenic media containing 5 mM βGP and 2.6 mM $CaCl^{2+}$ for three weeks and treated with EMPs generated from human aortic endothelial cells stimulated with TNFα (AoEMPs) to study their effects on vascular calcification (Figure 12). HCoASMCs and AoEMPs were chosen for this study as the coronary artery and the aorta are two areas prone to calcify and reflect both macro and micro vessels (10), and their normal function is paramount in disease.

As discussed in section 1.2.5. MEJs and potentially MMP activity in EMPs, together with increased membrane permeability in endothelial dysfunction, are mechanisms that could regulate the cross-talk between the endothelial cells and the smooth muscle cell layer. However, this study focused on understanding the effects of EMPs on smooth muscle calcification, thus the mechanisms involved in EMP-driven cross-talk remain to be elucidated.

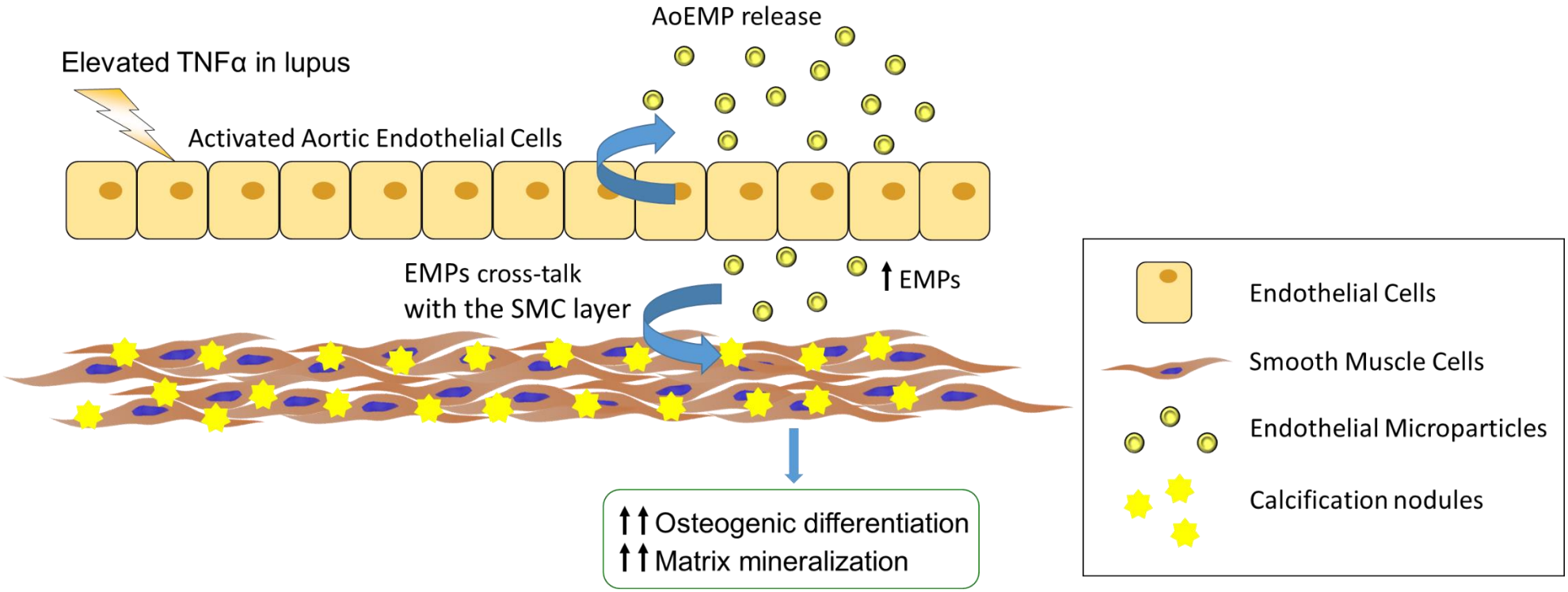

Figure 12. Proposed *in vitro* model of calcification. HCoASMCs were cultured in osteogenic media and treated with AoEMPs to investigate their effects on vascular smooth muscle cell calcification. TNFα: tumor necrosis factor alpha; EMPs: endothelial microparticles; SMC: smooth muscle cell.

1.4. Hypothesis

We hypothesise that EMPs have a dual role, depending on the stimuli involved in their release, potentially playing a role in vascular homeostasis, but also in exacerbating vascular damage under disease conditions and this can be executed via activating the endothelium, and also in the cross-talk to the smooth muscle layer, in terms of depositing a calcified matrix. The overarching aim of this study was to identify the role of EMPs in vascular disease using an *in vitro* endothelial and smooth muscle cell model.

1.5. Aims and objectives

1. Develop an *in vitro* model of SLE using human umbilical vein and aortic endothelial cells stimulated with TNFα for the isolation of EMPs from different vascular beds and study their protein and miRNA profile. In order to achieve this aim, the following objectives were addressed:

    - To identify the protein and microRNA content of two distinct EMP populations using a proteomic and microRNA screen.
    - To determine whether a correlation exists between protein content, function and morphology of EMPs.

2. To establish the role of two distinct EMP populations generated from human umbilical vein endothelial cells under i) unstimulated (uEMPs) conditions, to reflect those generated in healthy subjects, and ii) TNFα-stimulated (sEMPs) conditions, reflecting the inflammatory milieu associated with SLE, in order to establish whether the content of EMPs effects their function on vascular cells. The following objectives were addressed:

    - To determine whether EMPs enhance EMP generation under different environmental conditions.
    - To elucidate the differences between untreated (healthy) and stimulated (disease) EMPs on endothelial cell function.
    - To establish the mechanism of action responsible for such effects.

3. To elucidate the effect on EMPs on the osteogenic differentiation of SMCs using a well-established *in vitro* SMC calcification model. In order to achieve this aim, the following objectives were addressed:

    - To determine whether AoEMP treatment of HCoASMCs enhances vascular calcification compared to untreated cells grown in osteogenic conditions.
    - To elucidate the content of AoEMPs (proteins, microRNAs and Ca^{2+}) in order to identify relevant molecules and pathways involved in vascular calcification.
    - To identify novel molecular components of AoEMPs using a microRNA and proteomic analyses and their effects on osteogenic differentiation.

CHAPTER 2:
MATERIALS AND METHODS

CHAPTER 2: MATERIALS AND METHODS

The following sections describe the general methods and techniques used in the experimental design presented in this thesis.

2.1. Mammalian cell culture

All cells were grown in either 25 cm^2, 75 cm^2 flasks, 12 or 6-well plates (Nunc™, Thermo Scientific, Paisley, UK) and incubated at 37 ºC with 5 % CO_2 (v/v). The media was replaced every 48 or 72 hours. All cell culture work was carried out in a class II safety cabinet and performed under sterile conditions.

2.1.1. Maintenance of Human Umbilical Vein Endothelial Cells (HUVECs)

HUVECs were obtained from Caltag Medsystems (Buckingham, UK) from pooled donors, seeded into 0.1 % (w/v) gelatin-coated flasks or plates, and cultured in M199 medium (SLS, Nottingham, UK) supplemented with 20 µM L-Glutamine (Lonza, Verviers, Belgium), 10 µg/mL of Heparin (Sigma, Dorset, UK), 30 µg/mL Endothelial cell growth supplement (ECGS) and 20 % (v/v) heat inactivated Fetal Bovine Serum (FBS) from Gibco (Paisley, UK). HUVECs from passage 3 to 10 were used in experiments and were passaged at approximately 80 % confluency at 1:3.

2.1.2. Maintenance of Human Aortic Endothelial Cells (HAoECs)

HAoECs were sourced from Promocell (Heidelberg, Germany) from pooled donors and were cultured in endothelial cell growth medium MV2 (Promocell) supplemented with 25 % (v/v) heat inactivated FBS, 5 ng/mL epidermal growth factor, 10 ng/mL basic fibroblast growth factor, 20 ng/mL insulin-like growth factor, 0.5 ng/mL vascular endothelial growth factor 165, 1 µg/mL ascorbic acid and 0.2 µg/mL hydrocortisone according to the manufacturer's instructions. HAoECs from passage 3 to 10 were used in experiments and were passaged at approximately 80 % confluency at 1:3.

2.1.3. Maintenance of Human Coronary Artery Smooth Muscle Cells (HCoASMCs)

HCoASMCs were obtained from Caltag Medsystems and were cultured in smooth muscle media (Promocell), supplemented with 25 % (v/v) Fetal Calf Serum, 0.5 ng/mL epidermal growth factor, 2 ng/mL basic fibroblast growth factor and 5 µg/mL

insulin). HCoASMCs from passage 3 to 6 were used in experiments and were passaged at approximately 90 % confluency at 1:2.

2.1.4. Passaging cells

Once cells had reached 80-90 % confluency, the media was removed and cells were washed twice with pre-warmed Phosphate Buffered Saline (PBS; Lonza) and incubated with pre-warmed trypsin-ethylenediaminetetra-acetic acid (EDTA) (Lonza; 3 mL per 75 cm^2 flask) for 2 minutes at 37 ºC with 5 % CO_2 (v/v). Trypsin was inhibited by adding twice the volume of complete media and centrifuged at 304 x g for 5 minutes at room temperature. The supernatant was discarded and the cells were resuspended in warm complete media before plating evenly into 75 cm^2 flasks as outlined above.

2.1.5. Mammalian cell freezing and revival

To cryopreserve cells from a 25 cm^2 flask, cells were trypsinised as described (section 2.1.4), resuspended in 1 mL complete media containing 10 % (v/v) dimethylsulphoxide (DMSO) (Hybri-Max, Sigma) and transferred to 1.2 mL cryopreservation tubes. Cells were then placed in a Mr. Frosty (Thermo Scientific) freezing container at -80 ºC overnight prior to long-term storage in liquid nitrogen.

2.2. Generation, isolation and quantification of endothelial microparticles *in vitro*

Microparticles were generated from HUVECs and HAoECs in order to study the effects of distinct populations of EMPs on endothelial function and vascular calcification respectively.

2.2.1. Generation of HUVEC-derived EMPs (uEMPs and sEMPs)

HUVEC-derived EMPs were generated and used to study their effects on endothelial function and homeostasis. HUVECs were cultured in 75 cm^2 flasks until they reached 90 % confluence. Cells were washed with PBS twice and treated with 10 ng/mL TNFα (PromoCell) for 24 hours at 37 ºC with 5 % CO_2 (v/v) to generate TNFα-stimulated EMPs (sEMPs). EMPs derived from unstimulated HUVECs (uEMPs) were isolated from conditioned media of healthy growing cells 24 hours after a media change. In both cases, conditioned media was collected and sEMPs and uEMPs isolated as described in section 2.2.3.

2.2.2. Generation of HAoEC-derived EMPs (AoEMPs)

HAoEC-derived EMPs (Aortic-EMPs: AoEMPs) were generated using an established protocol from the Alexander laboratory (21) and used to study their effects on vascular calcification. HAoECs were cultured in 75 cm^2 flasks until they reached 90 % confluence. Cells were washed with PBS three times and incubated in serum-free endothelial cell medium (supplemented with 5 ng/mL epidermal growth factor, 10 ng/mL basic fibroblast growth factor, 20 ng/mL insulin-like growth factor, 0.5 ng/mL vascular endothelial growth factor 165, 1 µg/mL ascorbic acid and 0.2 µg/mL hydrocortisone) for 24 hours at 37 ºC with 5 % CO_2 (v/v). Cells were then treated with 10 ng/mL TNFα for further 24 hours. Conditioned media was collected and AoEMPs isolated as described in section 2.2.3.

2.2.3. Isolation of EMPs generated *in vitro*

To isolate uEMPs, sEMPs and AoEMPs, conditioned media was collected and centrifuged at 4,300 x g for 5 minutes at room temperature in order to remove cell debris. MPs are present in the supernatant and as such, 90-95 % of supernatant was collected into sterile 50 mL falcon tubes and stored at -80 ºC before isolation using ultracentrifugation. For large volumes of conditioned media (>200 mL), an Optima™ XE ultracentrifuge (Beckman Coulter, High Wycombe, UK) was used. Samples were transferred to 31 mL thick-walled polycarbonate ultracentrifugation tubes (Beckman Coulter) and centrifuged in a swing out SW32Ti rotor at 100,000 x g for 2 hours at 4 ºC. Pellets were carefully washed in PBS and centrifuged again under the same conditions. Finally, pellets were resuspended in 1 mL PBS and stored at -80 ºC for quantification.

2.2.4. Quantification of EMPs generated *in vitro*

EMP quantification was carried out by flow cytometry using a BD FACSVerse flow cytometer. EMP suspension (50 µL) was diluted in AnnexinV binding buffer (900 µL, Becton Dickinson, Oxford, UK). Flow-Count™ Fluorospheres (50 µL; Beckman Coulter) were added in order to assess absolute number of EMPs. Photomultiplier tube (PMT) voltages and microparticle gates were defined using the Megamix-Plus SSC size beads (Stago, Marseille, France) of 0.5 µm, 0.24 µm, 0.2 µm and 0.1 µm. Samples were labelled with AnnexinV-FITC (5 µL) mouse anti-human IgG_1 (Becton Dickinson) and incubated on ice in the dark for 15 minutes. Flow cytometry analysis was performed by gating the counting fluorospheres on Forward scatter (FSC) vs

Side Scatter (SSC) (linear scale). An example of the gating strategy can be seen in Figure 13. Samples were acquired at low flow rate until 1000 counting beads were detected. AnnexinV-FITC-positive events were selected as microparticles. Absolute EMP numbers were calculated using the following equation:

$$V = \frac{Z/(X/Y)}{20}$$

Where z = total volume of sample; x = total number beads added; y = number of beads counted; and 20 is the dilution factor. Once the volume of EMPs analysed is known, the total number of AnnexinV positive events is multiplied by (1000/v) to generate a number of EMPs/mL.

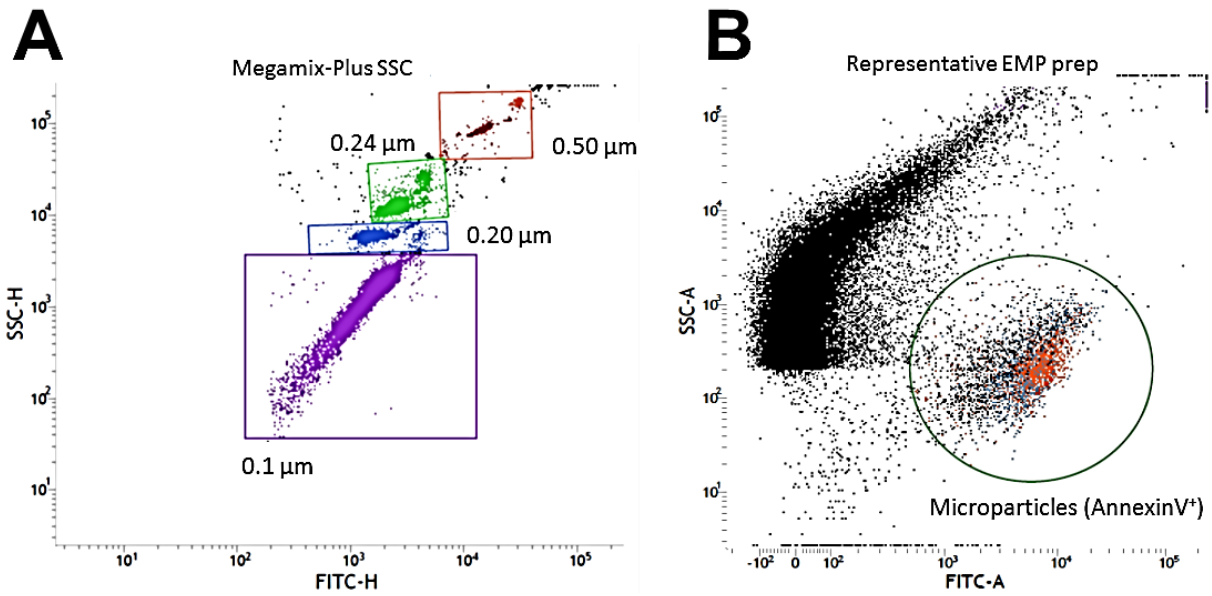

Figure 13. Representative dot plots of the EMP gating strategy. Flow cytometry analysis was performed using a BD FACSVerse and samples were acquired at low flow rate. A) Photomultiplier voltages were optimised using the Megamix-Plus SSC sizing beads. B) AnnexinV$^+$ events were gated and considered as MPs.

After quantification, a known volume of EMPs suspension was centrifuged at 100,000 x g for 2 hours at 4 ºC. After centrifugation, supernatant was discarded and EMP pellets were resuspended in a determined volume of PBS at a final concentration of 10^5 EMPs/µL of PBS.

2.3. RNA analysis

2.3.1. RNA isolation

All RNA work was carried out in a designated RNA workstation. Cells were lysed directly in flasks by adding 1 mL of TRIzol reagent (Invitrogen, Paisley, UK) per 10 cm^2 and scraped and stored in RNase-free tubes at -80 ºC until RNA isolation was performed.

Cell lysates were defrosted and sonicated for 1 minute in a water bath sonicator to ensure complete cell lysis; tubes were cleaned after sonication using RNAse ZAP solution (Invitrogen) Chloroform (0.2 mL per mL of TRIzol) was added, shaken by hand for 15 seconds and incubated at room temperature for 3 minutes. Samples were then centrifuged at 12,000 x g for 15 minutes at 4 ºC and the upper clear aqueous phase (RNA containing fraction) was transferred to a fresh RNase free tube, carefully avoiding the DNA-containing interphase. 0.5 mL of 2-propanol per mL of TRIzol were added to precipitate the RNA at -20 ºC overnight. Samples were incubated at room temperature for 10 minutes and centrifuged at 12,000 x g for 10 minutes at 4 ºC. The supernatant was discarded and the RNA pellet was washed with 1 mL of 75 % (v/v) ethanol, by vortexing briefly, and centrifuging at 7,500 x g for 5 minutes at 4 ºC. The ethanol was discarded and the pellet was left to air-dry for 15 minutes before resuspending in RNase-free water (15 µL). Samples were incubated at 55 ºC in the heat block for 10 minutes to allow the pellets to dissolve completely.

RNA content and purity were quantified using a NanoDrop. If RNA purity was lower than 1.6 (A260/280 nm < 1.6), samples were DNase-treated as follows: 1 µg of total RNA was treated with 1 unit of DNAse I amplification grade (Invitrogen) in 1 µL of 1 x DNase I Reaction Buffer in a total volume of 10 µl. Samples were incubated for 15 minutes at room temperature. DNase I was inactivated by adding 1 µL of 25 mM EDTA and heated for 10 minutes at 65 ºC. RNA samples were then ready to reverse transcribe into complementary DNA (cDNA)

2.3.2. Reverse transcription

Total RNA was reverse transcribed using the Tetra cDNA synthesis kit (Bioline, London, UK) in a PCR machine (Agilent Surecycle 8800). Typically, a master mix containing Oligo (dT)18, 10 mM deoxynucleotides (dNTP) mix, 5 x RT Buffer, RiboSafe RNase Inhibitor, Reverse Transcriptase (200 units/μL) and RNase free dH_2O was prepared and used to reverse-transcribe 1 μg of RNA into cDNA in a final volume of 20 μL: samples were incubated at 45 ºC for 40 minutes and the reaction was terminated by incubation at 85 ºC for a further 5 minutes. The resulting cDNA was stored at -20 ºC until real-time PCR was performed.

2.3.3. Quantitative real-time PCR (RT-qPCR)

PCR reactions were set up as follows: 1 μL cDNA (50ng), 5 μL of SensiFAST™ SYBR® Lo-ROX Kit (Bioline), 0.4 μL of forward primer (10 μM), 0.4 μL of reverse primer (10 μM) and 3.2 μL of RNase-free water. RT-qPCR was performed using a Stratagene Mx3000P. All primers used in real time PCR were obtained from Invitrogen and are listed with the PCR parameters in Table 6. Transcripts were normalised to GAPDH and mRNA abundance was calculated using the $2^{-\Delta\Delta CT}$ method.

Primer Name	Sequence (5’ -> 3’)	Ta	Product size (bp)
GAPDH F	GGAGCGAGATCCCTCCAAAAT	56	197
GAPDH R	GGCTGTTGTCATACTTCTCATGG		
VCAM-1 F	CAGGCTAAGTTACATATTGATGACAT	52	116
VCAM-1 R	GAGGAAGGGCTGACCAAGAC		
ICAM-1 F	CCTATGGAACGACTCCTTC	52	110
ICAM-1 R	TCTCCTGGCTCTGGTTCC		
IκBα F	CTATTCTCCCTACCAGCTCAC	55	114
IκBα R	CTCTCCTCATCCTCACTCTCT		
CCL20 F	GCAAGCAACTTTGACTGCT	55	150
CCL20 R	ATTTGCGCACACAGACAACT		
OPG F	CCTGGCACCAAAGTAAACGC	55	163
OPG R	GCACGCTGTTTTCACAGAG		
OPN F	GCCGAGGTGATAGTGTGGTT	55	149
OPN R	AACGGGGATGGCCTTGTATG		
OCN F	TGCTCCCTGCCTGCTAAGAC	56	178
OCN F	GGCAGCACAAACGCCAAAAG		
C-met F	GAAGTCCCAGCTACCAGTGTC	55	89
C-met R	CTGCCAGTAGACACCTGCTTC		
PCR conditions:	95 ºC for 10 minutes, then 40 cycles of: 95 ºC (denaturing step) for 30 seconds, annealing temperature (Ta) for 30 seconds and 72 ºC for 30 seconds (extension step). Finally, one additional cycle of 95 ºC for 1 minute, Ta for 1 minute and 72 ºC for 1 minute.		

Table 6. DNA oligonucleotide primers for quantitative real-time PCR. Primers were obtained from Invitrogen and were reconstituted in nuclease-free water at a concentration of 100 μM and stored at -20 ºC. Working solutions were made as required by diluting the stock solution 1:10 in nuclease-free water (final working concentration 10 μM). F= forward primer. R = reverse primer.

2.4. Protein analysis

Protein extraction for the calcium deposition assay was carried out using RIPA buffer and quantified using the bicinchoninic acid (BCA) assay (see section 2.4.1). Protein extraction for western blotting analysis was performed using FractionPREP™ Cell Fractionation Kit (BioVision, Milpitas, US) and quantified using the Bradford assay.

2.4.1. Protein extraction and quantification

RIPA buffer was used to extract protein from HCoASMCs for calcium deposition assays, and from EMPs (uEMPs, sEMPs and AoEMPs) for proteomic quantification by Olink Bioscience (see section 2.4.1). Briefly, cells were washed twice in ice-cold

PBS, and 100 µL of RIPA buffer was added to the cells, which were thoroughly scraped off the cell culture dish and incubated on ice for 30 minutes, vortexing every 5 minutes. Samples were then centrifuged at 20,000 x g for 10 minutes at 4 ºC and the supernatant was transferred to a fresh Eppendorf tube and stored at -20 ºC before quantification. RIPA extracted protein quantification was carried out using the BCA assay (Thermo Scientific). Albumin standards ranging from 0.05 mg/mL to 2 mg/mL were prepared and 50 parts of reagent A were mixed with 1 part of reagent B in a Falcon tube. BCA reagent mix (200 µL) was added to each sample or standard (10 µL) and incubated for 30 minutes at 37 ºC. Absorbance was read at 562 nm using a Synergy HT plate (Biotek) reader and protein concentration determined using Gene5 Microplate Reader software, which generates a standard curve.

Protein extraction using the FractionPREP™ Cell Fractionation Kit was carried out according to manufacturer's instructions. Briefly, cells were trypsinised (as described in section 2.1.4) and washed in ice-cold PBS. Cell pellets were resuspended and incubated for 20 minutes in 400 µL of Cytosol Extraction Buffer-Mix (containing Protease Inhibitor Cocktail and 0.1 M dithiothreitol (DTT)). Samples were then centrifuged at 700 x g for 10 minutes and the cytosol-containing supernatant was stored at -20 ºC. Pellets were resuspended in 400 µL of Membrane Extraction Buffer-A (containing Protease Inhibitor Cocktail and 0.1 M DTT); 22 µL Membrane Extraction Buffer-B was added and samples were incubated for 1 minute prior to centrifugation at 1,000 x g for 5 minutes. The membrane-containing supernatant fraction and the nuclear/cytoskeleton-containing pellets were stored in -20 ºC until quantification was carried out. Protein quantification of fractionated samples was carried out using the Bradford assay (Bio-Rad, Hertfordshire) as the protein extraction buffer used for fractionation was not compatible with the BCA method. Bovine serum albumin (BSA) standards ranging from 0.05 mg/mL to 0.5 mg/mL were prepared. Briefly, dye reagent was prepared by diluting 1 part of Dye Reagent Concentrate with 4 parts deionised water and filtered through an 0.2 µM filter. 10 µL of each sample were used and 200 µL of diluted dye were added and incubated for 5 minutes at room temperature. Albumin ranging from 0.05 mg/mL to 0.5 mg/mL were prepared and used as standards. Absorbance was read at 595 nm using a Synergy HT plate reader (Biotek) and standard curve and protein concentration determined using Gene5 Microplate Reader software.

10 KDa molecular weight cut-off protein concentration columns (Thermo Scientific) were used in those cases where protein concentration was low. Briefly, protein lysate was centrifuged at 15,000 x g in protein concentration columns for 15 minutes. Concentrated protein was recovered and quantified again as described above.

2.4.2. Western blotting (gel electrophoresis, transfer and protein detection)

Proteins were separated by SDS polyacrylamide gel electrophoresis using the Thermo Fisher system with pre-made NuPAGE® Bis-Tris gels (4-12 % acrylamide/bisacrylamide). Protein samples (20 µg) were prepared by boiling 1 x NuPAGE LDS loading buffer (containing 250 mM DTT) for 5 minutes at 100 ºC. All samples were loaded onto the gel and electrophoresed in 1 x MOPS SDS Running Buffer (50 mM MOPS, 50 mM Tris Base, 0.1 % (w/v) SDS, 1 mM EDTA, pH 7.7) at 200 V for 50 minutes or until the dye front hand reached the bottom of the gel. SeeBlue Plus2 Pre-Stained protein standard molecular weight markers (Thermo Fisher) were also loaded.

Following gel electrophoresis, wet transfer was performed using the XCell II™ Blot Module. Blotting pads and filter papers were soaked in 1 x NuPAGE Transfer Buffer (containing 10 % (v/v) methanol); in the meantime, PVDF membranes (New England BioLabs, Hitchin, UK) were activated in methanol for 30 seconds, washed in dH_2O and soaked in transfer buffer. The gels were gently removed from the cassettes and a transfer assembly was prepared by bringing together the blotting pads, filter paper, the PVDF activated membrane, the gel, filter paper and blotting paper (in that order). Protein transfer was performed at 30V for 1 hour.

After transfer, membranes were blocked in PBST (0.5 % (v/v) Tween 20) containing 4 % (w/v) skimmed milk powder (Marvel) for 1 hour at room temperature. Primary antibodies (Table 7) were prepared in blocking buffer and membranes were incubated overnight at 4 ºC on a rocking platform. Membranes where washed with PBST 4 times (5 minutes each) and incubated with the appropriate horseradish peroxidase (HRP)-conjugated secondary antibody for 1 hour at room temperature on a rocking platform. Following incubation, membranes were washed in PBST 5 times over an hour prior to being developed in enhanced chemiluminescence (ECL) reagent. Pierce ECL Western-Blotting substrate mix (Thermo Fisher) was prepared

by mixing equal parts of reagents A and B and adding 1 mL of the substrate to each membrane. Membranes were incubated for 5 minutes with ECL prior to be analysed using the Chemidoc Touch system, with exposure times varying from 30 seconds to 3 minutes, depending on the antibody.

Antibody	Supplier	Catalogue number	Dilution used
Rabbit anti-VCAM-1	Abcam	ab134047	1:200
Rabbit anti-ICAM-1	Abcam	ab53013	1:200
Rabbit anti-IκBα	Santa Cruz	sc-203	1:500
Rabbit anti-NFκB	Santa Cruz	sc-372	1:500
Mouse anti-α-tubulin	Abcam	ab7291	1:500
Rabbit anti-Mouse-HRP	Dako	P0161	1:2000
Goat anti-Rabbit-HRP	Dako	P0448	1:2000

Table 7. Antibodies used for western blot analysis. Antibodies were stored at -20 or 4 ºC according to manufacturer's instructions and diluted to the appropriate concentration in blocking solution before use. VCAM-1: vascular cell adhesion molecule 1; ICAM: intercellular adhesion molecule 1; IκBα: inhibitor-kB alpha; NFκB: nuclear factor kappa-B; HRP: horseradish peroxidase

2.4.3. Densitometry

Densitometry analysis of western blot images acquired with the Chemidoc Touch system was performed using ImageJ analysis package. Each of the bands in the blot was selected using the rectangular selection tool and histograms indicating the intensity of each of the bands were generated. A numerical value for densitometry was generated by calculating the area in each of the histograms.

2.5. EMP content analysis

uEMPs, sEMPs and AoEMPs were generated as described in sections 2.2.1 and 2.2.2 and were subjected to proteomic and microRNA screening to characterise their molecular components. Protein and microRNA extraction and validation experiments were performed as described in the sections below. All EMP subsets were also analysed by Scanning Electron Microscopy to investigate phenotypical differences as detailed in section 2.6.

2.5.1. Proteomic analysis and Ca^{2+} content of *in vitro* generated EMPs

For proteomic screening, 10^7 uEMPs, sEMPs and AoEMPs were centrifuged at 100,000 x g for 2 hours at 4 ºC. The supernatant was removed and the EMP pellets were resuspended in 50 µL of RIPA buffer (containing Protease Inhibitor Cocktails) and protein content was quantified as described in section 2.4.1. Proteomic screening was performed by Olink Bioscience (Uppsala, Sweden) against set panels of 92 inflammatory and CVD associated proteins identified using Proseek® Multiplex technology (Figure 14). The subsequent downstream targets were then detected and quantitative analysis was carried out using standard RT-qPCR. Proseek Multiplex data are normalised for both intra- and inter-plate variation. In the final step of the data pre-processing procedure, the values are set relative to a fixed correction factor determined by Olink Bioscience. The generated normalised protein expression unit is on a log2 scale where a larger number represents a higher protein level in the sample, typically with the background level at around zero.

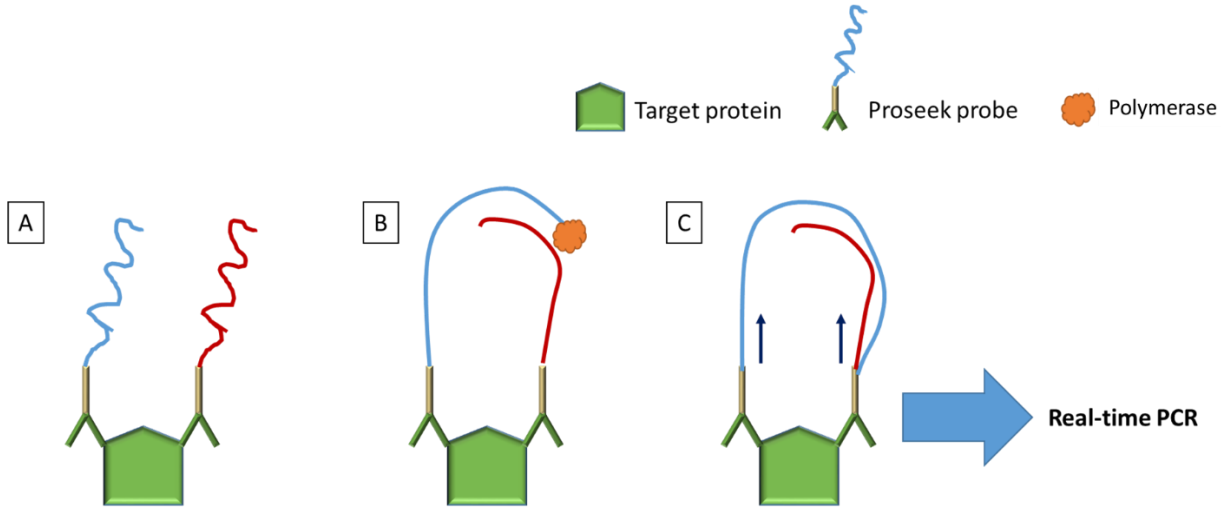

Figure 14. Main steps involved in a Proseek assay. A) A pair of oligonucleotide-labelled antibodies (Proseek probes) are allowed to bind to the target protein present in the sample by proximity. B) When the two probes are in close proximity, a new PCR target sequence is created by a proximity-dependent DNA polymerisation event. C) The resulting sequence is detected and quantified using standard real-time PCR. Adapted from Olink (191)

Subcellular localisation analysis was carried out using fatiGo (Babelomics 5). Further target validation was performed using enzyme-linked immunosorbent assay (ELISA) and flow cytometry.

For determining Ca^{2+} in EMPs, 10^7 uEMPs, sEMPs and AoEMPs were incubated with 1 N HCL (50 µL) overnight to extract the calcium. Ca^{2+} was then measured as described in section 2.9.1.2 using a calcium deposition quantification kit.

2.5.1.1. Validation of proteomic content by flow cytometry

Flow cytometry was used to further validate the presence of CCL20 in uEMPs and sEMPs and its relative abundance in the two different subsets. 10^7 uEMPs and 10^7 sEMPs were centrifuged at 100,000 x g for 2 hours at 4 ºC and incubated in 1 x Cytofix/Cytoperm buffer (100 µL, Becton Dickinson) for 30 minutes. Perm/Wash buffer was added (2 mL) and samples were centrifuged at 100,000 x g for 2 hours at 4 ºC. The supernatant was removed and samples incubated in the dark in 50 µL of 1 x Perm/Wash buffer containing CCL20-APC (5 µL, R&D systems, Abingdon, UK). After incubation, AnnexinV solution mix (containing 5 µL of AnnexinV, 50 µL of counting beads and 895 µL of 1x AnnexinV binding buffer) was added. Flow cytometry was performed using a BD FACSVerse using the gating strategy described in section 2.2.4. An IgG1 APC-conjugated Isotype Control was used to confirm specific staining.

2.5.2. microRNA array analysis of EMPs generated *in vitro*

10^7 uEMPs, sEMPs and AoEMPs were centrifuged at 100,000 x g for 2 hours at 4 ºC and the pellets were washed in 1 mL of cold PBS and centrifuged for further 2 hours under the same conditions. The supernatant was removed and TRIzol (1 mL) was added to extract the total RNA. 20 µg of molecular biology grade Glycogen was added to each sample to act as a carrier and increase the recovery of nucleic acids during RNA precipitation, mixed well and transferred to microfuge tubes. RNA was isolated as described in section 2.3.1. microRNA screening was performed by Ocean Ridge Biosciences (Florida, USA): microRNA was purified from total RNA by ultrafiltration and quantified by fluorometry and subjected to Ocean Ridge Biosciences proprietary microRNA microarray analysis. Validation of the identified microRNAs was carried out by RT-qPCR in our laboratory.

2.5.2.1. Validation of microRNA analysis

microRNA was extracted from 10^7 uEMPs, sEMPs and AoEMPs using the Isolate II miRNA kit from Bioline, according to manufacturer's instructions, and quantified

using a Qubit BioAnalyzer (Thermo Scientific). cDNA amplification and RT-qPCR were carried out as described in sections 2.3.2 and 2.3.3. Primers for microRNA RT-qPCR validation were designed using miRprimer2 software (Table 8) and obtained from Thermo Scientific. Bioinformatic analysis of validated microRNAs was performed to identify relevant pathways and targets using DIANA-miRPath and microRNA.org (TargetScan and miRBase). Target predictions with low mirSVR scores were considered as relevant and were pursued.

Primer (hsa-miRNA)	Sequence (5' -> 3')	Ta	Score
1224-3p F	CCCACCTCCTCTCTCCT	53	0.72
1224-3p R	GGTCCAGTTTTTTTTTTTTTTCTGA		
34a F	GCAGTGGCAGTGTCTTAG	52	0.49
34a R	GGTCCAGTTTTTTTTTTTTTTTACAAC		
608 F	GGGTGGTGTTGGGACA	53	0.64
608 R	GTCCAGTTTTTTTTTTTTTTTACGGA		
328 F	GCCCTCTCTGCCCTTC	52	0.44
328 R	GGTCCAGTTTTTTTTTTTTTTTACG		
1231 F	TGTCTGGGCGGACAG	52	0.33
1231 R	GTCCAGTTTTTTTTTTTTTTTGCAG		
532-3p F	GCCTCCCACACCCA	52	0.33
532-3p R	GTTTTTTTTTTTTTTGCAAGCCT		
483-3p F	GCAGTCACTCCTCTCCTC	52	0.34
483-3p R	GTCCAGTTTTTTTTTTTTTTTAAGACG		
595 F	GAAGTGTGCCGTGGTG	51	0.64
595 R	GGTCCAGTTTTTTTTTTTTTTTAGAC		
129-5p F	CAGCTTTTTGCGGTCTG	51	0.24
129-5p R	TCCAGTTTTTTTTTTTTTTTGCAAG		
210-3p F	GCTGTGCGTGTGACA	54	0.26
210-3p R	GTTTTTTTTTTTTTTTCAGCCGCT		
574-3p F	ACGCTCATGCACACAC	52	0.29
574-3p R	GTCCAGTTTTTTTTTTTTTTTGTGG		
1225-3p F	GTGAGCCCCTGTGC	52	0.42
1225-3p R	GGTCCAGTTTTTTTTTTTTTTTCTG		
185-3p F	GCAGTGGGCGTATCTGT	53	0.44

185-3p R	GGTCCAGTTTTTTTTTTTTTTTAGCA		
551a F	GCGACCCACTCTTGGT	53	0.49
551a R	GGTCCAGTTTTTTTTTTTTTTTGGAA		
1538 F	CGGGCTGCTGCTGT	52	0.72
1538 R	GGTCCAGTTTTTTTTTTTTTTTAGGA		
423-3p F	GCAGAGCTCGGTCTGAG	52	0.33
423-3p R	GGTCCAGTTTTTTTTTTTTTTTACTGA		
423-5p F	CAGTGAGGGGCAGAGAG	52	0.39
423-5p R	GGTCCAGTTTTTTTTTTTTTTTAAAGTC		
3148 F	CAGTGGAAAAAACTGGTGTGT	53	0.48
3148 R	GGTCCAGTTTTTTTTTTTTTTTAAGCA		
let-7b-5p F	CAGTGAGGTAGTAGGTTGTGT	53	0.81
let-7b-5p R	GGTCCAGTTTTTTTTTTTTTTTAACCA		
let-7a-5p F	GCAGTGAGGTAGTAGGTTG	51	0.16
let-7a-5p R	GGTCCAGTTTTTTTTTTTTTTTAACTATAC		
221-3p F	GCAGAGCTACATTGTCTGCT	51	0.64
221-3p R	CAGTTTTTTTTTTTTTTTGAAACCCA		
125b-5p F	GCAGTCCCTGAGACCCT	51	0.42
125b-5p R	CCAGTTTTTTTTTTTTTTTCACAAGT		
149-3p F	AGGGACGGGGGCT	52	0.21
149-3p R	GTCCAGTTTTTTTTTTTTTTTGCAC		
222-3p F	GCAGAGCTACATCTGGCT	52	0.49
222-3p R	CCAGTTTTTTTTTTTTTTTACCCAGT		
PCR conditions:	95 ºC for 10 minutes, then 40 cycles of: 95 ºC (denaturing step) for 30 seconds, annealing temperature (Ta) for 30 seconds and 72 ºC for 30 seconds (extension step). Finally, one additional cycle of 95 ºC for 1 minute, Ta for 1 minute and 72 ºC for 1 minute.		

Table 8. DNA oligonucleotide primers for miRNA validation using quantitative real-time PCR. Primers were designed using miRprimer2 software and obtained from Invitrogen and were reconstituted in nuclease-free water at a concentration of 100 µM and stored at -20 ºC. Working solutions were made as required by diluting the stock solution 1:10 in nuclease-free water (final working concentration 10 µM). A lower score means that primer pairs are less likely to form dimers. F= forward primer. R = reverse primer.

2.6. Scanning electron microscopy analysis of HUVECs and EMPs

Square glass coverslips (22 mm x 22 mm) were coated with 0.1 % (w/v) gelatin overnight at 37 ºC and washed once in PBS. EMPs (10^6), unstimulated and TNFα-stimulated HUVECs (10^5) were added to the centre of the cover slips, fixed with 2.5 % (v/v) glutaraldehyde in 0.1 M PBS at 4 ºC for 15 minutes and washed twice with 0.1 M PBS. Sequential steps using increasing concentrations of methanol were performed to dehydrate the sample (20 minutes each of 20 %, 40 %, 60 %, 80 % and 100 % (v/v) methanol in dH_2O) and samples were left to air-dry overnight. Gelatin coated coverslips, without EMPs, were included as controls. Samples were gold-coated using a Polaron SC7640 sputter coater and Scanning Electron Microscopy was performed using a Zeiss Supra 40VP microscope.

2.7. Specific protein analysis of EMPs using ELISA

A Human MIP3a/CCL20 ELISA Kit (Abcam, Cambridge, UK) was used to further validate CCL20 content following extraction from uEMPs and sEMPs. A Human HGF Quantikine ELISA Kit (R&D, Abingdon, UK) was used to validate HGF content following extraction from the AoEMPs.

2.7.1. MIP3a/CCL20 assay procedure

For MIP3a/CCL20 ELISA, 10^7 uEMPs and 10^7 sEMPs were isolated by ultracentrifugation at 100,000 x g for 2 hours at 4 ºC and resuspended in 1 x cell extraction buffer PTR (50 µL, as supplied by the manufacturer) for protein extraction. For performing the ELISA, protein from uEMPs and sEMPs (50 µL) were added to the wells, as well as MIP3a/CCL20 standards ranging from 2,500 pg/mL to 39.06 pg/mL and an antibody cocktail was added (50 µL per well). The plate was sealed and incubated for 1 hour at room temperature on a plate shaker (400 rpm). Sample wells were then washed 3 times with 1 x wash buffer PT prior to adding TMB substrate (100 µL) to each sample well. Samples were then incubated for 10 minutes in the dark on a plate shaker (400 rpm). After incubation, stop solution (100 µL) was added to each well and the plate was shaken for a further minute to allow complete mixing. Absorbance was measured at 450 nm using a Synergy HT plate reader (Biotek, Swindon, UK).

2.7.2. HGF Quantikine assay procedure

For the HGF Quantikine ELISA, 10^7 AoEMPs were isolated by ultracentrifugation for 2 hours at 100,000 x g at 4 ºC, resuspended in PBS at 4 ºC (50 µL), and sonicated for 15 minutes in a water bath sonicator for protein extraction. Assay diluent RD1W was added to each well (150 µL), prior to adding the samples (50 µL), as well as HGF standards ranging from 8,000 pg/mL to 125 pg/mL, and the plate was sealed and incubated for 2 hours at room temperature. After incubation, wells were washed four times with washing buffer (400 µL) and human HGF conjugate was added to each well (200 µL) and incubated for 1 hour and 45 minutes at room temperature. The plate was then washed four times with washing buffer (400 µL) and substrate solution (200 µL) was added to each well and incubated for 30 minutes at room temperature protected from light. After incubation, stop solution (50 µL) was added to each well and the plate was shaken for a further minute to allow complete mixing. Absorbance was measured at 450 nm as described above.

2.8. HUVEC treatment with EMPs as an *in vitro* model of inflammation

In order to investigate the effects of inflammation-derived microparticles (sEMPs) and to understand the effects of the microenvironment on EMP generation and role in endothelial function, a second set of healthy-derived microparticles (uEMPs) was used. HUVECs from passages 3 to 8 were seeded into 25 cm^2 flasks (Thermo Scientific) for EMP release experiments and protein assays, or into 6-well plates for RT-qPCR or wound healing, at a density of 5 x 10^3 cells/cm^2.

Cells were treated with uEMPs or sEMPs at a concentration of 10^6 EMPs/mL and in the presence or absence of TNFα (to simulate an inflammatory environment) (10 ng/mL) for 6 hours for the scratch assays, and for 24 hours for EMP generation experiments, RT-qPCR and western blotting.

2.8.1. Quantification of EMPs released *in vitro*

HUVECs were cultured on gelatin-coated 25 cm^2 flasks until confluent and treated with either uEMPs or sEMPs for 24 hours. Conditioned media was collected and centrifuged at 4,300 x g for 5 minutes at room temperature and 90-95 % of supernatant was ultracentrifuged at 100,000 x g for 2 hours at 4 ºC using a Beckman Coulter ultracentrifuge. EMP-containing pellets were resuspended in PBS (50 µL)

and EMP quantification was carried out using flow cytometry (AnnexinV$^+$ events) as described in section 2.2.4.

2.8.2. Functional analysis of EMPs on endothelial cells

2.8.2.1. Wound healing (scratch assays)

HUVECs were seeded on gelatin-coated 6-well plates and cultured to confluence in M199 complete media for 24 hours. A straight scratch was made across the centre of the cell monolayer in each well using a sterile 200 µL pipette tip, followed by treatment with 10^6 uEMPs or sEMPs per mL (in the presence or absence of 10 ng/mL of TNFα) for 6 hours. Phase contrast imaging was performed with a 10 x objective lens (Zeiss) at 6 hours. Cell migration was determined using ImageJ and calculated as percentage of initial cell-free areas vs percentage of cell-free areas after treatment.

2.8.2.2. Endothelial cell proliferation assays

In parallel with the functional scratch assays, the level of cell proliferation was determined using a cell proliferation kit (Abcam) according to manufacturer's instructions. Briefly, HUVECs were cultured sub-confluently (2.5 x 10^3 cells/cm^2) in 96-well plates in 100 µL/well of complete M199 media in the presence or absence of TNFα (10 ng/mL), and treated with uEMPs and sEMPs for 6 hours. WST-1 reagent and Electro Coupling Solution (10 mL) was added per well and cells were incubated for further 30 minutes. To ensure homogenous color distribution, the plate was shaken for a minute and the absorbance was read at 420 nm.

2.8.2.3. Adhesion assays (RT-qPCR and western blot)

Inflammation is linked with an increase in the endothelial cell adhesion markers VCAM-1 and ICAM-1. Western blot and RT-qPCR were performed to investigate the effects of both uEMP and sEMPs on adhesion markers at a proteomic and RNA level respectively. HUVECs were seeded on gelatin coated 6-well plates (for RT-qPCR) or 25 cm^2 flasks (for western blot analysis) and treated with uEMPs or sEMPs (10^6 per mL) for 24 hours in the presence or absence of TNFα (10 ng/mL; positive control). Cells were then collected in TRIzol as described in section 2.3.1 for RT-qPCR analysis of VCAM-1 and ICAM-1 mRNA expression, or in FractionPREP™

Cell Fractionation buffer as described in section 2.4.1 for western blot analysis of VCAM-1 and ICAM-1 protein quantification.

2.8.2.4. Immunofluorescence of NFκB

HUVECs were cultured subconfluently in µ-Slides VI 0.4 ibiTreat (Ibidi, Glasgow, UK) and left overnight. The M199 complete media was replaced 24 hours later with low serum M199 media (1 % (v/v) FBS, no heparin and no ECGS) and left to equilibrate for a further 24 hours. uEMP or sEMP treatments were performed for 30 minutes and 16 hours, using 10 ng/mL TNFα as a positive control. After treatment, culture media was removed and cells washed twice with PBS. Samples were fixed with 4 % (v/v) paraformaldehyde(PFA)/PBS for 15 minutes at room temperature and washed twice with PBS prior to incubation for one hour in blocking buffer (5 % (v/v) goat serum/0.1 % (v/v) Triton X-100/ PBS). Samples were then incubated overnight with primary antibody (rabbit anti-human anti-NFκB diluted 1/500 in blocking buffer; Santa Cruz, Heidelberg, Germany) at 4 ºC. Samples were washed with PBS 4 times (5 minutes per wash) and secondary antibody Alexa 488-labelled goat anti-rabbit IgG (1/500 in blocking buffer) was added for one hour at room temperature in the dark. Finally, samples were washed quickly in PBS 4 times, mounted in prolong gold antifade mountant (containing diamidino-2-phenylindole (DAPI); Vector Laboratories, Peterborough, UK) and left to set overnight in dark at 4 ºC. Slides were analysed using a Leica DMI6000B fluorescent microscope; 10 x and 20 x images were taken.

2.9. *In vitro* model of calcification

HCoASMCs were seeded in 6-well plates at a density of 1.5 x 10^4 cells/cm^2 and cultured in osteoinductive media (DMEM 10 % (v/v) FBS, 1 % (v/v) L-Glutamine, 1 % (v/v) Penicillin-Streptomycin, 5 mM βGP (β-glycerophosphate) and 2.6 mM $CaCl^{2+}$) for up to 21 days and treated with 10^6 AoEMPs per mL. Alizarin red S, calcium deposition, Bioplex analysis, ELISA and transfection experiments were performed. All experiments were performed in triplicate and the media was removed (and stored at -80 ºC for secretome analysis, where appropriate) every 72 hours and fresh media added.

2.9.1. Quantification of smooth muscle cell osteogenic differentiation

2.9.1.1. Alizarin red S staining

Alizarin red S was used to assess the level of calcification in AoEMP-treated SMCs; the staining produces a red-orange staining of calcium deposits observed by eye under the microscope and can be quantified colorimetrically. After 21 days of treatment with AoEMPs in osteoinductive conditions, the media was discarded and cells were washed three times with room temperature PBS. Cells were then fixed in 4 % (v/v) PFA for 10 minutes at room temperature and washed with PBS. Cells were stained with 500 mL of 2 % (w/v) Alizarin red S pH 4.2 (Sigma) for 5 minutes on a rocking platform. Excess dye was removed and the cells were washed 5 times with distilled water over a period of an hour, prior to observation under a microscope. Alizarin red S dye was then eluted to allow quantification of the staining: 10 % (v/v) formic acid (800 µL) was added to each well and the plate was incubated at room temperature for 5 min with shaking. 200 µL of elution was transferred per triplicate to a flat bottom 96 well plate and absorbance was measured at 414 nm using a Synergy HT plate reader (Biotek).

2.9.1.2. Calcium deposition assays

Calcium deposition was measured using a colorimetric Ca^{2+} detection kit (Abcam). Media was discarded and cells were washed three times with PBS. Cells were incubated in 800 µL of 0.6 N HCL overnight at 37 ºC and 5 % CO_2 (v/v) to extract the calcium. 50 µL of Calcium-containing HCL samples were incubated for 5 minutes at room temperature with 90 µL of the chromogenic reagent and 60 µL of calcium assay buffer and protected from light. Calcium standards ranging from 2 µg/well to 0.4 µg/well were prepared, and calcium content was quantified by measuring absorbance at 575 nm using a Synergic HT plate reader (Biotek).

Finally, Calcium content was normalised to total protein content, which was extracted from every sample using RIPA buffer and measured using the BCA assay and BSA as the control standard protein (see section 2.4.1).

2.9.2. AoEMPs internalisation by HCoASMCs

Calcein-AM (Thermo Fisher) was used to stain AoEMPs in order to investigate their uptake by target HCoASMCs. 10^6 AoEMPs were pelleted by ultracentrifugation for 2 hours at 100,000 x g at 4 ºC and incubated with 10 µM Calcein-AM for 30 minutes at 37 ºC in the dark. After incubation, AoEMPs were washed by adding PBS and concentrated by ultracentrifugation as outlined above. The supernatant was removed and Calcein-AM-labelled AoEMPs were resuspended in osteogenic media and added to the HCoASMCs. A control with Calcein-AM in the absence of AoEMPs was used to identify baseline and background fluorescence. Pictures were taken after 3, 6 and 24 hours using a Leica DMI6000B fluorescent microscope and uptake was quantified in ImageJ.

2.10. Bioplex suspension array analysis

Bioplex technology (also named Multiplex) is based on immunoassay and fluorescent principles, allowing the detection of multiple analytes in a single sample using a mixture of antibody-conjugated fluorescent beads. Bioplex human angiogenesis/growth factor and bone-panel kits were obtained from Merck Millipore (Watford, UK; Table 9) and were used to analyse the content of EMPs and the secretome of AoEMP-treated HCoASMCs using a Luminex LX100/LX200.

2.10.1. Sample preparation

For analysing EMP content, protein was extracted by sonicating 10^7 uEMPs and 10^7 sEMPs for 15 minutes in a water bath sonicator and used in the Bioplex on the same day. For analysing the secretome of HCoASMCs, conditioned media from AoEMP-treated cells was collected twice a week and centrifuged at 4,300 x g for 10 minutes to remove cell debris, and supernatant was stored at -80 ºC until the assays were conducted.

2.10.2. Assay protocol

All reagents were brought to room temperature. Antibody-immobilised beads were prepared in bead diluent buffer, sonicated and vigorously vortexed; quality controls and protein standards were reconstituted in 250 µL of deionised water. 200 µL of assay buffer were added intro each well of the microtiter plates and incubated for 10 minutes at room temperature on a plate shaker. Assay buffer was discarded and

25 µL was added again to every well on the plate. Standards and quality controls were added to the corresponding wells (25 µL) and topped up to a 50 µL with PBS (25 µL). Samples (25 µL) were added into the appropriate wells, and topped up with assay buffer (25 µL) to a final volume of 50 µL. Antibody-binding beads were vortexed and added to each well (25 µL); plates were sealed and incubated overnight on a plate shaker at 4 ºC. Following incubation, plates were washed 3 times using an automated plate washer (Biotek), detection antibodies (50 µL) were added into each well and plates were incubated on a plate shaker for 1 hour at room temperature. Streptavidin-Phycoerythrin substrate (50 µL) was added to each well and incubated for further 30 minutes at room temperature on a shaker. Plates were washed 3 times using the automate plate washer and sheath fluid (provided with the kits) was added (100 µL) and samples were incubated for 5 minutes on a plate shaker prior to being analysed in the Luminex.

	Protein	**Minimum concentration detected (pg/mL)**	**Maximum concentration detected (pg/mL)**
Angiogenesis/Growth factor panel kit	Angiopoietin-2, FGF-1, FGF-2, VEGF-A	13.7	10,000
	Endoglin	27.4	20,000
	Endothelin-1	2.7	2,000
	IL-8	1.4	1,000
	VEGF-C	6.9	5,000
Bone panel kit	OPG	7	30,000
	OC	146	600,000
	OPN	98	400,000
	SOST	24	100,000
	IL-6	1	6,000
	TNFα	0.24	1,000

Table 9. Characteristics of the bioplex kits used in the study. The angiogenesis/growth factor kit was used to identify proteins in uEMP and sEMP lysates. The bone panel kit was used to investigate the secretome of AoEMP-treated HCoASMCs. Maximum and minimum detection limits for the kits are described in the table. FGF-1: fibroblast growth factor-1; FGF-2: fibroblast growth factor-2; VEGF-A: vascular endothelial growth factor-A; IL-8: interleukin-8; VEGF-C: vascular endothelial growth Factor-C; OPG: osteoprotegerin; OC: osteocalcin; OPN: osteopontin; SOST: sclerostin; IL-6: interleukin-6; TNFα: tumor necrosis factor-α.

2.11. miRNA analysis using transfection of human vascular cells

2.11.1. hsa-miRNA-129-5p and hsa-miRNA-3148 plasmids

pEZX-MR04 plasmids, containing either hsa-miRNA-129-5p or hsa-miRNA-3148 or a scrambled control with a CMV promoter and carrying ampicillin and Puromycin resistant genes, as well as eGFP as a reporter gene, were purchased from GeneCopoeia (Figure 15) as bacterial glycerol stocks. A bacterial stab of the plasmids was grown in 100 mL of LB culture medium containing ampicillin and incubated overnight at 37 ºC with agitation. A scrambled control clone was also obtained from the same company.

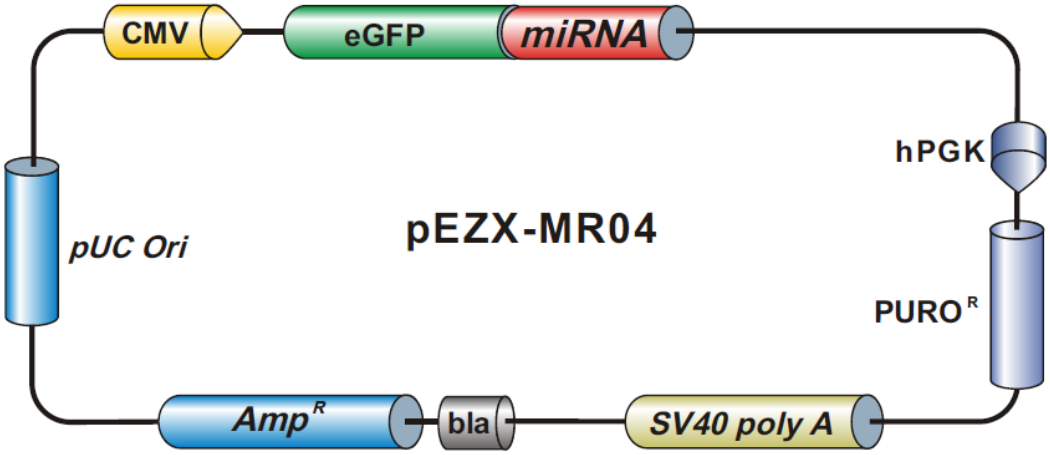

Figure 15. Schematic representation of pEZX-ME04. Puromycin resistant plasmids with an eGFP reporter gene were obtained from GeneCopoeia for hsa-miRNA-3148, hsa-miRNA-129-5p and a scrambled control.

2.11.2. Midi-preparation of plasmid DNA

The plasmid DNA was purified using the PureLink HiPure Plasmid Filter Midiprep Kit (Thermo Scientific). Briefly, cells were pelleted by centrifugation at 4,000 x g for 10 minutes and resuspended in Resuspension buffer R3 (10 mL), prior to the addition of Lysis buffer L7, mixed gently by inversion and incubated for 5 minutes at room temperature. Precipitation buffer N3 (10 mL) was added and mixed by inversion before centrifugation at 12,000 x g for 10 minutes at room temperature. The supernatant was loaded onto a pre-equilibrated column and the solution was allowed to drain by gravity. The column was washed twice with Wash buffer W8 (10 mL each wash) and the flow through was discarded. The plasmid DNA was eluted in Elution buffer E4 (5 mL) into fresh Falcon tubes. Isopropanol (3.5 mL) was added, followed by centrifugation at 12,000 x g for 30 minutes at 4 ºC. The supernatant was

discarded and the pellet was washed using 70 % (v/v) ethanol (3 mL), followed by centrifugation at 12,000 x g for 5 minutes at 4 ºC. The supernatant was discarded and the plasmid-containing pellet was allowed to air-dry for 10 minutes before resuspending in TE buffer (200 µL), sterile filtered and stored at -80 ºC. DNA concentration and quality (A260/280 ratio) was determined using a NanoDrop.

2.11.3. Plasmid transfection (AMAXA)

Plasmid DNA transfection was performed in a Nucleofector 2b device using Amaxa Nucleofector® technology (Lonza), where specific suspension buffers are used for each cell type being transfected. The solution and program used in this study was optimised for HUVEC and HCoASMC transfection using electroporation principles, in which an electrical field being applied to the cells increases the permeability of the cell membrane, allowing cells which are normally resistant to the uptake of DNA, to be successfully and efficiently transfected with the recombinant miRNA plasmids.

Bioinformatic analysis of uEMPs and sEMPs content allowed the prediction of hsa-miRNA-129-5p which targets CCL20 mRNA, therefore, transfection experiments were performed to validate this observation. For transfection of HUVECs, a 12-well plate was prepared by filling two wells with 750 µL of complete M199 media (supplemented with Heparin and ECGS as detailed in section 2.1.1) and pre-incubated/equilibrated in a 37 °C and 5 % CO_2 (v/v) incubator. Cells were then trypsinised as described in section 2.1.4 and counted using a Neubauer chamber. 5 x 10^5 cells were centrifuged at 200 x g for minutes at room temperature, resuspended in room temperature Nucleofector Solution (100 µL), and combined with 5 µg of hsa-miRNA-129-5p plasmid. For transfection control, 5 x 10^5 cells were also centrifuged, resuspended in Nucleofector Solution, and combined with 2 µg pmaxGFP vector. HUVEC/plasmid suspension was then transferred to an Amaxa cuvette and electroporation was performed using program A-034 in the Nucleofector 2b device. Pre-incubated/equilibrated M199 complete media (500 µL) was then added to the cuvette and transfected cells were gently transferred and distributed into the two pre-equilibrated wells in the 12-well plate (avoiding repeated aspiration of the sample) and incubated overnight in the incubator at 37 °C and 5 % (v/v) CO_2. 24 hours after transfection, efficiency was measured by fluorescence microscopy of the FITC channel, and an efficiency of 70 % was considered successful. pmaxGFP transfected cells were used as transfection controls. Media was replaced with M199 media (supplemented with 0.25 µg/mL of Puromycin) for positive selection of

transfected cells (Puromycin resistant), and was replaced every 24 hours for 3 days. Cells were washed twice in PBS and treated with TNFα (10 ng/mL) in serum free M199 media for 24 hours to stimulate CCL20 transcription (192). RNA was then collected in TRIzol and CCL20 mRNA levels were assayed by RT-qPCR as described in section 2.3.

Bioinformatic analysis of AoEMPs miRNA content predicted hsa-miRNA-3148 targets OPG mRNA, therefore, transfection experiments were performed to validate this observation. For transfecting HCoASMCs, a 6-well plate was prepared by filling 3 wells with HCoASMC complete media (1 mL each) and pre-incubated/equilibrated in a 37 °C and 5 % CO_2 (v/v) incubator. Cells were then trypsinised as described in section 2.1.4 and counted using a Neubauer chamber. 1 x 10^6 cells were centrifuged at 100 x g for minutes at room temperature, resuspended in room temperature Nucleofector Solution (100 µL), and combined with 5 µg of hsa-miRNA-3148 plasmid. For transfection control, 1 x 10^6 cells were also centrifuged, resuspended in Nucleofector Solution, and combined with 2 µg pmaxGFP vector. HCoASMC/plasmid suspension was then transferred to an Amaxa cuvette and electroporation was performed using program A-033 in the Nucleofector 2b device. Pre-equilibrated HCoASMCs complete media (500 µL) was then added to the cuvette and transfected cells were gently transferred and distributed into the three pre-equilibrated wells in the 6-well plate (avoiding repeated aspiration of the sample) and incubated overnight in the incubator at 37°C and 5 % CO_2 (v/v). 24 hours after transfection, efficiency was measured by fluorescence microscopy of the FITC channel, and an efficiency of 70 % was considered successful. pmaxGFP transfected cells were used as transfection controls. Media was replaced with HCoASMC media (supplemented with 0.25 µg/mL of Puromycin) for positive selection of transfected cells (Puromycin resistant), and was replaced every 24 hours for 3 days; cells were then washed twice in PBS and cultured in osteogenic media and collected in TRIzol after 4 days for RT-qPCR of OPG or left in osteogenic media for 21 days in order to perform Alizarin Red S staining (as described in section 2.9.1.1). Fluorescence microscopy was used at 4, 7, 14 and 21 days to confirm sustained plasmid expression. In addition to OPG, OPN, OCN and C-met were also investigated due to their role as either inhibitors or promoters in the vascular calcification process.

A dose-response experiment with HUVECs and HCoASMCs to determine the optimal concentration of Puromycin for positive selection of transfected cells was performed. HUVECs and HCoASMCs were seeded on 12-well plates and 6-well plates respectively, and treated with Puromycin concentrations ranging from 0.1 µg/mL to 2 µg/mL for 72 hours in M199 or HCoASMC media. Cells were observed every day and cell death was assessed visually; fluorescence microscopy was used to confirm that surviving cells were GFP^+. A summary of the workflow in this section is presented in Figure 16.

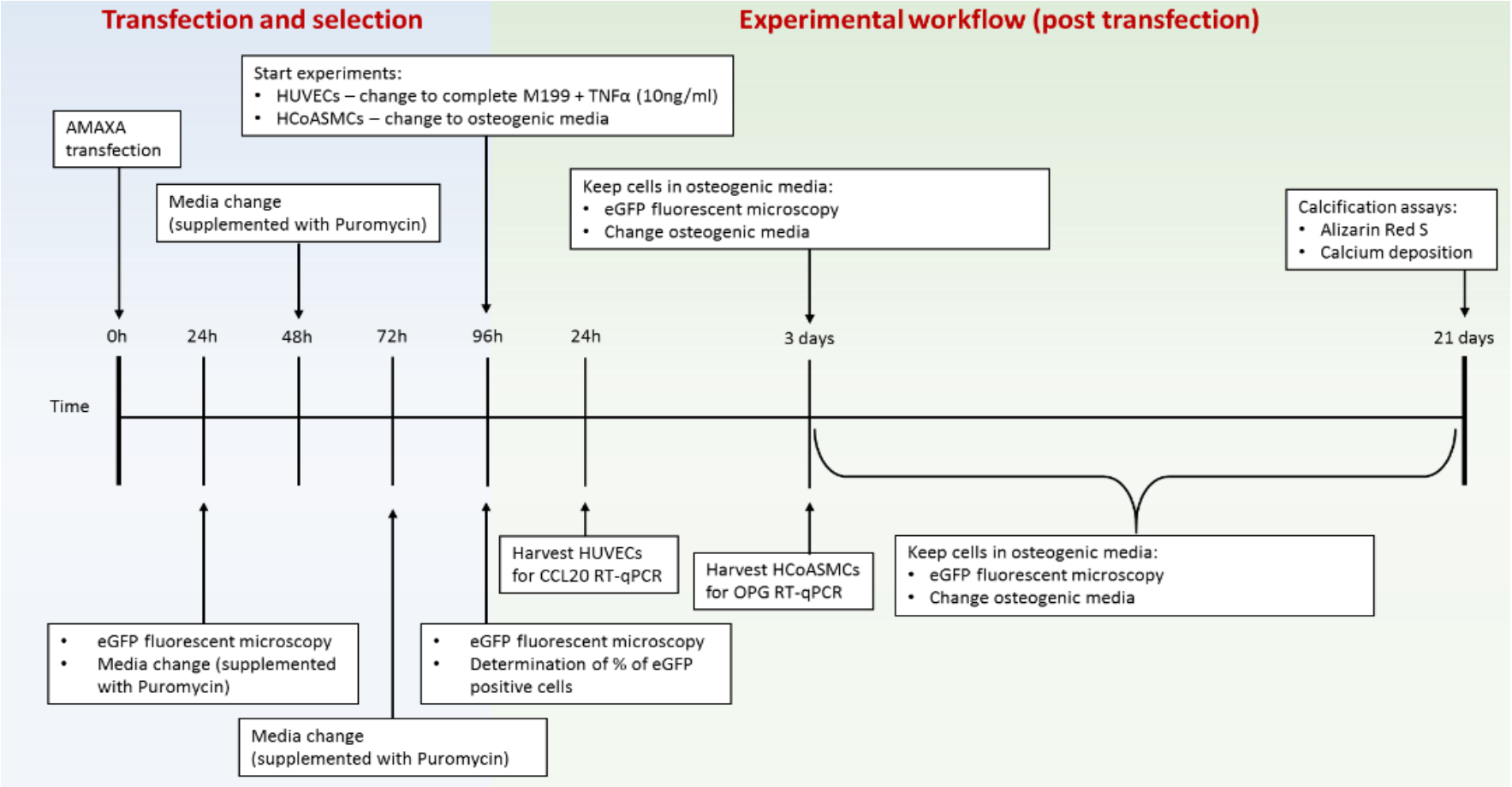

Figure 16. Experimental timeline for HUVEC and HCoASMC transfection. Cells were transfected using AMAXA kits from Lonza and selected in Puromycin for 3 days as described above. After Puromycin selection, cells were cultured either in Puromycin-free M199 osteogenic media for the experiments.

2.12. Statistical analysis

Data obtained from the experiments described in this thesis are representative of at least 3 independent experiments using cells from three different populations of cells representing biological triplicates as well as technical triplicates. Statistical analysis was carried out using GraphPad Prism 6 software and data are expressed as ± standard error mean (± SEM). Differences between groups were analysed with a Student's t test or one-way ANOVA (with Tukey correction for multiple comparisons) as appropriate. P values < 0.05 were considered significant unless stated otherwise.

CHAPTER 3:
THE EFFECT OF EMPS ON ENDOTHELIAL CELL FUNCTION

CHAPTER 3: THE EFFECT OF EMPS ON ENDOTHELIAL CELL FUNCTION

3.1. EMPs – agents of damage and protection

SLE and other connective tissue diseases are characterised by increased inflammation and in turn, these inflammatory disorders are also associated with endothelial dysfunction, leading to an increased risk of CVD. Previous work from the Alexander group have shown that circulating levels of EMPs are increased in different disease conditions (33), however, whether EMPs act either to exacerbate the damage in the vessel wall or as a protective factor to enhance repair of the endothelial layer remains to be established and is one of the aims of this programme of work.

The aim of the experiments presented in this chapter was to study the protein and miRNA profile of two distinct EMP populations generated from human umbilical vein endothelial cells under i) unstimulated (uEMPs) conditions, to reflect those generated in healthy subjects, and ii) TNFα-stimulated (sEMPs) conditions, reflecting the inflammatory milieu associated with SLE, in order to establish whether content of EMPs effects their function on vascular cells. In order to achieve this aim, the following 5 objectives were addressed:

1. To identify the protein and microRNA content of two distinct EMP populations, uEMPs and sEMPs, using a proteomic and microRNA screen and validation of specific proteins and miRNAs, using flow cytometry, bioplex suspension arrays and RT-PCR analysis.
2. To determine whether a correlation exists between protein content, function and morphology of EMPs, using scanning electron microscopy.
3. To determine whether EMPs enhance EMP generation under different environmental conditions using flow cytometry for quantification.
4. To elucidate the differences between untreated (healthy) and stimulated (disease) EMPs on endothelial cell function focusing on migration, proliferation and adhesion.
5. To establish the mechanism of action responsible for such effects using fluorescence microscopy and western blot.

3.2. Results

3.2.1. uEMPs and sEMPs as models of health and disease

TNFα, a known inflammatory stimulus, and one of which is raised in SLE, was used in this study to stimulate the release of MPs from HUVECs in order to investigate their function under inflammatory conditions compared to EMPs generated from untreated cells in standard physiological conditions. For the purposes of this study the 2 groups of EMPs generated from TNFα-stimulated and untreated HUVECs will be referred to as sEMPs and uEMPs respectively. Given that it is recognised that different stimuli and vascular beds lead to generation of distinct EMPs, we investigated the differences in the contents and roles of uEMPs and sEMPs, as well as their effects on endothelial function and the pathways associated with these effects.

3.2.1.1. sEMPs and uEMPs are phenotypically similar

Scanning Electron Microscopy (SEM) analysis was performed on unstimulated and TNFα-stimulated HUVECs. There appeared to be elevated EMP release in TNFα-treated cells compared to untreated cells (Figure 17), which was investigated further by flow cytometric analysis and quantification of these findings are presented in section 3.2.3.

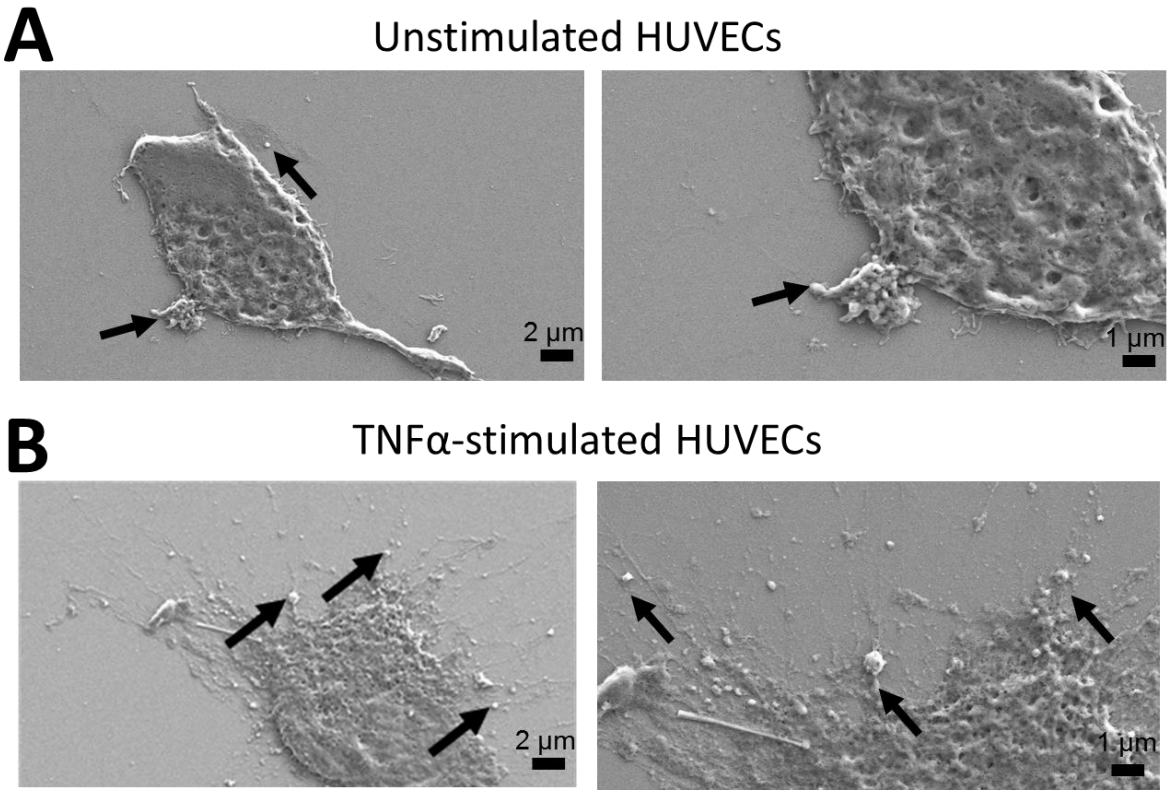

Figure 17. Representative Scanning Electron Microscopy micrographs of HUVECs releasing EMPs. A) Unstimulated HUVECs and B) TNFα-treated cells were grown on 0.1 % (w/v) gelatin coated cover slides and subjected to SEM analysis to observe EMP release. Black arrows indicate formation of EMPs. n = 3 independent experiments. HUVECs: human umbilical vein endothelial cells; TNFα: tumor necrosis factor alpha.

As shown in Figure 17A, unstimulated cells also release EMPs and therefore, SEM was performed to examine preparations of uEMPs and sEMPs as described in section 2.6 (Figure 18A and 18B). In all preparations, particles ranging from 200 nm to 1 µm were found. However, uEMPs appear to be slightly smaller than sEMPs (~ 200 nm), as well as more rounded. Since it is likely that the phenotypical differences observed between the two EMP populations was due to differences in their content, a proteomic and a microRNA analysis of the two EMP populations was performed.

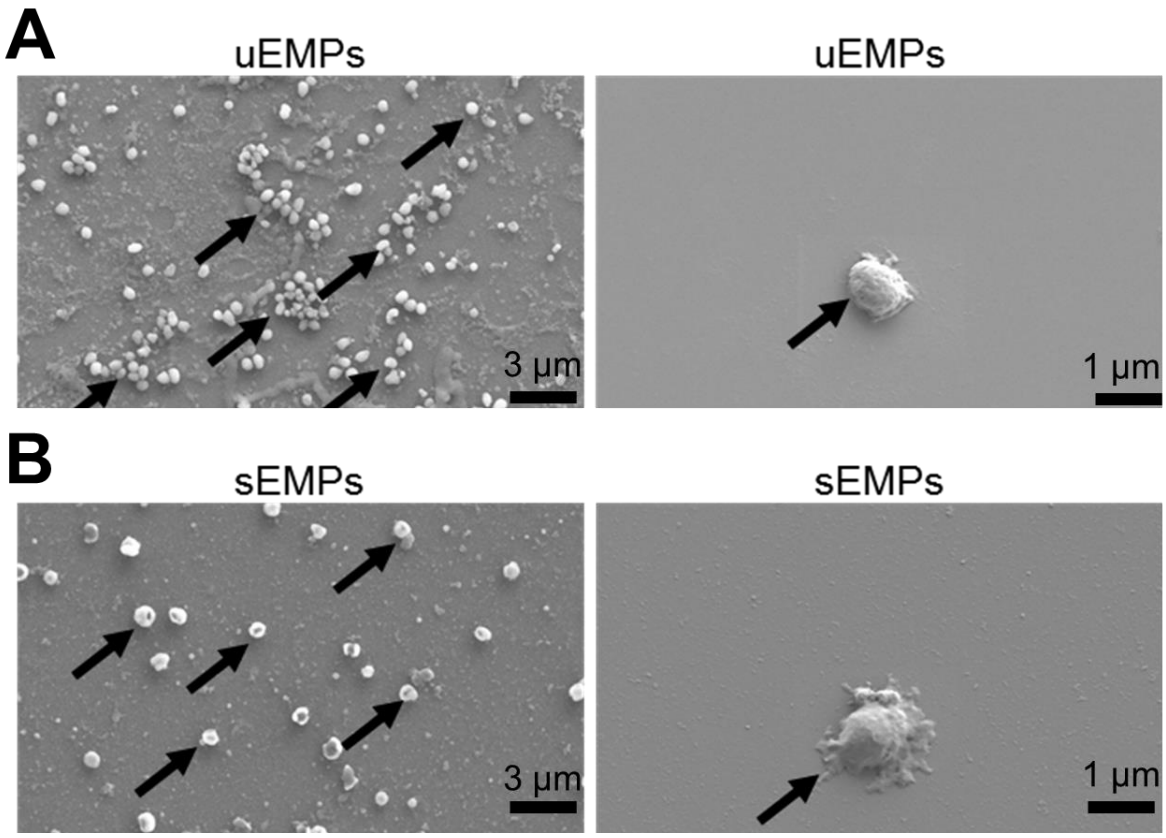

Figure 18. Phenotypic differences in uEMPs and sEMPs. Representative Scanning Electron Microscopy micrographs of uEMP (A) and sEMP (B) preparations. Particles ranging from 200 nm to 1 µm (± 400 nm SEM) were found in all preparations. Black arrows indicate the presence of EMPs. n = 3 (different uEMPs and sEMPs preparations).

3.2.1.2. uEMPs and sEMPs carry molecular components involved in endothelial function and inflammation

Since SLE is an inflammatory disorder associated with endothelial damage, it was of interest to establish whether any endothelial repair processes may be activated. A proteomic screen of inflammatory and proteins associated with CVD, a multiplex array of angiogenic/growth factor molecules were performed on concentrated preparations of EMPs. For the proteomic screen, proteins were extracted from the same number of uEMPs and sEMPs as detailed in section 2.5.1 in Methods and proteomic analysis performed by Olink Bioscience using Proseek technology as described in Figure 14 (n = 2 using different EMP batches). Out of the 92 cardiovascular and inflammatory proteins screened, 21 were found in both uEMPs and sEMPs, and only those in which SD < 3 between replicates were considered for further analysis (Figure 19). Proteomic screening demonstrated that uEMPs and sEMPs carry the same proteins, albeit in different concentrations, strengthening the

finding of others that the microenvironment during EMP generation underpins their proteomic content (193). Proteins identified in both uEMPs and sEMPs include the CXC chemokines; CXCL10, CXCL5 and CXCL6, as well as CC chemokines; MCP-1 and MCP-3 (Figure 19), albeit in increased concentration in sEMPs. Inflammatory cytokines TNFα, VEGF-A and IL-8 were also found in relatively similar levels, but a trend towards higher abundance in the sEMPs was found. However, of note, CCL20, was found to be more abundant in sEMPs than uEMPs, which is of interest because a parallel study in our laboratory also identified that circulating EMP levels correlate with circulating CCL20 levels in SLE patients (personal communication, unpublished data).

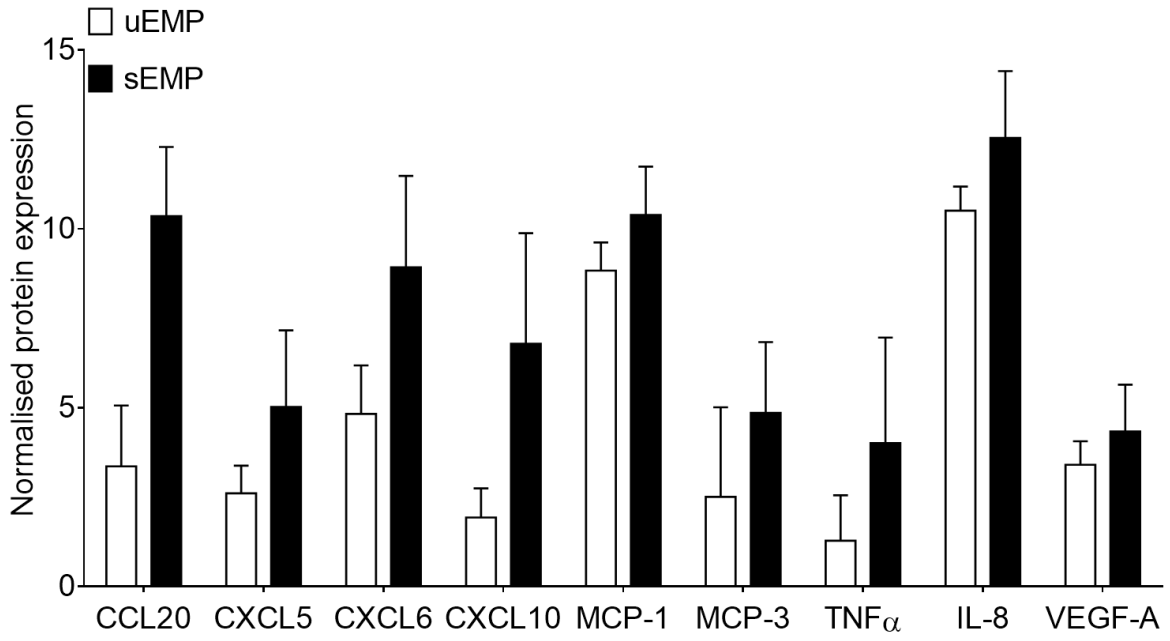

Figure 19. Analysis of proteomic profiles of isolated uEMPs and sEMPs. Protein from 10^7 uEMPs/µL of PBS and 10^7 sEMPs/µL of PBS was extracted in RIPA buffer (containing Protease Inhibitor Cocktail) and quantified using a BCA assay. The proteomic screening was outsourced to Olink Bioscience and the results presented are normalised for both intra- and inter-plate variation by Olink Bioscience. Proteins identified in uEMPs and sEMPs include CCL20, a regulator of macrophage recruitment to sites of injury. Error bars are presented as SEM. n = 2 (Olink Bioscience screenings performed on two different occassions using two different uEMPs and sEMPs preparations). CCL20: Chemokine (C-C motif) ligand 20; CXCL5: C-X-C motif chemokine 5; CXCL6: C-X-C motif chemokine 6; CXCL10: C-X-C motif chemokine 10; MCP-1: Monocyte chemotactic protein 1; MCP-3: Monocyte chemotactic protein 3; TNFα: Tumor necrosis factor alpha; IL-8: Interleukin 8; VEGF-A: Vascular endothelial growth factor A.

Parallel to the proteomic screen in EMPs, Multiplex analysis 8 molecules (angiopoietin-2, endoglin, VEGF-C, FGF-1, FGF-2, endothelin-1, IL-8 and VEGF-A) of uEMP and sEMP lysates confirmed the presence of IL-8 and VEGF-A (also found in the Olink Bioscience proteomic screening). Of note, two key angiogenic factors, i) Angipoietin-2, a molecule involved in the detachment of smooth muscle cells, matrix degradation and inhibition of VEGF-mediated angiogenesis, and ii) Endoglin, which is involved in vessel maturation, were found to be elevated in uEMPs in comparison to sEMPs (1.5 and 1.46 fold-change respectively; Figures 20A & 20B). Similarly, VEGF-C, which is has been shown to stimulate angiogenesis in adults, as well as FGF-1 and FGF-2 which regulate cell proliferation and differentiation, were also elevated in uEMPs in comparison to sEMPs (1.4, 1.6 and 1.94 fold-change respectively; Figures 20C, 20D & 20E). In addition, Endothelin-1, a potent vasoconstrictor, was found to be elevated in sEMPs in comparison to uEMPs (1.2 fold-change; Figure 20F). Finally, the pro-angiogenic molecules IL-8 and VEGF-A, which were also identified in the Olink Bioscience proteomic screening, were elevated in sEMPs in comparison to EMPs (10.4 and 6.3 fold-change respectively; Figures 20G & 20H). These results suggest that the content of both uEMPs and sEMPs may play a role in the disruption of endothelial repair mechanisms.

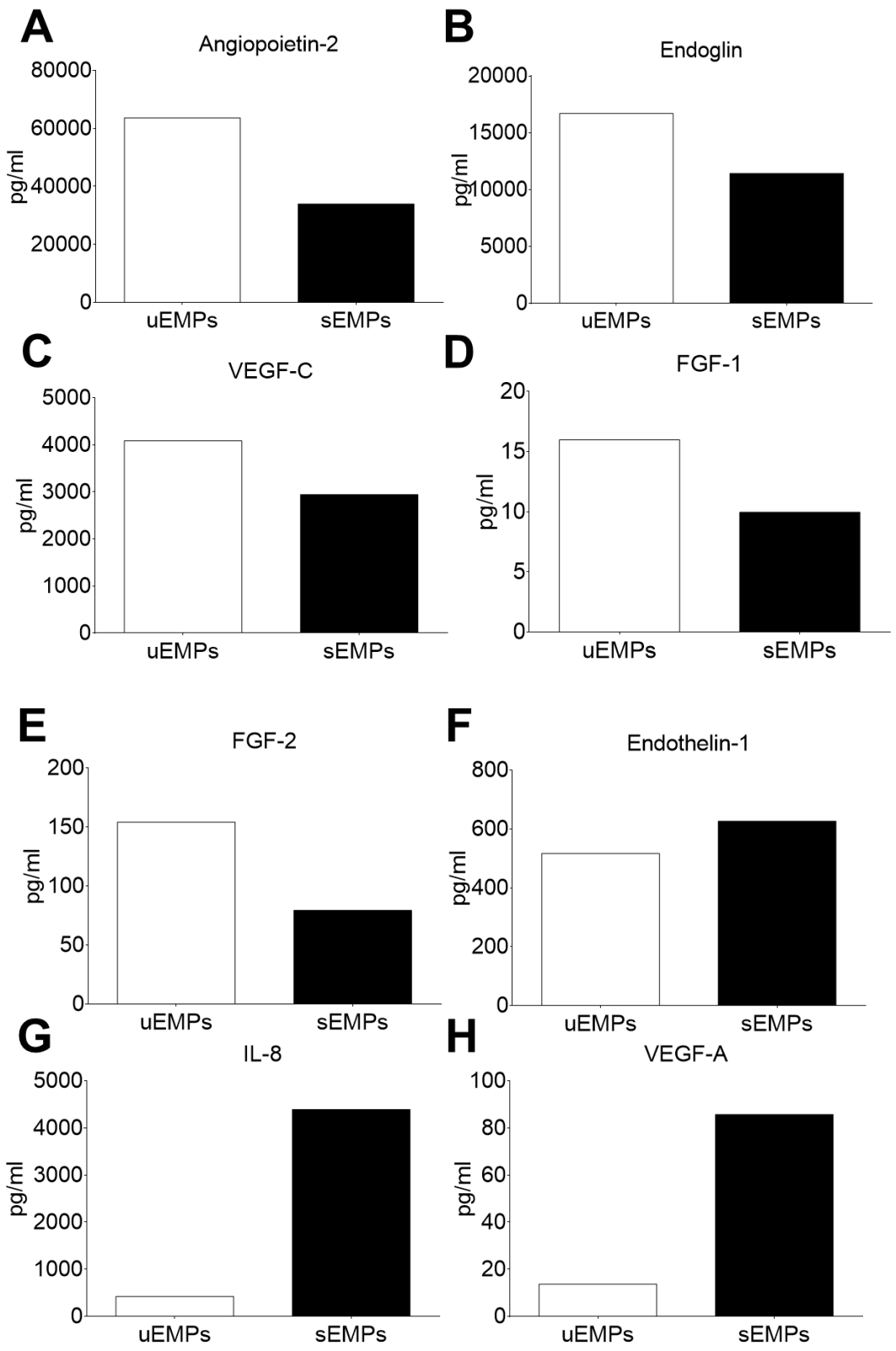

Figure 20. Angiogenic and growth factor molecules carried by uEMPs and sEMPs. Bioplex was carried out in single lysates of 10^7 uEMPs/µL of PBS and 10^7 sEMP/µL of PBS to investigate the presence of angiogenesis/growth factor molecules. A) Angipoietin-2, B) Endoglin, C) Vascular Endothelial Growth Factor-C: VEGF-C, D) Fibroblast Growth Factor-1: FGF-1, E) Fibroblast Growth Factor-2: FGF-2, F) Endothelin-1, G) Interleukin-8: IL-8, H) Vascular Endothelial Growth Factor-A: VEGF-A. n = 1.

The data from the proteomic screenings (n = 2) was pooled and UniProtKB and Gene Ontology databases were used to determine the function and location of the proteins identified in the proteomic screening of the uEMPs and sEMPs. These data confirmed that the majority of proteins carried by the EMPs are either secreted (59 %) or membrane-bound proteins (34 %), with just 7 % of proteins having their origin in the cytoplasm or the nucleus (Figure 21), strengthening the idea that EMPs act as paracrine signalling molecules or vehicles of biological information.

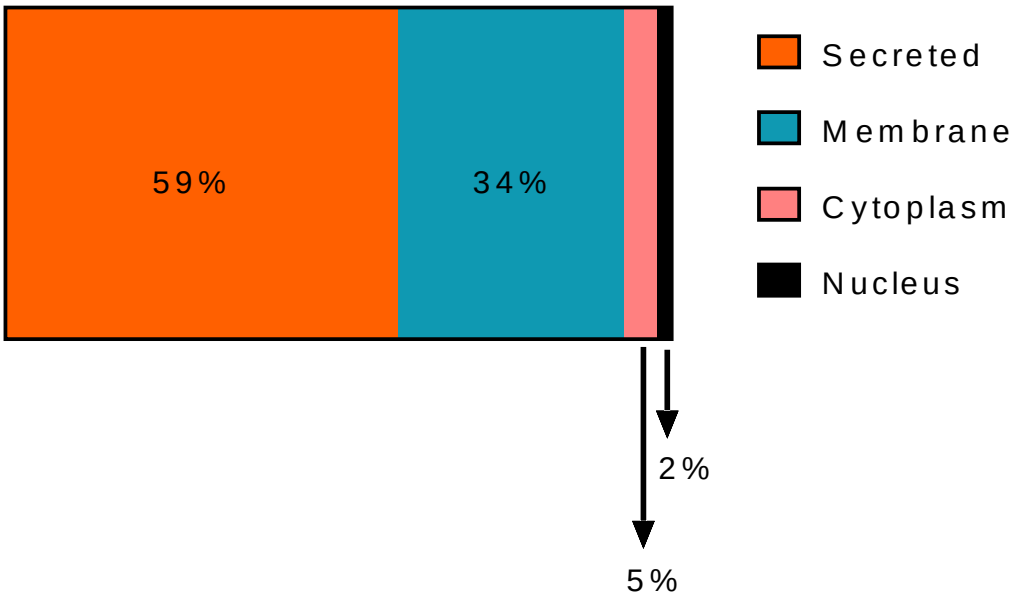

Figure 21. Proteins categorised by location using proteomic technology. uEMPs and sEMPs were lysed and sent for proteomic analysis by Olink Bioscience. Identified proteins were classified according to subcellular location using UniProtKB and Gene Ontology. % refer to the number of proteins.

3.2.1.3. sEMPs carry CCL20

Validation of the proteomic screening was performed in our laboratory using ELISA and flow cytometry. As described in 3.2.1.2, the proteomic screening found that CCL20, a protein involved in macrophage recruitment to sites of injury, was more abundant in sEMPs than uEMPs. CCL20 content in uEMPs and sEMPs was validated by ELISA and flow cytometry as described in section 2.5.1.1. CCL20 was detected in both uEMPs and sEMPs lysates by ELISA with a trend towards elevated levels in the sEMPs compared to uEMPs (~1.3 fold-change; Figure 22A). Since

CCL20 levels were close to the detection limit of the ELISA kit, further validation was carried out using an alternative method.

Flow cytometry confirmed that sEMPs carried significantly more CCL20 compared to uEMPs (~8.75 fold, $p < 0.05$). Flow cytometry analysis also demonstrated that approximately 20 % of the total sEMP population (AnnexinV$^+$ events) are CCL20$^+$, in contrast with just 2 % of the uEMP population (Figure 22B, 22C). These observations, together with the fact a CCL20 was found to correlate with EMP levels in SLE patients (personal communication, unpublished), provided a rationale for further investigation of the role of CCL20 in SLE and the function EMPs have in its signalling.

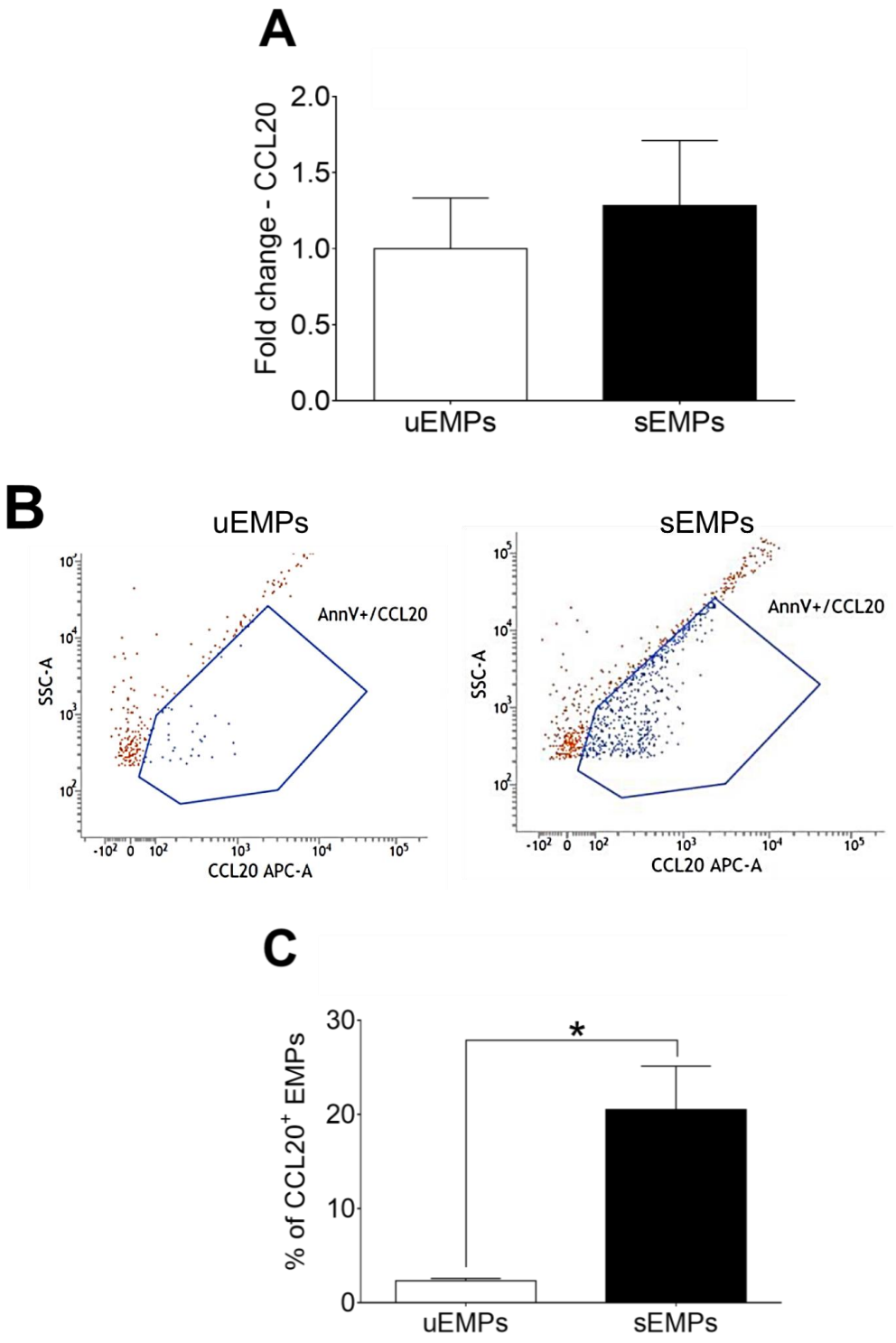

Figure 22. Validation of CCL20 in uEMPs and sEMPs. A) Protein lysates of 10^7 uEMPs/µL of PBS and 10^7 sEMPs/µL of PBS were used to validate CCL20 levels using ELISA (n = 2). B) Further validation of CCL20 content in EMPs was carried out by flow cytometry. A modified protocol for intra-cellular antibody labelling was used to investigate differences in CCL20 levels in uEMPs vs sEMPs. Two representative flow cytometry plots of AnnexinV$^+$/CCL20$^+$ events are shown. C) An unpaired t-student test was used to analyse the difference in the percentage of CCL20$^+$ in uEMPs and sEMPs. Error bars are presented as ± SEM. n = 3 (different uEMP and sEMP preparations); *p < 0.05. CCL20: chemokine (C-C motif) ligand 20.

3.2.1.4. miRNA-129-5p is elevated in uEMPs compared to sEMPs

It is now recognised that EMPs carry nucleic acids, among which microRNAs have been extensively studied as relevant effectors of microparticle function (73, 92, 149). To investigate the differences in miRNA content between uEMPs and sEMPs, total RNA was extracted, quantified and sent to Ocean Ridge Biosciences for microRNA screening; microRNA was purified from total RNA by ultrafiltration, quantified by fluorometry and subjected to Ocean Ridge Biosciences proprietary microRNA microarray analysis. Of the 300 miRNAs identified, only the 28 most abundant ones in sEMPs (compared to uEMPs) were considered for RT-qPCR validation and were investigated further in the context of endothelial function. A full list of the miRNAs validated by RT-qPCR are shown in Table 10.

miRNAs screened	Validated by RT-qPCR
hsa-miRNA-328	Yes
hsa-miRNA-595	Yes
hsa-miRNA-608	Yes
hsa-miRNA-1224-3p	Yes
hsa-miRNA-125b-5p	Yes
hsa-miRNA-129-5p	Yes
hsa-miRNA-149-3p	Yes
hsa-miRNA-185-3p	Yes
hsa-miRNA-221-3p	Yes
hsa-miRNA-222-3p	Yes
hsa-miRNA-423-3p	Yes
hsa-miRNA-423-5p	Yes
hsa-miRNA-483-3p	Yes
hsa-miRNA-532-3p	Yes
hsa-miRNA-551a	Yes
hsa-miRNA-let-7a-5p	Yes
hsa-miRNA-let-7b-5p	Yes
hsa-miRNA-1231	No
hsa-miRNA-1538	No
hsa-miRNA-1225-3p	No
hsa-miRNA-574-3p	No
hsa-miRNA-34a	No
hsa-miRNA-210-3p	No

Table 10. miRNA analysis of uEMPs and sEMPs. The most abundant miRNAs in sEMPs (compared to uEMPs) identified in the screen were shortlisted and their presence was validated using RT-qPCR. microRNA was extracted from 10^6 uEMPs or sEMPs using the Isolate II miRNA kit from Bioline, quantified using a Qubit BioAnalyzer, and only those miRNAs in which a unique amplicon was found in the dissociation curve, were considered validated.

The validated microRNAs were subjected to bioinformatic analysis using an alignment algorithm in microRNA.org, which finds potential mRNA targets for

miRNAs, and predicted that CCL20 is a target of miRNA-129-5p (mirSVR score: -0.2911; Figure 23A). miRNA-129-5p abundance in uEMPs and sEMPs was investigated by RT-qPCR and normalised to miRNA-222-3p levels, which has been shown to be a suitable single gene housekeeper miRNA, is highly expressed in endothelial cells, and was found to be similarly abundant in uEMPs and sEMPs in our proteomic screening (194, 195). Amplification plots and dissociation curves shown on Figure 23C. miRNA-129-5p was found to be significantly more abundant in uEMPs than in sEMPs (~4 fold-change; Figure 23B), suggesting that miRNA-129-5p could be partially responsible for the reduced CCL20 levels found in uEMPs in comparison to sEMPs. As a result of this observation, the role of miRNA-129-5p on CCL20 signalling was investigated further.

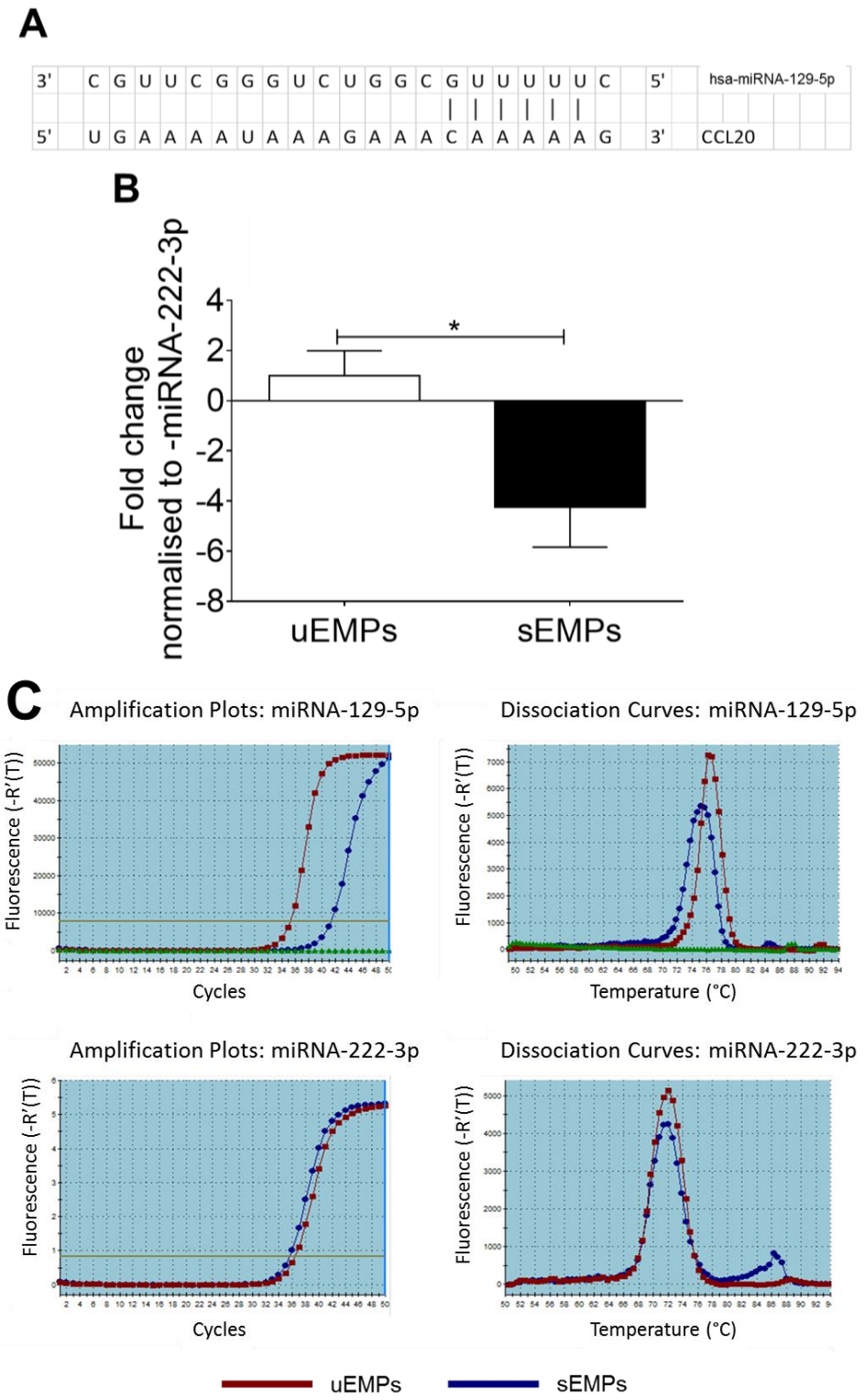

Figure 23. Bioinformatic prediction of miRNA-129-5p targets and quantification in EMPs. microRNA was extracted from 10^6 uEMPs and sEMPs using the Isolate II miRNA kit from Bioline and quantified using a Qubit BioAnalyzer. A) miRNA-129-5p and CCL20 alignment and target prediction was performed using microRNA.org and DIANA-miRpath algorithms. An unpaired t-student test was used and error bars are presented as ± SEM. n = 3; *p < 0.05. B) RT-qPCR of miRNA-129-5p (normalised to miRNA-222-3p) shows that uEMPs carry more miRNA-129-5p than sEMP. C) Amplification plots and dissociation curves of miRNA-129-5p and housekeeper miRNA-222-3p are shown, demonstrating the presence of a single amplicon.

3.2.2. uEMPs and sEMPs effects on CCL20

In order to determine the effects of uEMPs and sEMPs on TNFα-induced CCL20 expression, HUVECs were treated with uEMPs or sEMPs in combination with TNFα and analysed using RT-qPCR. Results showed that CCL20 mRNA abundance was decreased in uEMP-treated cells in comparison to TNFα-treated control and to sEMP-treated cells (~2.3 fold-change, $p < 0.005$, Figure 24), suggesting that uEMPs (but not sEMPs) can reduce TNFα-induced CCL20 expression, potentially due to a higher abundance of miRNA-129-5p; therefore, transfection experiments were performed to validate CCL20 as a target of miRNA-129-5p.

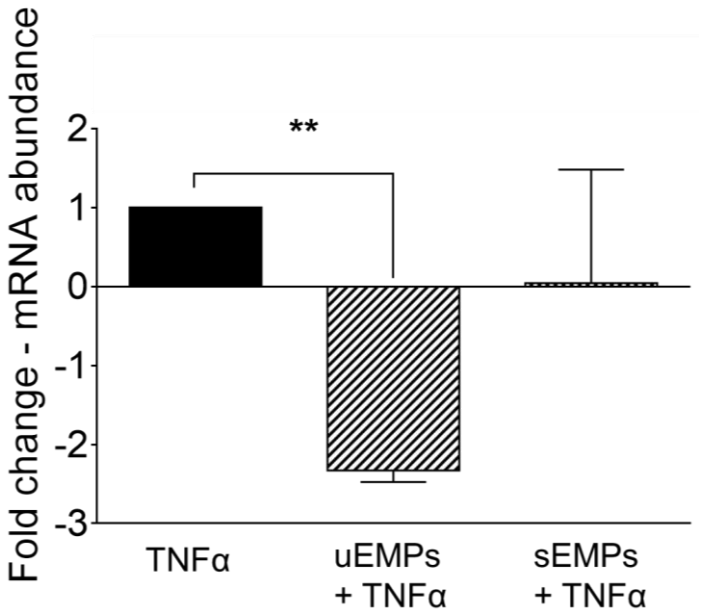

Figure 24. The effect of uEMPs and sEMPs on CCL20 mRNA abundance in the presence of TNFα. HUVECs were treated with TNFα (10 ng/mL of media) in combination with 10^6 uEMPs/mL of media or 10^6 sEMPs/mL of media for 24 hours and total RNA was isolated and analysed using RT-qPCR. Reduced CCL20 mRNA levels in uEMP treated cells compared to TNFα and sEMP-treated cells. A one-way ANOVA test with Tukey correction was used for statistical analysis. Error bars represent ± SEM. n = 3 (different uEMP and sEMP preparations); **$p < 0.005$.

3.2.2.1. miRNA-129-5p does not regulate CCL20 mRNA levels

To investigate if these effects were due to miRNA-129-5p content in uEMPs, HUVECs were transfected with miRNA-129-5p precursor or a scrambled control using an Amaxa Nucleofector® kit as described in section 2.11.3. Since miRNA-129-5p and scrambled control plasmid carry a Puromycin resistant gene, transfected cells were selected in 0.25 µg/ml of Puromycin for 4 days (Figure 25A). After selection, an apparent 50-65 % transfection efficiency was achieved (visual

observation; Figure 25B). miRNA-129-5p and scrambled control transfected cells were treated with TNFα for 24 hours (in parallel with control-transfected cells) and harvested for RT-qPCR to elucidate the effects of miRNA-129-5p on CCL20 mRNA abundance.

RT-qPCR for CCL20, which is only expressed upon TNFα activation and it is not present in untreated endothelial cells (192), showed that mRNA abundance was increased in miRNA-129-5p transfected HUVECs compared to the TNFα positive control after 24 hours (~27 fold-change, $p < 0.001$). Scrambled control transfected cells also showed increased CCL20 mRNA levels (~13.5 fold-change, $p < 0.005$) compared to the TNFα control but was still significantly lower than the miRNA-129-5p transfected cells (Figure 26). This observation could be explained as follows: i) Puromycin treatment of the cells could have caused changes in the cells, thereby affecting CCL20 regulation in the scrambled and miRNA-129-p transfected cells, and upregulating CCL20 expression during the selection process, an effect not observed in the TNFα-treated control-transfected cells as they were not exposed to Puromycin; ii) the plasmid construct is partially responsible for the observed effects and therefore the elevation in CCL20 mRNA abundance in miRNA-129-5p transfected cells cannot be attributed to the presence of the microRNA, or iii) miRNA-129-5p has a different, unknown target, that leads to increased CCL20 mRNA abundance.

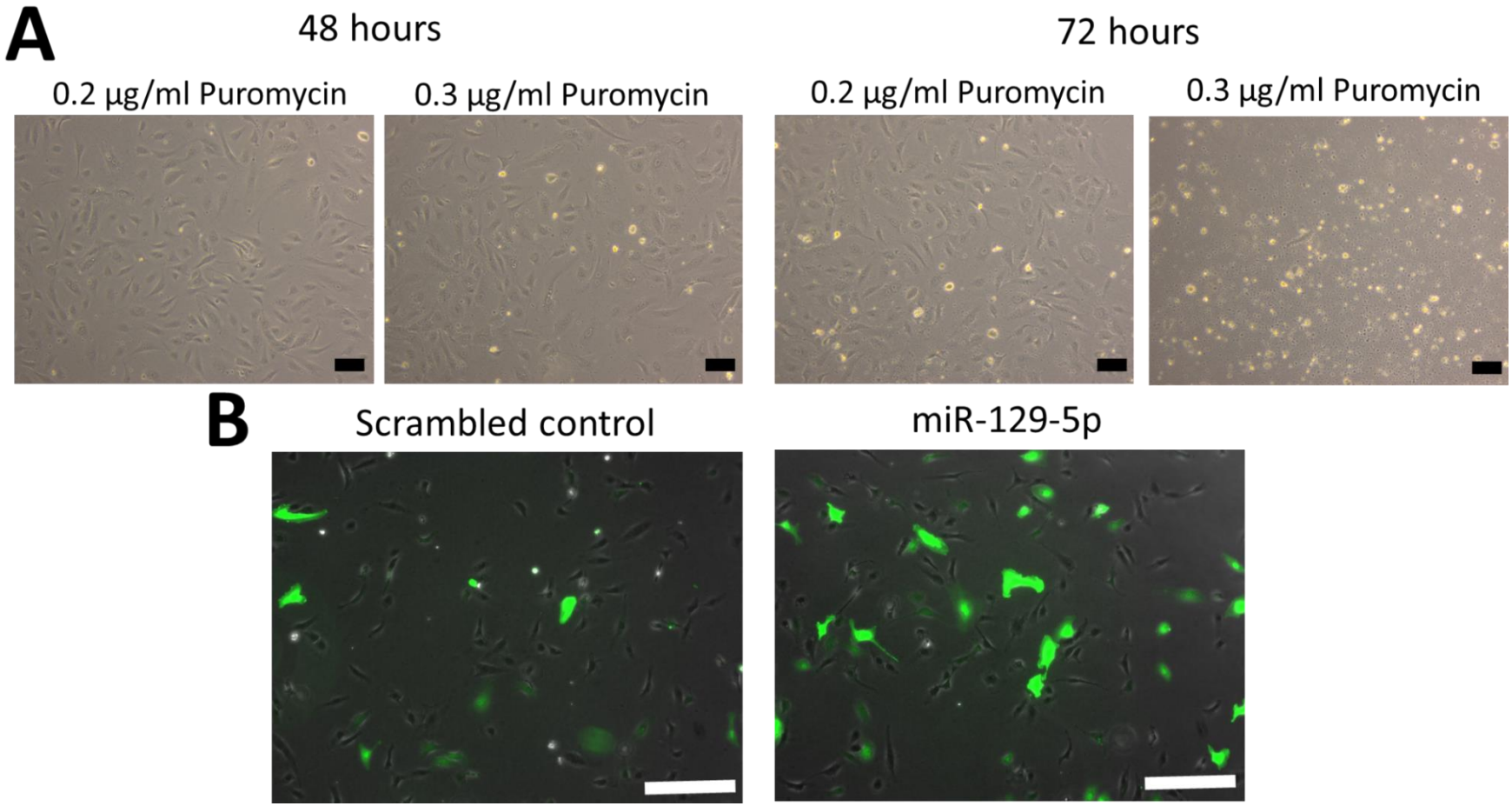

Figure 25. Transfection and selection of transfected HUVECs. HUVECs were transfected using an Amaxa Nucleofector® kit and Puromycin was used to select the transfected cells. Representative micrographs taken at 10x magnification are shown. A) Non-transfected cells were used to identify the concentration of Puromycin for the selection of the successfully transfected cells. Scale bar = 100 µM. B) Transfected HUVECs were observed under the fluorescence microscope after 72 hours of Puromycin selection. An apparent transfection efficiency of 50-65 % was achieved (visual observation). Scale bar = 100 µM.

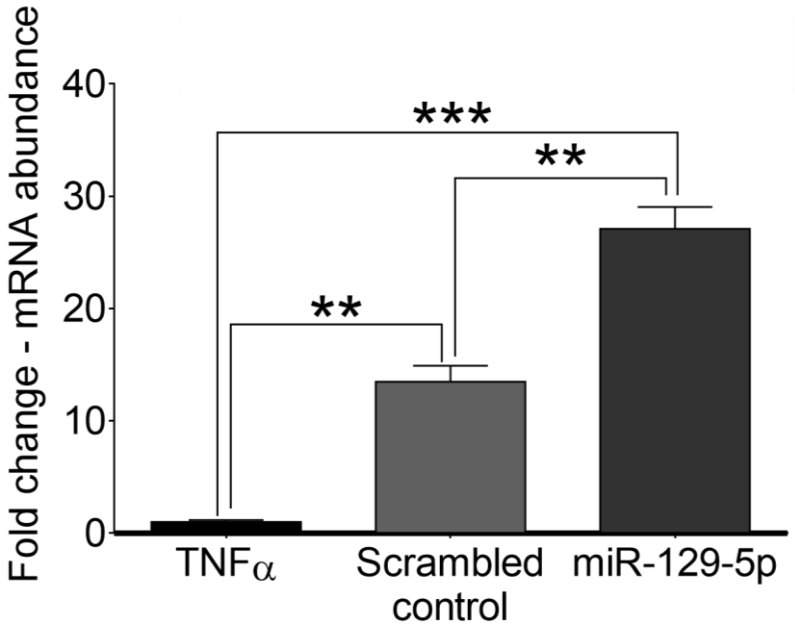

Figure 26. Abundance of CCL20 mRNA in miRNA-129-5p transfected HUVECs. RT-qPCR of TNFα-treated cells (positive control for CCL20 mRNA expression), scrambled control-transfected cells and miRNA-129-5p transfected cells showed CCL20 mRNA levels are increased in both miRNA-129-5p and scrambled control transfected cells. These results demonstrate that i) the bioinformatic prediction was not precise and that miRNA-129-5p does not target CCL20 or ii) Puromycin selection affects CCL20 expression. A one-way ANOVA test with Tukey correction was used for statistical analysis. Error bars represent ± SEM. n = 3 (independent transfections); **p < 0.005; ***p < 0.001.

3.2.3. EMP release by activated HUVECs

In order to establish whether EMPs exerted any additional effects on activated HUVECs, two populations of MPs (sEMPs or uEMPs) were used, either on their own or in combination with TNFα, to treat HUVECs for 24 hours. After treatment, EMPs were isolated as described in 2.2.3 and quantified using flow cytometry as in 2.2.4. As expected, TNFα stimulated EMP release (~1.5 fold-change, $p < 0.05$, Figure 27A) compared to untreated cells. These results are representative of the uEMP and sEMP generation process and consistently, 10^6 uEMPs and 5×10^6 sEMPs were generated per mL of media.

When cells were treated with sEMPs, a significant increase in EMP release compared to untreated or uEMP-treated cells was detected (~1.5 fold-change, $p < 0.001$, Figure 27B). Furthermore, uEMP treatment in the presence of TNFα significantly reduced EMP release ($p < 0.05$) compared to sEMPs, to almost untreated levels Figure 27C). These results suggest that EMPs play a role in

regulating EMP release, but their role depends on their mode of generation: uEMPs are protective against TNFα-driven EMP release, whereas sEMPs enhance EMP release, thus contributing to the elevated circulating EMP levels found in inflammatory diseases.

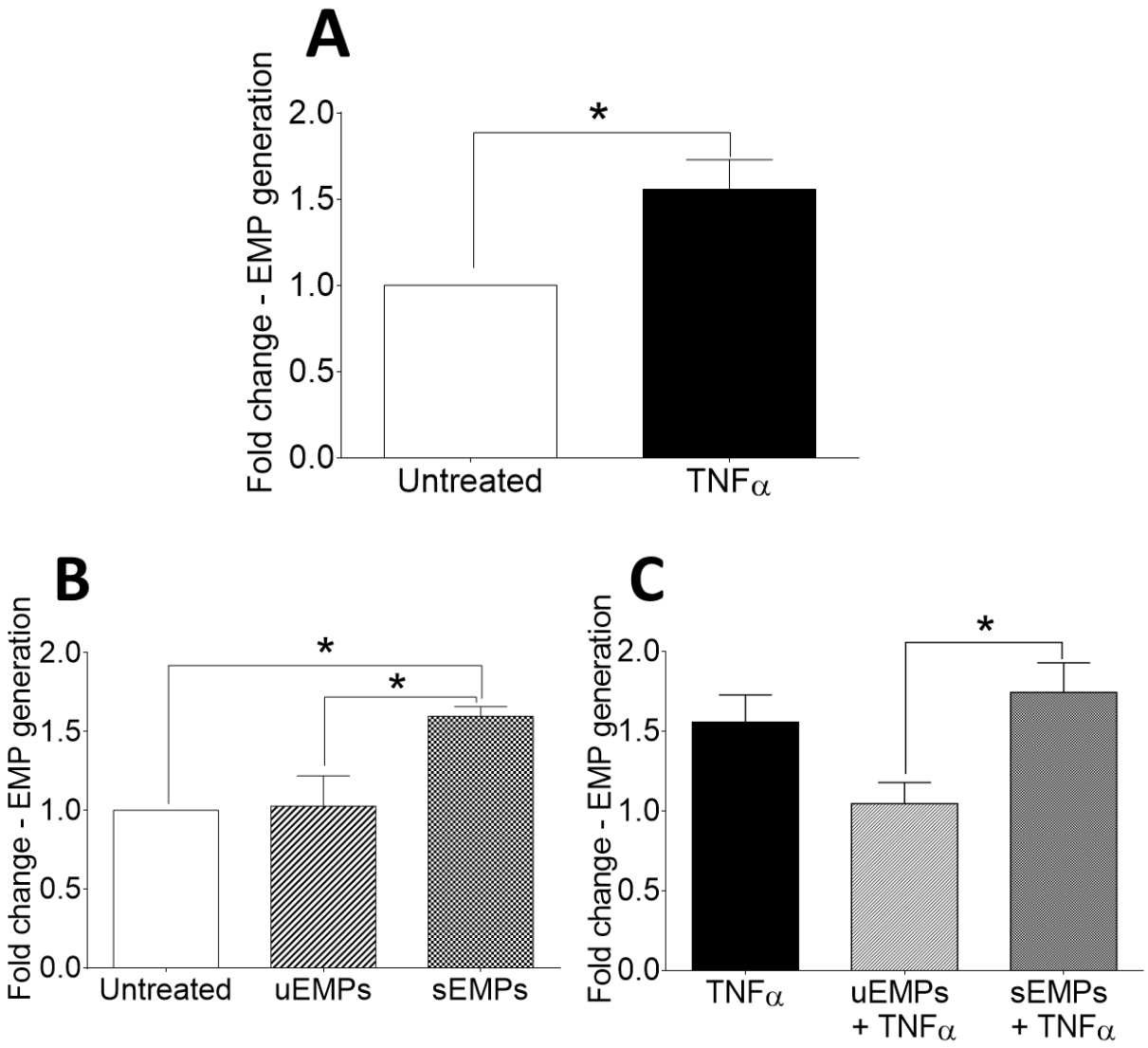

Figure 27. The effects of uEMPs and sEMPs on EMP generation under homeostatic and pro-inflammatory conditions. HUVECs were cultured in T25 flasks and treated with 10^6 uEMPs or 10^6 sEMPs/mL of media in the presence or absence of TNFα for 24 hours. Conditioned media was collected and EMPs were quantified by flow cytometry. A) Conditioned media from untreated and TNFα-treated cells after 24 hours was collected for EMP isolation and quantification. An unpaired student t-test was performed. B) EMPs were isolated and quantified from conditioned media from untreated, uEMP-treated and sEMP-treated cells. C) HUVECs were treated with TNFα in combination with uEMPs or sEMPs for 24 hours prior to EMP isolation and quantification. A one-way ANOVA test with Tukey correction was used for statistical analysis. (B, C) was used to determine differences. Error bars represent ± SEM. n = 3 independent experiments (three different populations of HUVECs and uEMP/sEMP preparations); *$p < 0.05$.

3.2.4. uEMPs and sEMPs enhance cell migration (wound healing assay)

Cell migration is a key process in endothelial homeostasis and vascular damage. To establish whether EMPs had any differential effects on migration, uEMPs and sEMPs were used alone or in combination with TNFα to treat HUVECs for 6 hours in a scratch assay, as described in section 2.8.2.1. Representative micrographs at 0 and 6 hours are shown in Figure 28A and cell migration was quantified using ImageJ (Figure 28B). TNFα enhanced cell migration significantly compared to untreated control cells (~1.8 fold-change, $p < 0.05$); uEMP- and sEMP-treated cells both showed an increased migration capacity compared to untreated cells and to a similar level as TNFα treatment (~1.5 and ~1.6 fold-change respectively, $p < 0.005$). However, TNFα treatment in combination with either uEMPs or sEMPs showed no significant increase in endothelial cell migration when compared to uEMP or sEMP treatment only, which differs from the effects detected on EMP release.

To ensure that the results observed were due to cell migration and not enhanced cell growth, proliferation was measured using a kit based on the MTT assay principle (Figure 28C). No statistically significant differences were found between uEMP- and sEMP-treated groups compared to untreated or TNFα-treated cells, suggesting that the reported effects are due to endothelial cell migration and not proliferation.

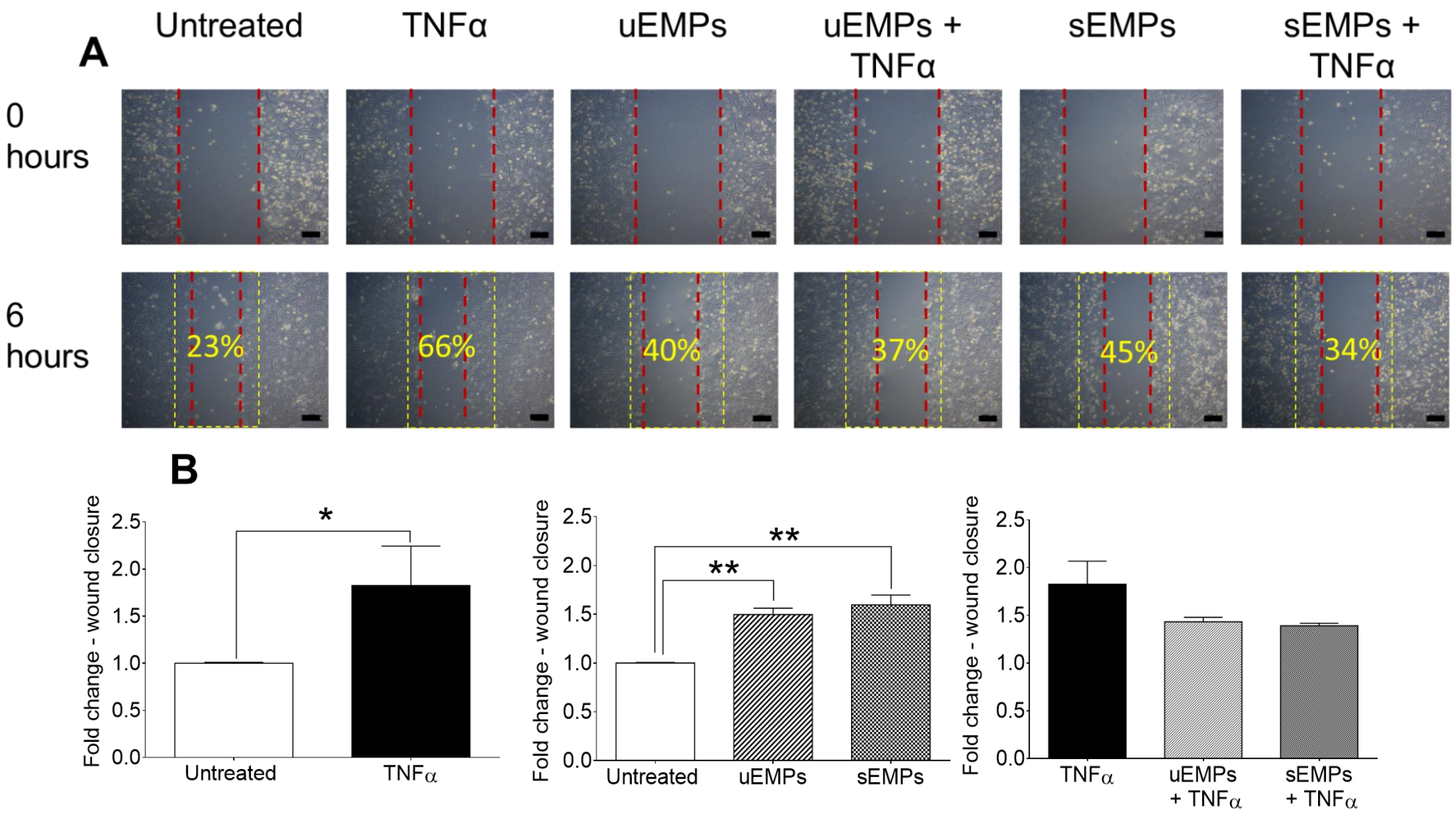
A
Untreated
TNFα
uEMPs
uEMPs + TNFα
sEMPs
sEMPs + TNFα
0 hours
6 hours
23%
66%
40%
37%
45%
34%
B
Fold change - wound closure
2.5
2.0
1.5
1.0
0.5
0.0
*
Untreated
TNFα
**
**
Untreated
uEMPs
sEMPs
TNFα
uEMPs + TNFα
sEMPs + TNFα

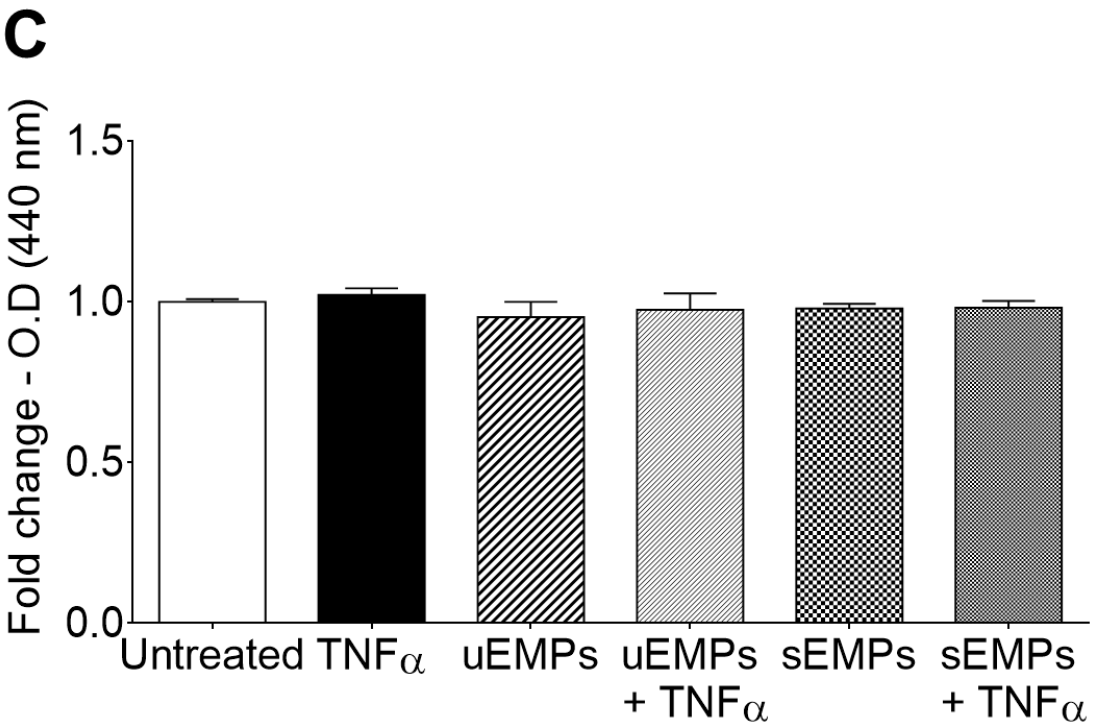

Figure 28. The effects of uEMPs and sEMPs on endothelial cell migration. HUVECs were cultured in 6-well plates and a scratch assay was performed. Cells were treated with TNFα, uEMPs or sEMPs (10^6 EMPs/ml), or in combination with TNFα. Images were taken at 0 and 6 hours. A) Representative images taken at 10x magnification at 0 and 6 hours. The red dotted line represents the wounded area, while the yellow dotted box represents the original wounded area. Percentage of wound closure is shown in yellow text (average of 3 independent experiments). Scale bar = 100 µm. B) Quantification of wound closure after 6 hours: both uEMPs and sEMPs enhance cell migration. An unpaired student t-test and one-way ANOVA test with Tukey correction were used for statistical analysis. Error bars represent ± SEM. n = 3; *$p < 0.05$, **$p < 0.005$. C) 2.5 x 10^3 cells/cm^2 were seeded in 96-well plates and proliferation assays at 6 hours confirmed that EMPs did not affect cell proliferation. All treated groups were normalised to untreated samples. Statistical analysis using a one-way ANOVA test with Tukey correction did not identify significant differences.

3.2.5. Gene expression and protein analysis in uEMP and sEMP-treated HUVECs versus untreated cells

The results show that EMPs enhance endothelial cell migration, which is often regulated by the expression adhesion molecules. It is well established that activated endothelial cells show an increase in adhesion molecule expression, therefore, the levels of VCAM or ICAM and associated pathways was investigated in cells treated with EMPs in the presence or absence of TNFα.

HUVECs were treated with uEMP and sEMP in with the presence or absence of TNFα for 24 hours and the RNA harvested for RT-qPCR analysis. As shown in the

literature, TNFα increased VCAM-1 and ICAM-1 mRNA abundance by ~2 fold and ~3 fold respectively compared to untreated cells (Figure 29A, 29D; $p < 0.0001$). Of note, the uEMPs increased VCAM-1 and ICAM-1 mRNA abundance by ~3 and ~4 fold respectively (Figure 29B, 29E; $p < 0.0001$) and sEMPs also increased mRNA abundance of VCAM-1 and ICAM-1 by 4.5 fold (Figure 29B, 29E; $p < 0.0001$). The sEMP treatment increased mRNA abundance of VCAM-1 and ICAM-1 significantly more than uEMPs (Figure 29B, 29E; $p < 0.001$ and $p < 0.05$ respectively). In addition, uEMP treatment in combination with TNFα, increased mRNA abundance of VCAM-1 and ICAM-1 by 2 fold compared to TNFα treated cells (Figure 29C, 29F; $p < 0.0001$). Finally, increased VCAM-1 (but not ICAM-1) mRNA levels were found in TNFα plus sEMP-treated cells (Figure 29C, 29F; $p < 0.0001$).

VCAM-1 and ICAM-1 are adhesion proteins present in the cell membrane of activated endothelial cells. In order to determine whether the changes in mRNA expression are also reflected at the protein level, western blot analysis of the membrane and cytoplasmic fraction of HUVECs treated with either uEMPs or sEMPs was performed. VCAM-1 and ICAM-1 were detected in HUVECs treated with TNFα. While there was no evidence of VCAM-1 or ICAM-1 protein in uEMPs nor sEMP-treated HUVECs, strong signals were found for both proteins in TNFα plus uEMP or sEMP-treated cells. This observation suggests that uEMPs nor sEMPs increase VCAM-1 nor ICAM-1 protein levels, as the proteins were only found in cells treated with TNFα, regardless of the presence of uEMPs or sEMPs. Alpha-tubulin was used as a loading control and showed equal loading in all lanes (Figure 30).

These results show that EMPs modulate the mRNA abundance of VCAM-1 and ICAM-1, but do not increase their protein levels, suggesting they may not have an effect on endothelial cell activation *per se* (although it is possible that they affect the expression of other adhesion molecules). Cell migration and activation often occur together, and given that EMPs enhance migration but not activation, such effect is potentially indirect. The inflammatory pathway NFκB regulates key cell aspects such as migration, proliferation and activation and as such, the next section will investigate whether uEMPs and sEMPs mediate their effects via this pathway.

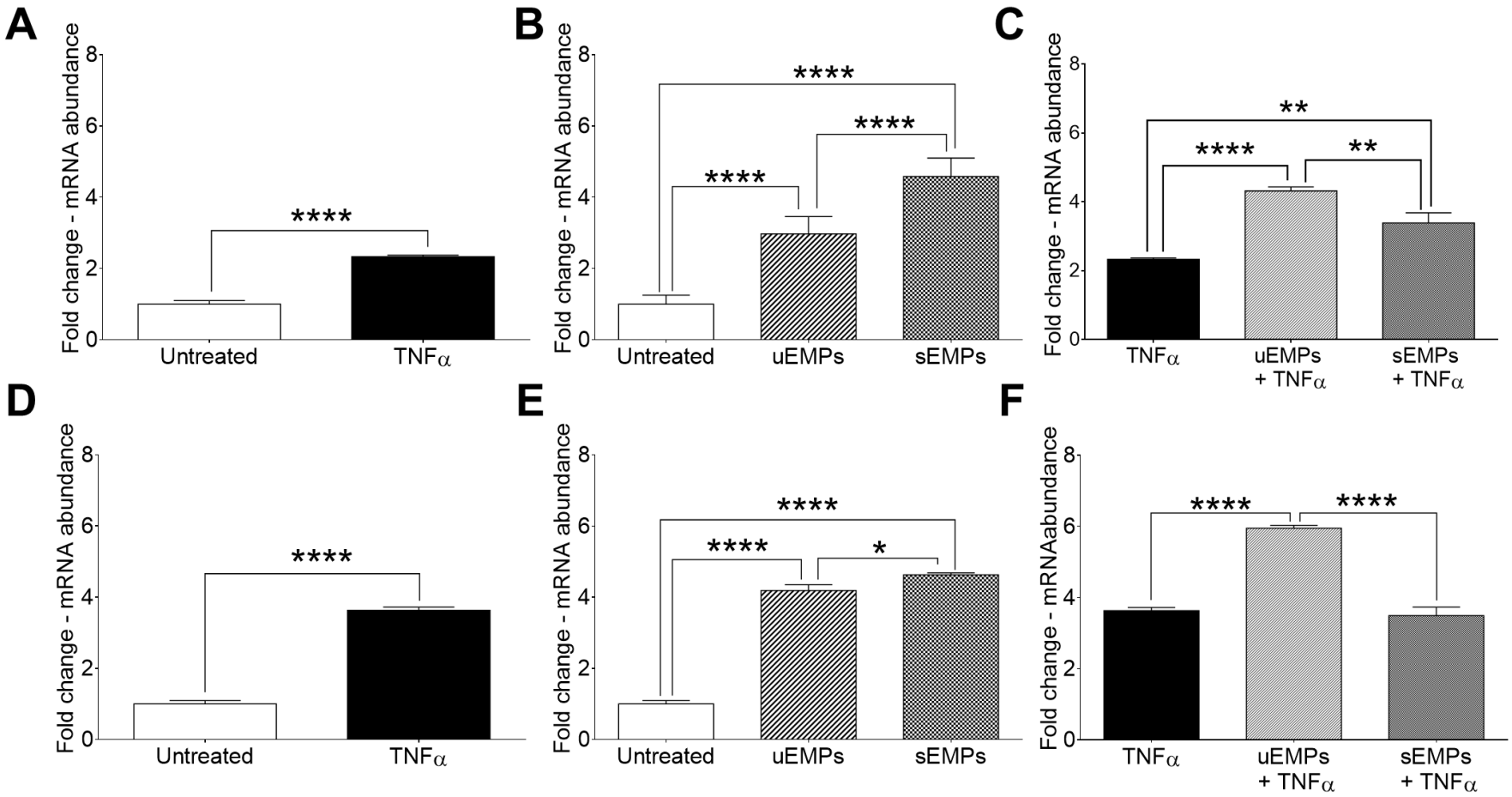

Figure 29. The effect of EMPs on mRNA abundance of adhesion molecules ICAM-1 and VCAM-1. HUVECs were seeded in 6-well plates (5×10^3 cells/cm^2) and treated with 10^6 uEMPs/mL of media or 10^6 sEMPs/mL of media for 24 hours prior to RNA isolation for RT-qPCR. A, D) TNFα increases VCAM-1 and ICAM-1 mRNA abundance. B, E) uEMPs and sEMPs increase mRNA abundance of VCAM-1 and ICAM-1. C, F) uEMPs, in combination with TNFα, increase VCAM-1 and ICAM-1 mRNA abundance. Unpaired student t-test (A, D) and one-way ANOVA with Tukey correction for multiple comparison (B, C, E, F) were used. Error bars represent ± SEM. n = 6 independent experiments; *$p < 0.05$, **$p < 0.005$, ****$p < 0.0001$.

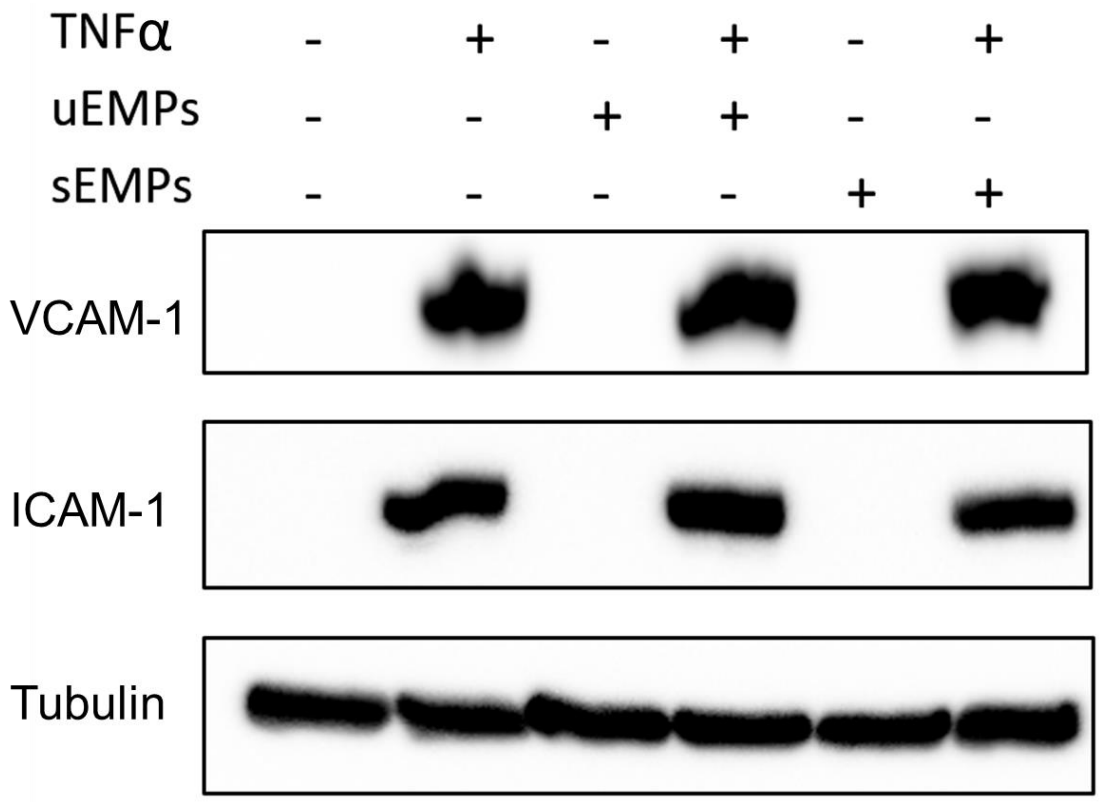

Figure 30. The effect of EMPs on VCAM-1 and ICAM-1 protein levels. HUVECs were seeded in 25 cm^2 flasks (5 x 10^3 cells/cm^2) and treated with 10^6 uEMPs/mL or 10^6 sEMPs/mL of media for 24 hours prior to protein extraction for western blotting. 20 µg of total protein was loaded per lane. A representative blot of both the membrane and cytoplasmic fraction is shown. VCAM-1 and ICAM-1 were only detected in the TNFα-treated samples, but not in the samples treated with uEMPs or sEMPs only. n = 3 independent experiments.

3.2.6. sEMPs, but not uEMPs, activate the NFκB pathway

NFκB is a key regulator of inflammation and endothelial cell function. Upon activation by TNFα, NFκB translocates from the cytoplasm to the nucleus where it acts as a transcription factor for many genes regulating cell survival and proliferation. Given the important role the NFκB pathway plays in inflammation, NFκB (p65 subunit) translocation to the nucleus was investigated in uEMP and sEMP-treated HUVECs after 30 minutes (Figure 31) and 16 hours (Figure 32) using immunofluorescence, with TNFα as the positive control (translocation is presented in turquoise colour; Figures 31B and 32B). sEMPs were shown to activate NFκB translocation at both time points investigated, at 30 minutes and 16 hours (Figures 31E and 32E), whereas uEMPs did not (Figures 31C and 32C). NFκB translocation was observed in cells treated with TNFα at either 30 minutes or 16 hours and regardless of the EMP treatment (Figures 31D, 31F and 32D, 32F).

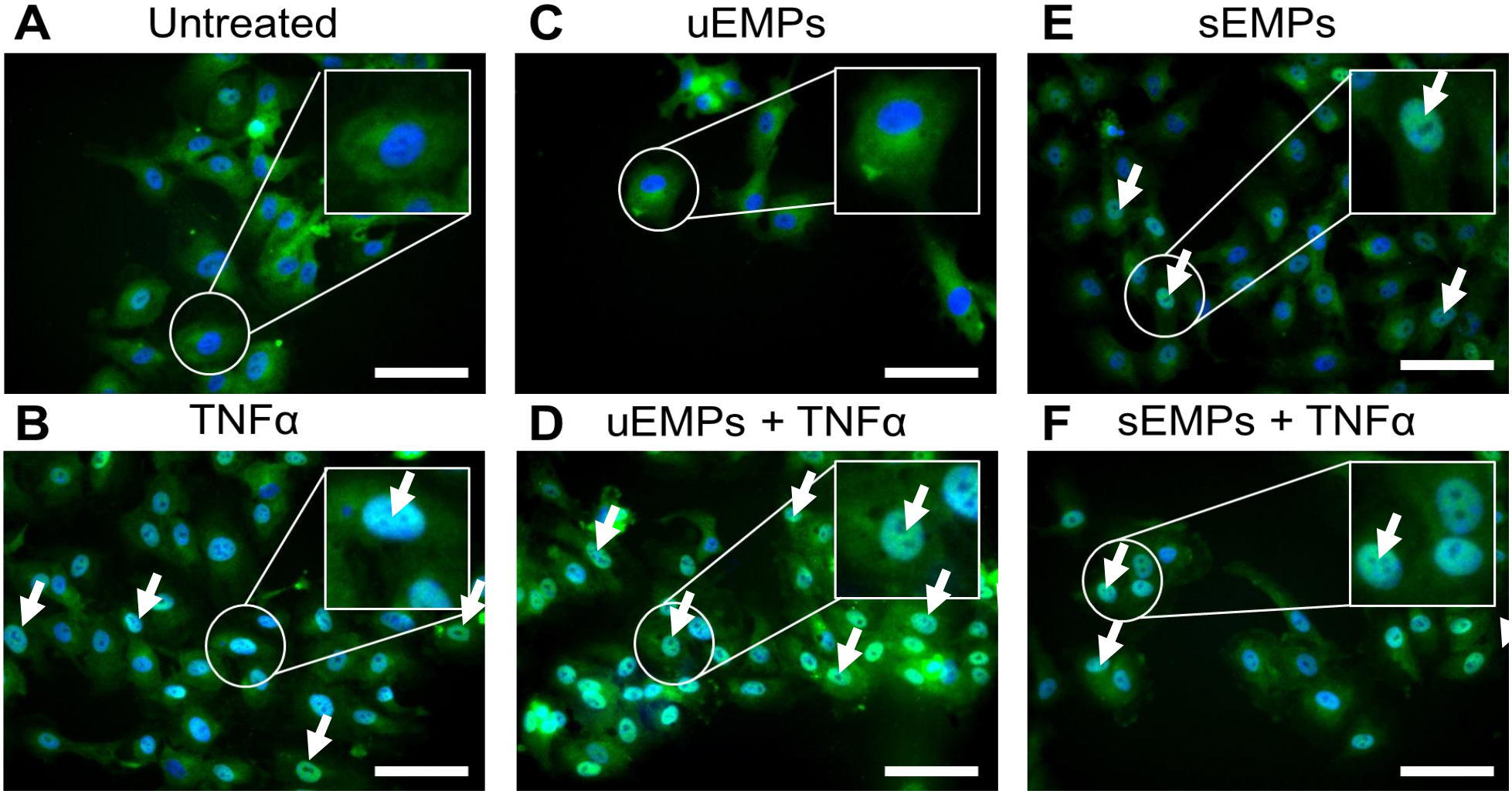

Figure 31. The effect of sEMPs on NFκB activity after 30 minutes. Representative immunofluorescence micrographs taken at 20x magnification of HUVECs treated with TNFα and uEMPs or sEMPs for 30 minutes and stained for NFκB (green) and DAPI (blue nuclei). NFκB translocation presents as turquoise colour. A) Untreated cells, B) TNFα-treated cells, C) uEMP-treated cells, D) uEMPs and TNFα-treated cells, E) sEMPs-treated cells, F) sEMPs and TNFα-treated cells. White boxes are inset zooms of the indicated area. Arrows indicate NFκB nuclear translocation. Scale bar = 25 μM. n = 3.

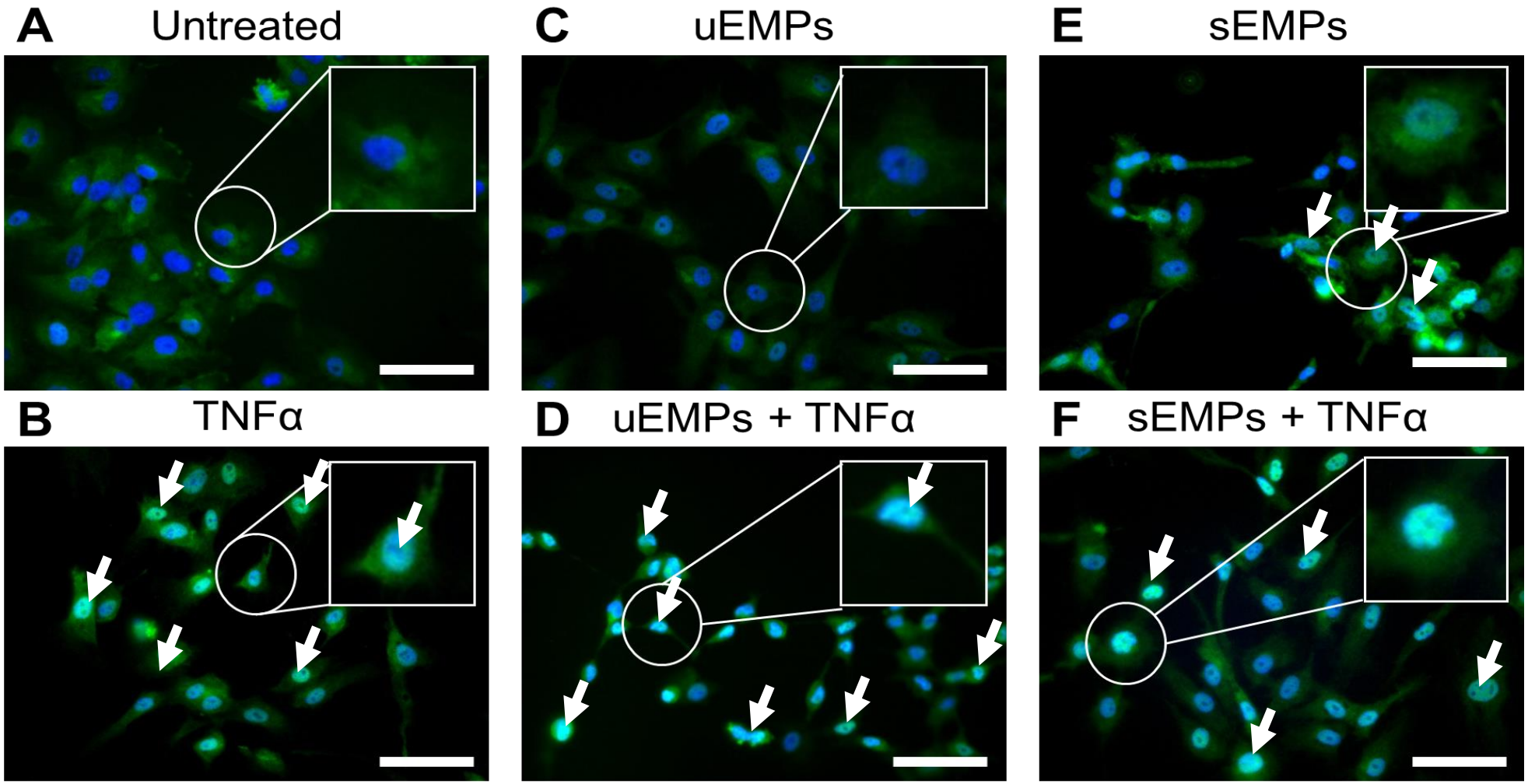

Figure 32. The effect of sEMPs on NFκB activity after 16 hours. Representative immunofluorescence micrographs taken at 20x magnification of HUVECs treated with TNFα and uEMPs or sEMPs for 16 hours and stained for NFκB (green) and DAPI (blue nuclei). NFκB translocation presents as turquoise colour. A) Untreated cells, B) TNFα-treated cells, C) uEMP-treated cells, D) uEMPs and TNFα-treated cells, E) sEMPs-treated cells, F) sEMPs and TNFα-treated cells. White boxes are inset zooms of the indicated area. Arrows indicate NFκB nuclear translocation. Scale bar = 25 μM. n = 3.

Upon activation, NFκB protein levels in the nucleus will increase in those cases where translocation occurred, therefore, a cell fractionation assay was carried out in order to confirm NFκB protein levels in the nuclear fraction of uEMP and sEMP-treated HUVECs (Figure 33). An elevated content of NFκB was detected in TNFα-treated cells (positive control; ~6 fold-change). Nuclear NFκB levels were higher in the sEMP-treated cells than in the untreated or uEMP-treated cells (~2.5 fold-change, Figure 33B). Although in low abundance, some NFκB was found also in the untreated or uEMP-treated cells, possibly due to cytoplasmic fraction contamination. NFκB nuclear levels in uEMP or sEMP-treated cells in combination with TNFα were lower than in the TNFα treatment only (~3 fold-change, Figure 33B).

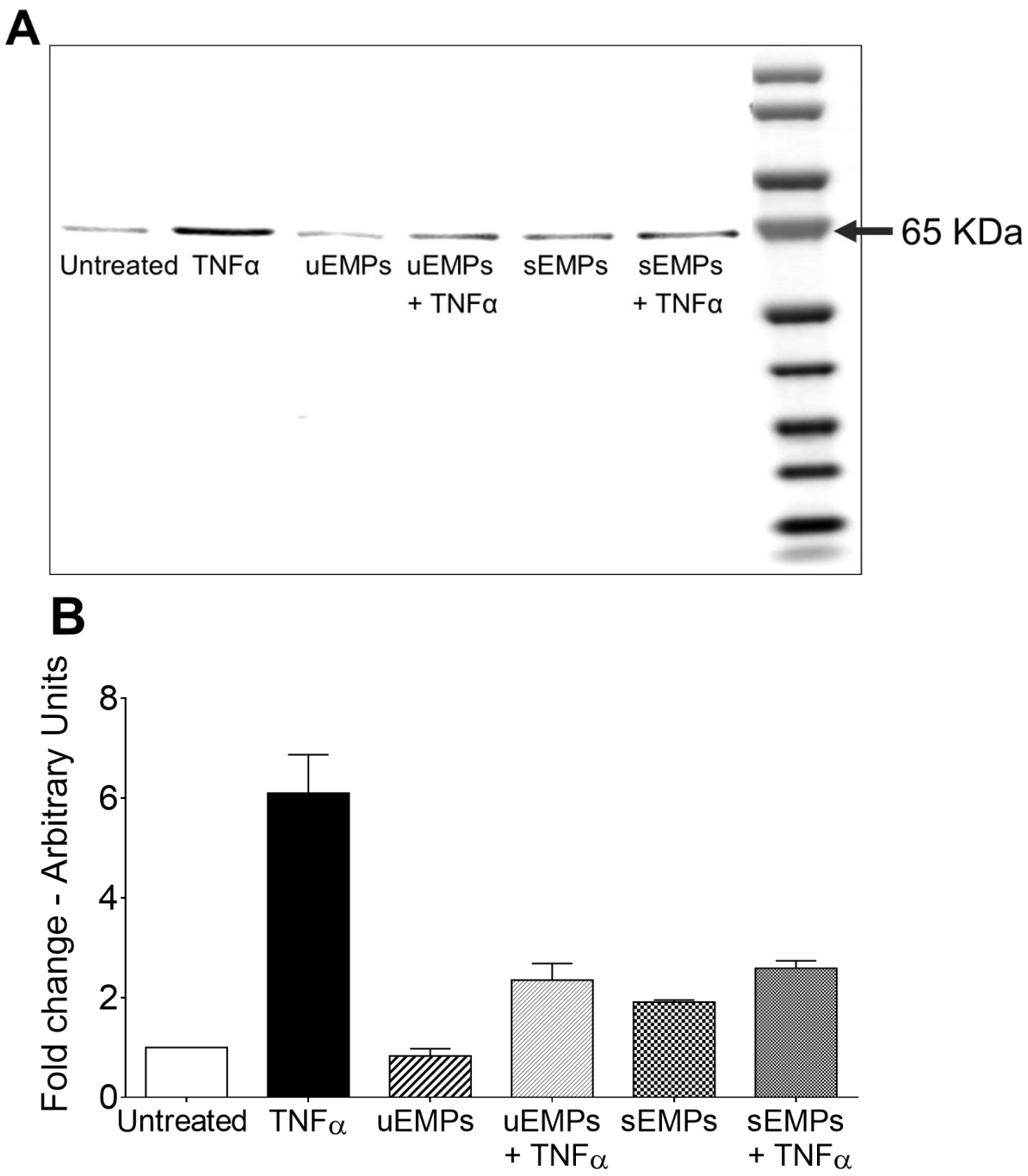

Figure 33. Quantification of NFκB protein translocation to the nucleus following HUVEC treatment of uEMPs and sEMPs. HUVECs were seeded in 25 cm^2 flasks (5 x 10^3 cells/cm^2) and treated with 10^6 uEMPs/mL or 10^6 sEMPs/mL of media for 24 hours prior to protein extraction for western blotting. A) A representative blot of the nuclear fraction is shown (20 µg of total protein was loaded/lane). B) Densitometry analysis using ImageJ revealed that NFκB protein levels were elevated in the TNFα and in the sEMP-treated samples compared to the untreated cells. Error bars represent ± SEM. n = 2 independent experiments.

To further validate these observations, RT-qPCR was used to measure mRNA abundance of IκB, a key adapter protein and a transcript of NFκB (Figure 34). As expected, IκB mRNA abundance was increased in TNFα-treated cells (positive control, ~1.5 fold-change, Figure 34A). An increase in IκB mRNA abundance was also found in sEMP-treated (~2 fold-change, Figure 34B), but not in uEMP-treated cells, supporting the immunofluorescence observations that NFκB is only activated by sEMPs (Figure 34B). No statistically significant differences in IκB mRNA abundance were found between TNFα, uEMPs or sEMPs plus TNFα treated-cells (Figure 34C).

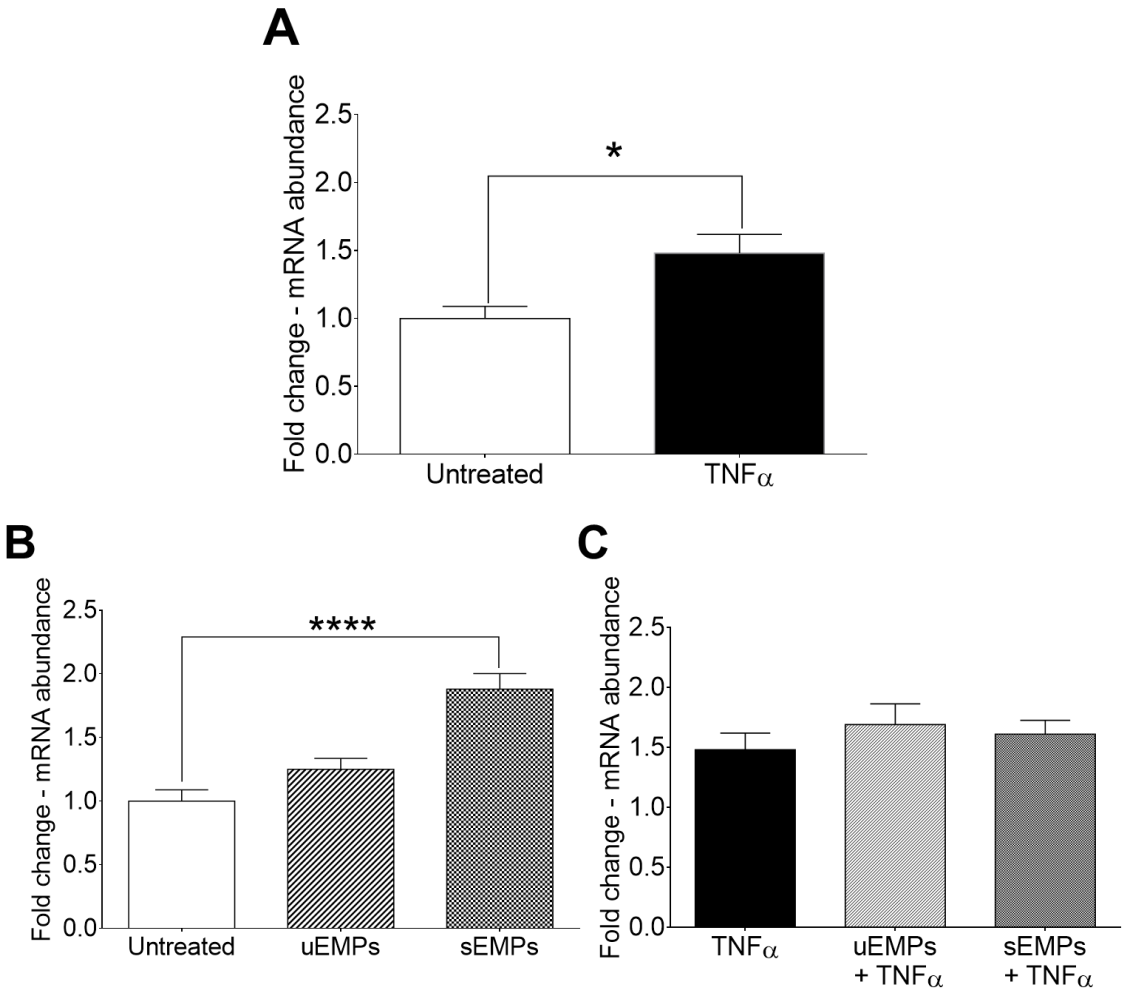

Figure 34. IκB mRNA abundance in uEMPs and sEMPs-treated HUVECs. HUVECs were seeded in 6 well plates (5 x 10^3 cells/cm^2) and treated with 10^6 uEMPs/mL or 10^6 sEMPs/mL of media for 24 hours prior to RNA isolation for RT-qPCR. A) IκB mRNA abundance was increased in TNFα-treated cells compared to untreated cells. B) sEMPs increased IκB mRNA abundance, whereas uEMPs did not. C) IκB mRNA levels were unaffected by either uEMP or sEMP-treatments in combination with TNFα compared to TNFα-treated cells. Unpaired student t-test (A) and one-way ANOVA test with Tukey correction (B, C) were used for statistical analysis. Error bars represent ± SEM. n = 6 independent experiments; *$p < 0.05$, ****$p < 0.0001$.

3.3. Key findings

The key findings of the experiments described in this chapter are:

1. This study is the first one to describe that CCL20 and miRNA-129-5p are carried by both healthy and disease-like EMPs and that their abundance depends on their mode of generation.
2. Although miRNA-129-5p is more abundant in uEMPs than sEMPs, it does not appear to target CCL20 mRNA and therefore it is unlikely to be responsible for reduced CCL20 mRNA levels in uEMP-treated ECs.
3. uEMPs and sEMPs appear to be phenotypically different; uEMPs being rounder and smaller than sEMPs, which appear to have a more spreading phenotype, possibly reflecting more adhesive properties.
4. EMPs generated with different stimuli play distinct roles in EC function:
    i. sEMPs enhance EMP release vs uEMPs,
    ii. uEMPs attenuate TNFα-driven EMP generation.
5. EMPs have common roles to play in endothelial function:
    i. Both uEMPs and sEMPs enhance EC migration,
    ii. uEMPs and sEMPs increase VCAM-1 and ICAM-1 mRNA abundance of targets cells, but not at the protein level.
6. Immunofluorescence, western blot and IκB RT-qPCR results demonstrate that sEMPs activate the NFκB pathway whereas uEMPs do not, reinforcing the idea that sEMPs and uEMPs work via different pathways under different circumstances.

3.4. Summary

We have established that EMPs released from cells under different conditions have distinct CCL20 and microRNA content and functional effects on cells; that EMPs are more highly released in activated endothelial cells compared to healthy cells and finally that EMPs have potential to exacerbate damage under disease conditions. Since EC damage also contributes to smooth muscle cell function, in particular facilitating vascular remodelling (196, 197), we hypothesised that EMPs could also have an effect on SMC function, therefore we questioned whether EMPs may ultimately affect SMC osteogenic differentiation. The series of experiments described in the next chapter aimed to shed light on the complex regulation of cell fate in the development of vascular calcification *in vitro*.

CHAPTER 4:
THE EFFECTS OF AoEMPs IN CALCIFICATION OF VASCULAR SMOOTH MUSCLE CELLS

CHAPTER 4: THE EFFECTS OF AoEMPs IN CALCIFICATION OF VASCULAR SMOOTH MUSCLE CELLS

4.1. EMPs as active regulators of vascular calcification

As previously described in our laboratory and reviewed by others (198, 199), aortic vascular calcification is a relevant clinical problem in SLE and it is considered to be an independent predictor of CVD. Previous research in our laboratory has shown that EMP levels are increased in SLE patients (33); therefore, it is possible that they play a role not only in endothelial dysfunction but also in vascular calcification (188). The mechanisms for the phenotypic reprogramming of VSMCs into osteoblast-like cells is only partly understood, thus it was of interest to determine whether they may play a role in aortic and coronary calcification via their molecular content.

The aim of the next series of experiments was to investigate the effects of EMPs on the osteogenic differentiation of vascular SMCs and to determine their mode of action. In order to achieve this aim, the following 3 objectives were addressed:

1. To determine whether AoEMP treatment of HCoASMCs enhances vascular calcification compared to untreated cells grown in osteogenic conditions using Alizarin Red S staining and calcium deposition assays.
2. To elucidate the content of AoEMPs (proteins, microRNAs and Ca^{2+}) using bioplex suspension arrays, ELISAs and RT-qPCR, in order to identify relevant molecules and pathways involved in vascular calcification.
3. To identify novel molecular components of AoEMPs using a microRNA and proteomic analyses and their effects on osteogenic differentiation, using transfection approaches.

4.2. Results

4.2.1. Calcein-AM-labelled AoEMPs are taken up by HCoASMCs

AoEMPs generated from serum-starved + TNFα-stimulated HAoECs were stained with 10 µM Calcein-AM and used to treat HCoASMCs to investigate their uptake. HCoASMCs were cultured in osteogenic media for 24 hours for pre-conditioning in order to avoid Calcein-AM uptake due to a sudden change of media. Fluorescent microscopy images were captured after 3, 6 and 24 hours of treatment with 10^6/mL Calcein-AM-labelled AoEMPs to visualise uptake (Figure 35A), which was quantified by measuring mean fluorescence intensity using ImageJ (Figure 35B). The results showed that the AoEMP internalisation was significantly increased ($p < 0.0001$) after 24 hours, suggesting that AoEMPs are taken up in a time dependant manner.

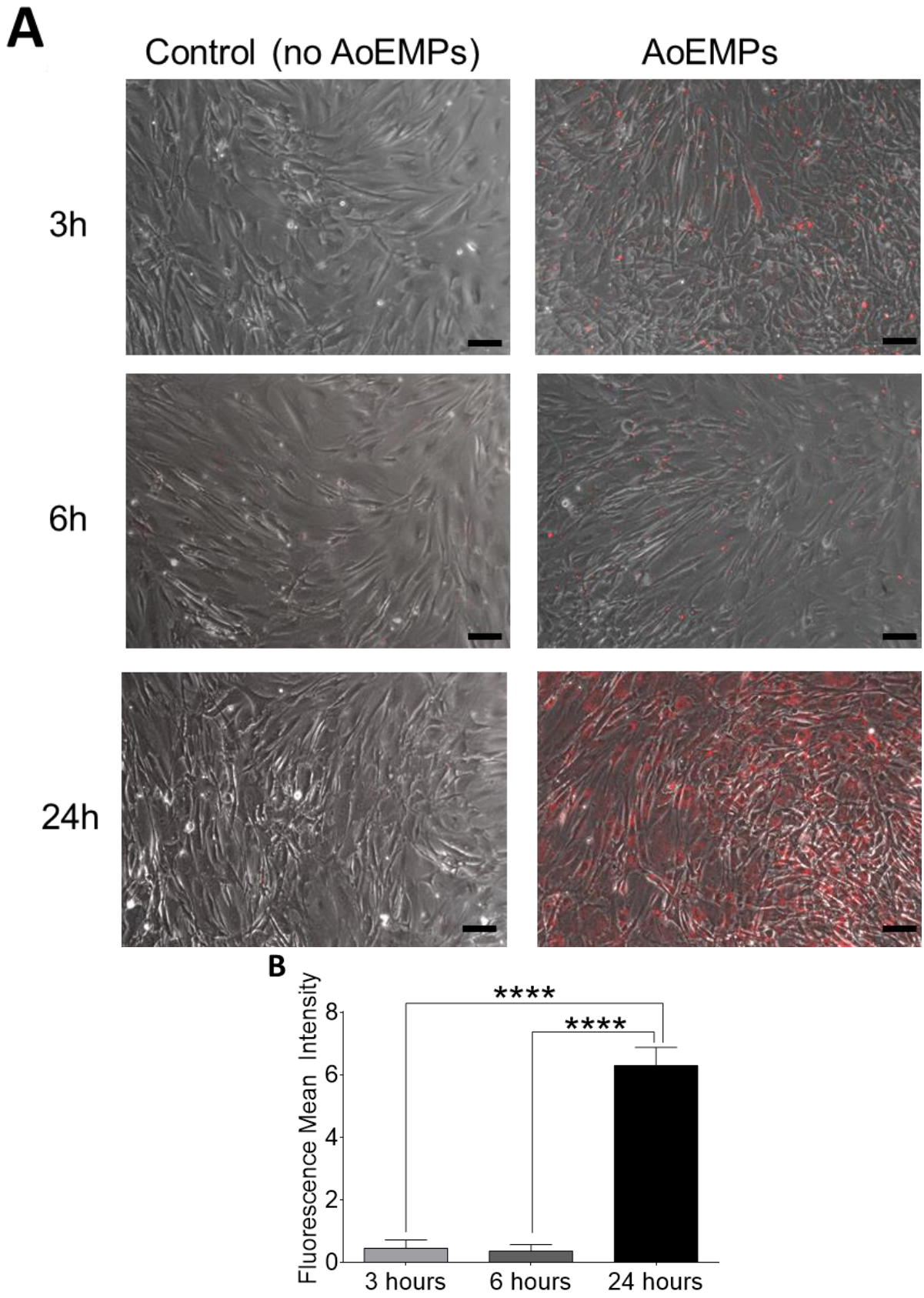

Figure 35. Internalisation of Calcein-AM-labelled AoEMPs by HCoASMCs. A) Representative micrographs taken at x10 magnification of HCoASMCs treated with 10^6/mL Calcein-AM-labelled AoEMPs (red) following 3, 6 and 24 hours, taken using a fluorescent microscope. 10 µM Calcein-AM + PBS was used as a control to establish the background fluorescence. Scale bar = 100 µM. B) Mean fluorescence intensity was used to quantify uptake from 3 different fields of view. A one-way ANOVA test with with Tukey correction was used for statistical analysis. Error bars represent ± SEM. n = 4 independent experiments (4 different AoEMP preparations and HCoASMC batches). ****p < 0.0001

4.2.2. AoEMPs enhance HCoASMC calcification *in vitro*

HCoASMCs were treated with and without AoEMPs and grown in osteogenic media *in vitro* for 21 days. In addition to the phenotypic differences observed between the untreated and the AoEMP-treated HCoASMCs (the later were more contracted and with larger calcification nodules), Alizarin Red S staining was performed and an increase in stained nodules in the AoEMP-treated cells was observed, reflecting enhanced osteogenic differentiation (Figure 36A). In order to quantify these observations, Alizarin Red S staining was eluted with 10 % (v/v) formic acid and quantified by measuring the absorbance at 414nm. These data confirmed a significant increase in calcification in AoEMP-treated cells compared to untreated cells ($p < 0.005$; Figure 36B).

Calcium levels were also measured in a parallel set of experiments and normalised to total protein content. AoEMP-treated cells showed significantly elevated levels of calcium compared to untreated cells ($p < 0.05$; Figure 36C), thus validating the Alizarin Red S findings.

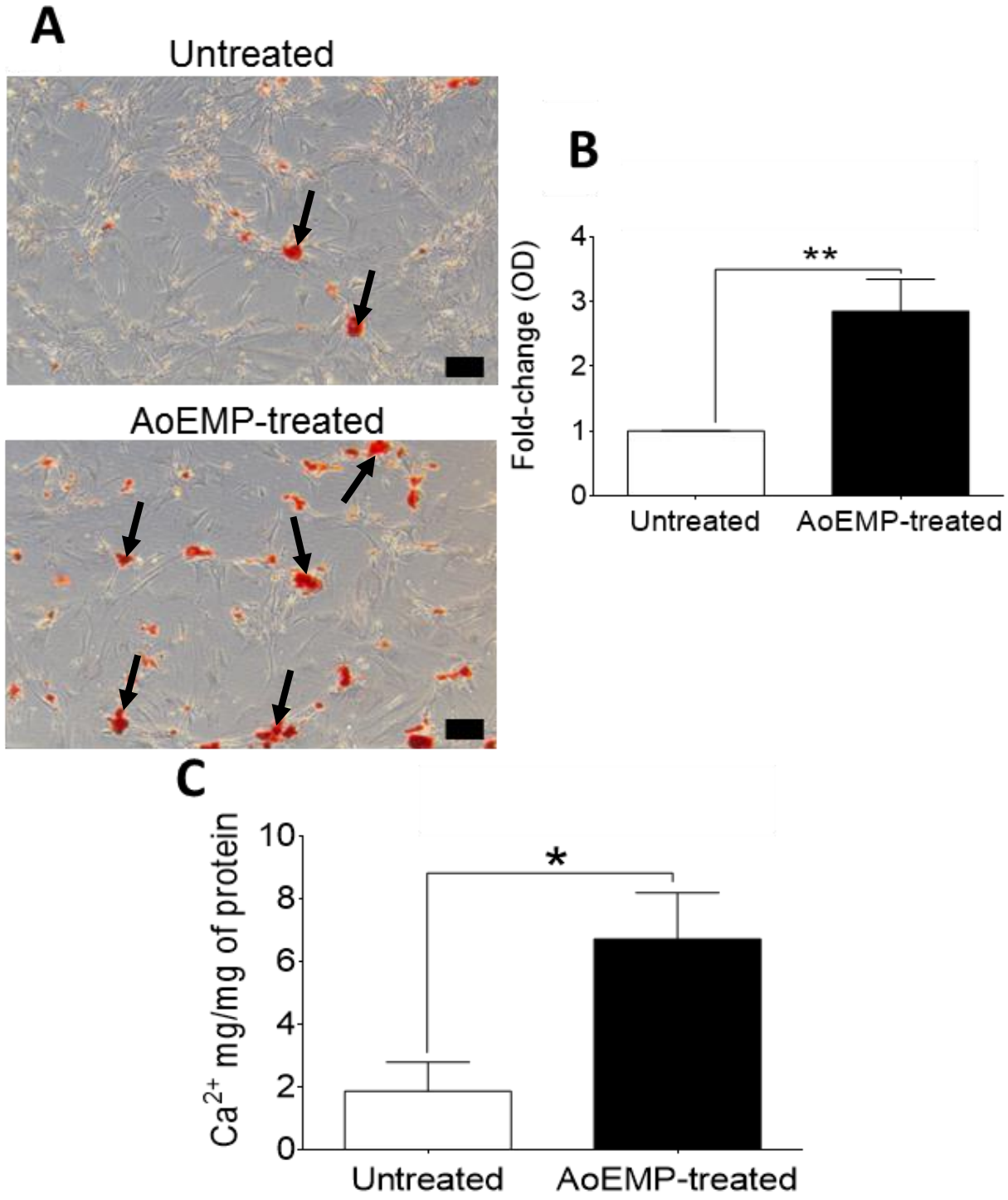

Figure 36. The effects of EMPs on HCoASMCs calcification. A) Representative micrographs taken at 10x magnification of Alizarin Red S staining of HCoASMCs cultured in osteogenic media and treated with 10^6 AoEMPs/mL of osteogenic media twice a week show enhanced calcification nodules (black arrows). Scale bar = 100 µm. B) Quantification of Alizarin Red S staining was performed by eluting the staining in 10 % (v/v) formic acid, confirming the visual observations. C) Calcium deposition assays also showed that more Ca^{2+} is deposited in the AoEMP-treated cells. An unpaired student t-test was used for statistical analysis. Error bars represent ± SEM. n = 4 independent experiments. *$p < 0.05$, **$p < 0.005$.

4.2.3. HCoASMC secretome is modulated by AoEMPs

Conditioned media from the experiments described in section 4.2.2 was used to investigate the effects of AoEMPs on the HCoASMC secretome after 4, 7, 14 and 21 days using a bone-panel multiplex assay containing proteins relevant in vascular calcification. The inflammatory cytokines IL-6 and TNFα were elevated throughout the 3 weeks in AoEMP-treated cells after 7 and 4 days respectively (Figure 37A and 37B), suggesting a pro-inflammatory effect of the AoEMPs. Secreted OPG, a known inhibitor of calcification was reduced in the media during the first week of treatment but increased at the later stages (Figure 37C), which suggests that AoEMPs mediate their effects at the early stages of the calcification process, whereas OPN and SOST levels were unaffected (Figure 37D and Figure 37E). OCN, which is a pro-osteogenic protein, was found to be elevated in AoEMP-treated media at 7 days in comparison to untreated cells, but no differences were detected at 4, 14 and 21 days (Figure 37F). Calcification is a highly regulated process and it is often the balance between calcification promoters and inhibitors that decides cell fate. In this study, the observation of increased OCN levels (calcification promoter) at day 7, together with the reduced OPG levels (calcification inhibitor) during first 7 days, may lead to the enhancement of calcification observed in AoEMP-treated HCoASMCs.

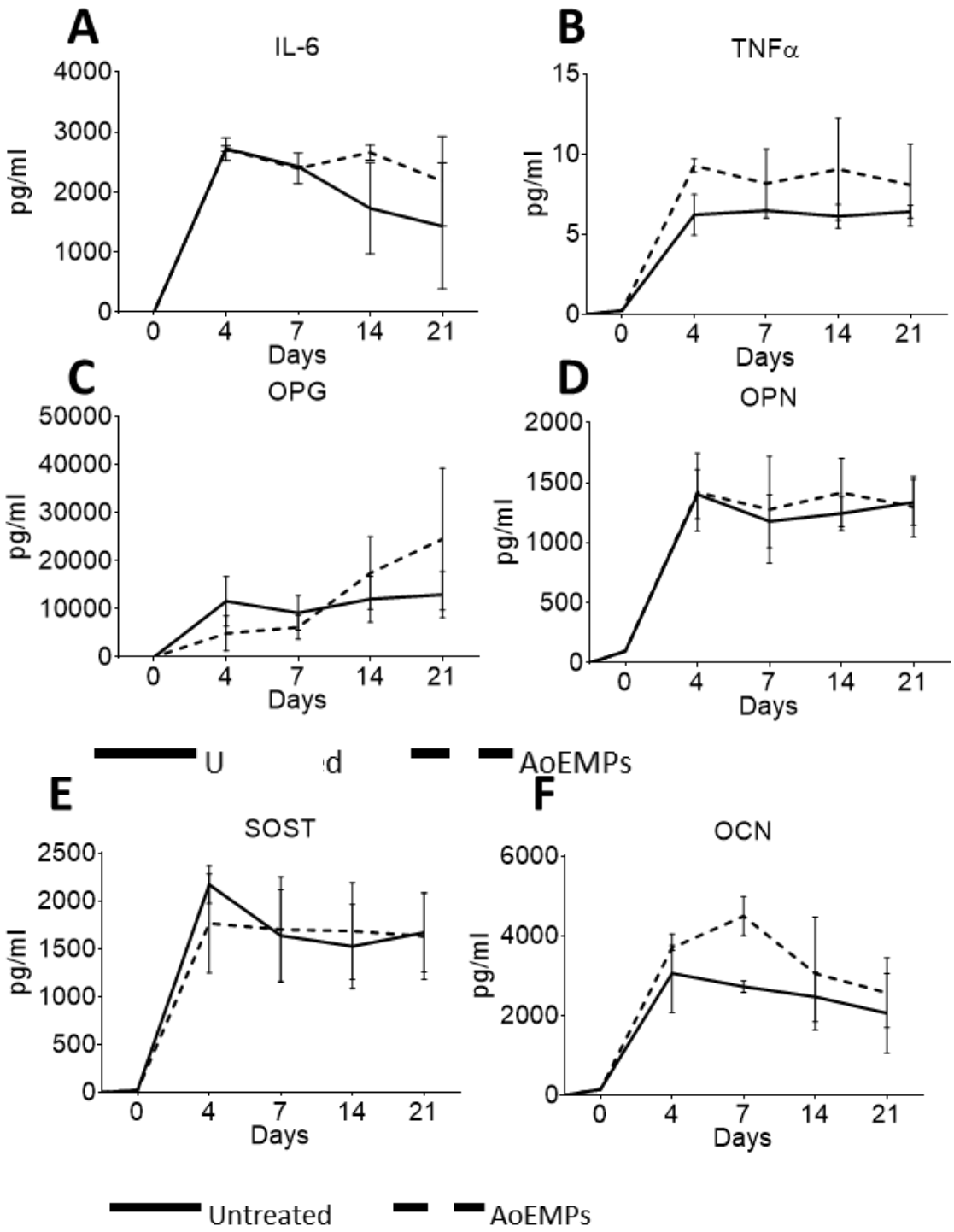

Figure 37. The effect of AoEMPs on HCoASMCs secretome during vascular calcification. Conditioned media of untreated and AoEMP-treated cells was collected during the 21-day experiments and analysed using a Multiplex immunoassay for bone-related proteins. A) IL-6: interleukin-6, n = 2; B) TNFα: tumour necrosis factor alpha, n = 2; C) OPG: osteoprotegerin, n = 3; D) OPN: osteopontin, n = 3; E) SOST: sclerostin, n = 3; F) OCN: osteocalcin. Solid and dotted lines represent untreated and AoEMP-treated HCoASMCs respectively. A two-way ANOVA was used for statistical analysis. Error bars represent ± SEM.

4.2.4. Molecular analysis of AoEMPs

Given that AoEMPs appear to enhance the osteogenic differentiation of SMCs by enhancing calcification, they were submitted to phenotypical, proteomic and microRNA analysis to identify any putative promoters of calcification that could be driving this process.

4.2.4.1. Phenotypical analysis of AoEMPs

Scanning Electron Microscopy of AoEMPs was performed as described in section 2.6. Of note, two differently sized particles were evident; particles in the range of 0.4-1 μm and others smaller than 200 nm were detected throughout the different AoEMP preparations analysed, suggesting the presence of exosomes in the MP preparations. It may be that the exosomes and their content may be different from that contained within EMPs and could be having their effect on vascular calcification (Figure 38). Therefore, it is difficult to determine if the enhanced calcification observed in AoEMP-treated cells is due the EMPs or to the smaller exosome fraction.

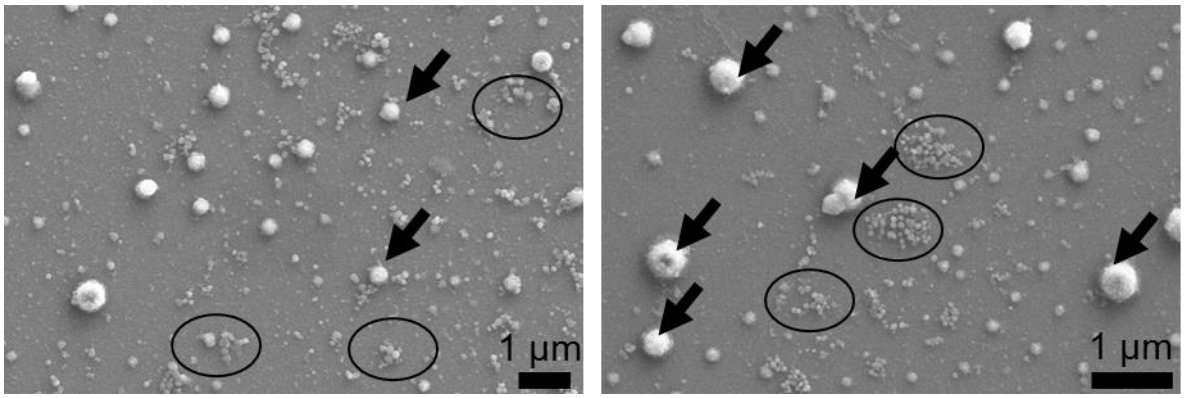

Figure 38. Representative phenotypical characteristics of AoEMPs. Representative Scanning Electron Microscopy micrographs of AoEMP preparations. Particles ranging from 200 nm to 1 μm (± 400 nm SEM) were found in all AoEMP preparations. Black arrows indicate the presence of AoEMPs. Black circles indicate the presence of exosomes. n = 3 (different AoEMP preparations).

4.2.4.2. Inflammatory proteomic analysis of AoEMPs

In order to assess the contents of AoEMPs and identify their molecular components, a proteomic screen was performed on concentrated preparations. Protein was extracted from the same number of AoEMPs as detailed in section 2.5.1 in Methods and subjected to proteomic analysis using an inflammatory panel of 92 molecules (n = 2; different AoEMP batches). Out of all proteins identified (41), only those in which SD < 3 between the two replicates (HGF, CXCL6, MMP-10, OPG, CCL23 and

MMP-1) were considered for further investigation in the context of vascular calcification. Protein screening identified the matrix metalloproteinases MMP-10 and MMP-1, as well as CXCL6, CCL23 and OPG. HGF (a protein that has been shown to be involved in the development of vascular calcification (166)) was also detected in the proteomic screening and was validated in our laboratory using an HGF Quantikine ELISA thus, confirming its presence (Figure 39).

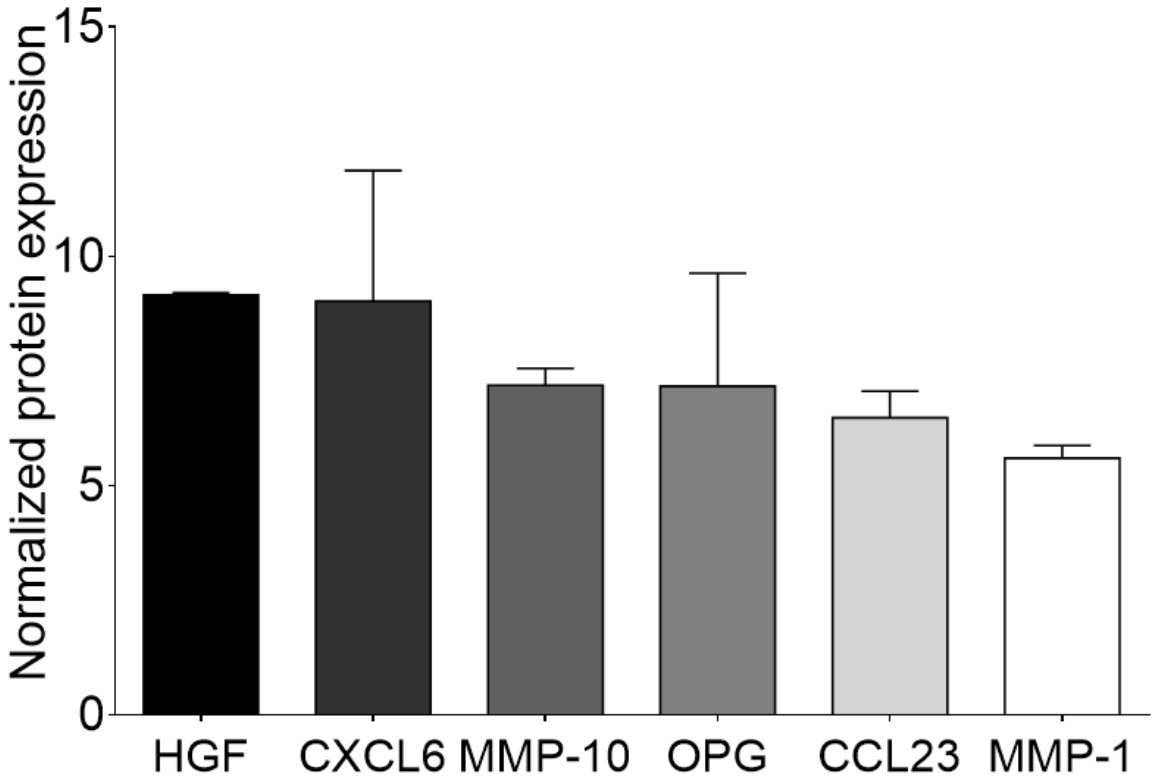

Figure 39. Proteomic screening of AoEMPs. Protein from 10^7 AoEMPs/µL of PBS was extracted in RIPA buffer (containing Protease Inhibitor Cocktail) and quantified using a BCA assay. Proteomic screening was performed by Olink Bioscience and results are presented as normalised protein expression (Proseek Multiplex data are normalised for both intra- and inter-plate variation). Error bars are presented as ± SEM. n = 2 (Olink Bioscience screenings performed on two different occasions using two different AoEMP preparations). HGF: Hepatocyte growth factor; CXCL6: Chemokine (C-X-C motif) ligand 6; MMP-10: Matrix metalloproteinase 10; OPG: osteoprotegerin; CCL23: Chemokine (C-C motif) ligand 23; MMP-1: Matrix metalloproteinase 1.

4.2.4.3. EMPs carry Ca^{2+}

Several studies have suggested that EMPs carry not only proteins, but also Ca^{2+}. In order to investigate this, uEMPs, sEMPs and AoEMPs were incubated in HCL to extract Ca^{2+}, which was measured using a calcium deposition quantification assay

as described in section 2.5.1. These data showed that uEMPs carry significantly more Ca^{2+} (~0.25 mg/10^7 EMPs) than inflammatory-derived sEMPs (~0.15 mg/10^7 EMPs) or AoEMPs (~0.12 mg/10^7 EMPs; Figure 40). The results suggest that EMPs carry and deliver calcium, thereby playing a role in vascular calcification, and confirm that the different microenvironments during EMP generation may have an impact on their final Ca^{2+} content.

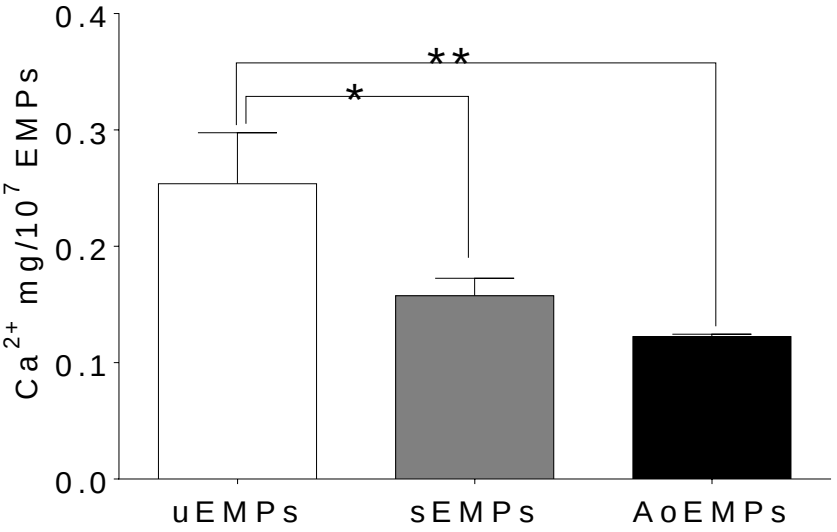

Figure 40. Ca^{2+} content in EMPs. Calcium content was measured from 10^7 uEMPs/µL, 10^7 sEMPs/µL and 10^7 AoEMPs/µL of PBS using a calcium deposition kit and expressed as mg/10^7 EMPs. A one-way ANOVA with Tukey correction was used and error bars are presented as ± SEM. n = 3 (different EMP preparations); *p < 0.05, **p < 0.005.

4.2.4.4. AoEMPs contain miRNA-3148

As reviewed by Goettsch *et al.*, it is now recognised that microRNAs play a role in regulating the vascular calcification process (200), therefore, a microRNA screening of extracts of AoEMPs was performed as described in section 2.5.2. Of all the miRNAs identified, only the 28 most abundant ones in AoEMPs were considered for RT-qPCR validation, followed by investigation in the context vascular calcification in a bioinformatic analysis. Among the 28 microRNAs identified, miRNA-3148 was found to be one of the most abundant ones, and a bioinformatic analysis using microRNA.org and DIANA-miRpath predicted that OPG is a target of miRNA-3148 (mirSVR score: -0.1687; Figure 41A) and could therefore be responsible the enhanced calcification observed in AoEMP-treated HCoASMCs in comparison to untreated cells. The presence of miRNA-3148 in AoEMPs was validated by RT-

qPCR and normalised to miRNA-222-3p levels. miRNA-3148 was found to be carried by AoEMPs (Figure 41B), suggesting that miRNA-3148 could be playing a role by reducing OPG mRNA levels during the first stages of AoEMP-induced vascular calcification.

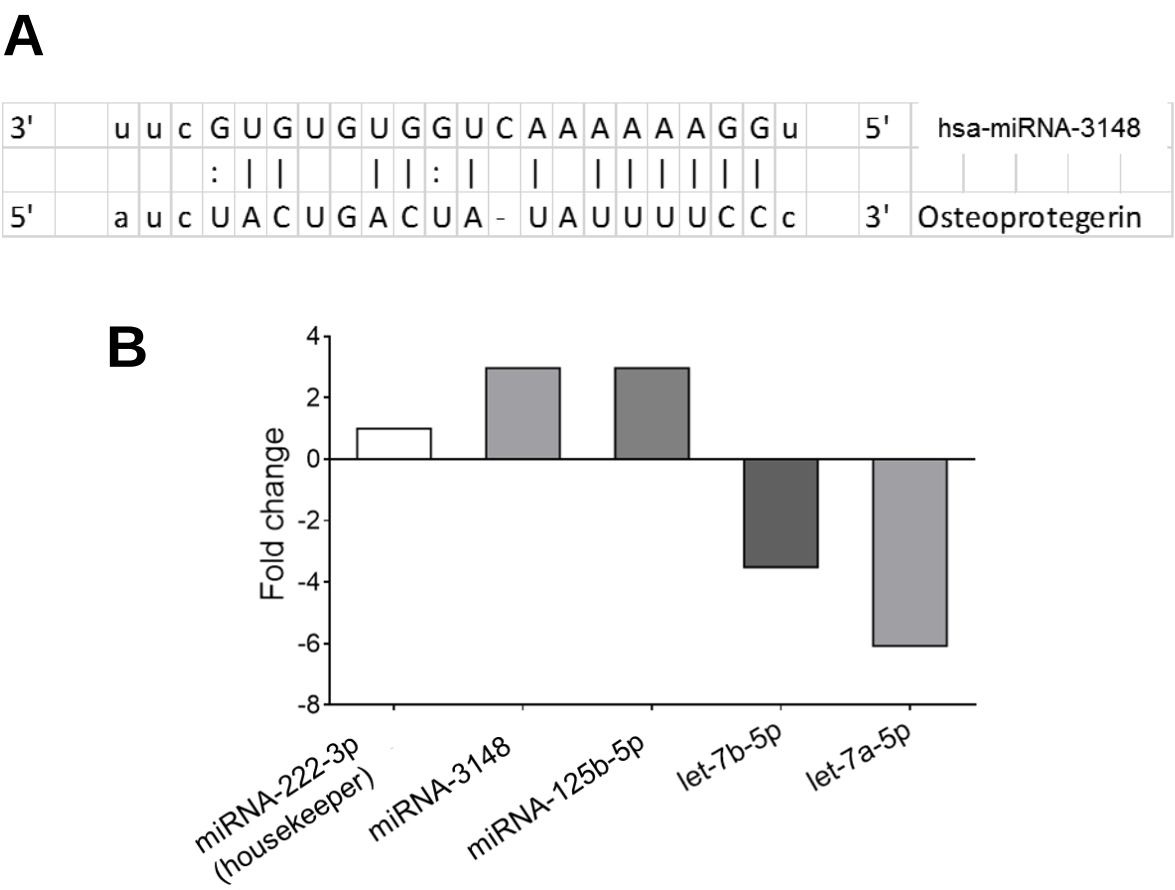

Figure 41. Bioinformatic prediction of miRNA-3148 targets and quantification in AoEMPs. A) A target prediction using microRNA.org and DIANA-miRpath algorithms predicted that OPG is a target of miRNA-3148. B) Validation of miRNA-3148 was performed by RT-qPCR and normalised to miRNA-222-3p. n = 1.

4.2.5. Vascular calcification is enhanced in miRNA-3148 transfected HCoASMCs

To elucidate the effects of miRNA-3148 on OPG mRNA, HCoASMCs were transfected with miRNA-3148 precursor and a scrambled control using an Amaxa Nucleofector® kit as described in section 2.11.3. Transfected cells were selected in 0.25 µg/ml of Puromycin for 4 days (Figure 42A) with an apparent 60-70 % transfection efficiency (Figure 42B). Transfected cells were harvested following incubation in osteogenic media for 21 days and RT-qPCR was used to investigate OPG mRNA levels, as well as Alizarin Red S staining to determine the level of calcification.

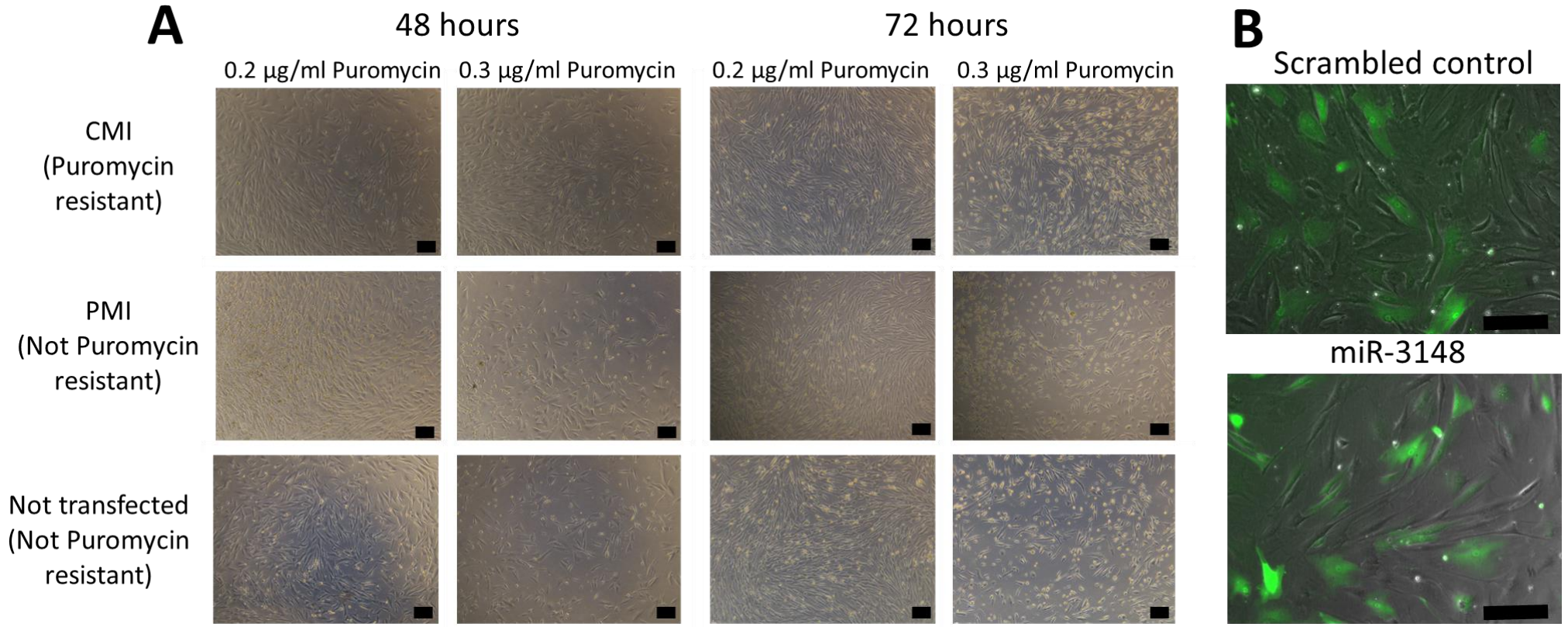

Figure 42. HCoASMC transfection using Amaxa Nucleofector® kit. A) Representative micrographs taken at 10x magnification of transfected HCoASMCs with the scrambled control (CMI), GFP transfection control (PMI) and non-transfected cells were used to identify the concentration of Puromycin for the selection of the successfully transfected cells. Scale bar = 50 µm. B) Representative micrographs taken at 20x magnification of transfected HCoASMC observed under the fluorescence microscope after 72 hours of Puromycin selection. An apparent transfection efficiency of 60-70 % was achieved. Scale bar = 50 µm.

4.2.5.1. OPG mRNA is reduced in miRNA-3148 transfected HCoASMCs

Calcification is a complicated process involving many proteins and secreted molecules, and it the balance between these molecules that decides cell fate. As such, RT-qPCR of the calcification inhibitors OPG and OPN, as well as the active regulators OCN and C-met was performed in transfected HCoASMCs in osteogenic media for 3 days. Our data showed a significant decrease (~6.5 fold-change) in mRNA abundance of the calcification inhibitor OPG compared to untreated and scrambled control cells ($p < 0.05$, $p < 0.005$ respectively), confirming that miRNA-3148 targets OPG mRNA (Figure 43A). OPN, another calcium inhibitor, was also decreased (~60 fold-change) in AoEMP-treated HCoASMCs (Figure 43B), whereas the calcium regulator OCN is increased (~4 fold-change) (Figure 43C). Furthermore, C-met mRNA abundance was also found to be reduced in both AoEMP and miRNA-transfected HCoASMCs (~1.5 fold and 1 fold-change respectively) (Figure 43D). A statistically significant difference was found between the untreated and the scrambled control groups in OPN mRNA abundance levels (Figure 43B), indicating that any effects on these genes in the transfected cells cannot be attributed to the presence of miRNA-3148. A statistically significant difference was found between the untreated and the scrambled control groups in OPN mRNA abundance levels (Figure 43B), which suggests that any effects on OPN in the transfected cells cannot be attributed to the presence of miRNA-3148.

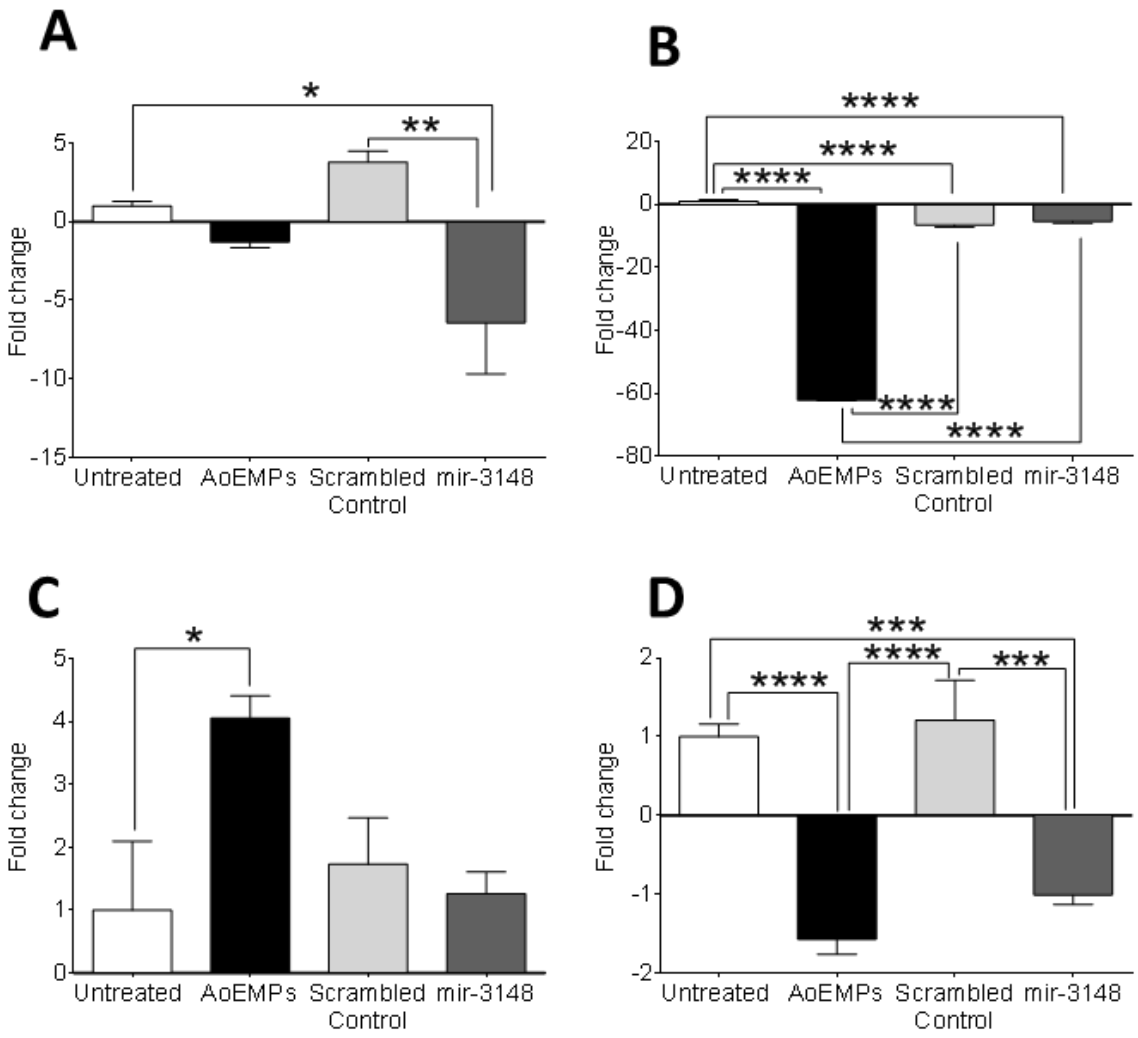

Figure 43. RT-qPCR analysis of molecules involved in vascular calcification in miRNA-3148 transfected HCoASMCs. RT-qPCR analysis of miRNA-3148 transfected HCoASMCs in osteogenic media for 4 days confirmed that A) miRNA-3148 targets the calcification inhibitor osteoprotegerin (OPG), reducing its mRNA abundance and validating the bioinformatic prediction. B) AoEMPs decrease osteopontin (OPN) and C) increase osteocalcin (OCN) mRNA levels. D) C-met mRNA levels were reduced in both AoEMP and miRNA-3148 transfected cells. A one-way ANOVA test with Tukey correction was used. Error bars represent ± SEM. n = 3 independent transfections; *p < 0.05, **p < 0.005; ***p < 0.001; ****p < 0.0001.

4.2.5.2. miRNA-3148 enhances matrix mineralisation

Our data demonstrated that miRNA-3148 targets and reduces mRNA abundance of the calcification inhibitor OPG, thus suggesting that miRNA-3148 could be responsible for the AoEMP-mediated calcification. To test this, miRNA-3148 transfected HCoASMCs were harvested in osteogenic media for 21 days in parallel with scrambled control transfected cells, untreated and AoEMP-treated cells (these last two were non-transfected). Representative Alizarin Red S images of transfected HCoASMCs in osteogenic media for 21 days showed increased calcification in miRNA-3148 transfected cells (Figure 44A), suggesting that miRNA-3148 could be partially responsible for the enhanced vascular calcification observed in AoEMP-treated HCoASMCs. These observations were confirmed by the quantification of Alizarin Red S elution (Figure 44B).

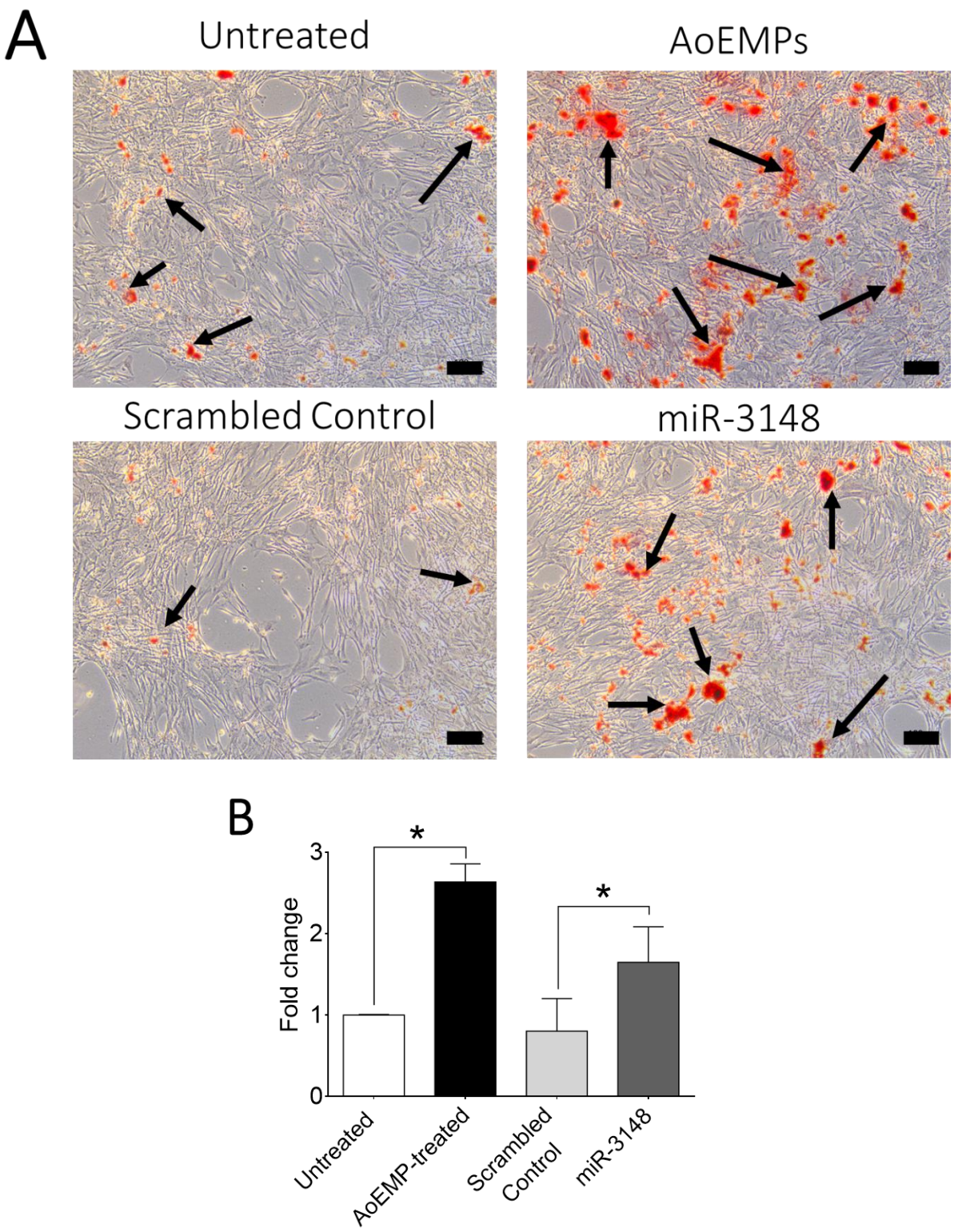

Figure 44. The effect of miRNA-3148 transfection on HCoASMC calcification. A) HCoASMCs were transfected with scrambled control or miRNA-3148 and cultured in osteogenic media for 21 days. Representative micrographs of Alizarin Red S staining taken at 10x magnification exhibited an elevated number of calcium deposits in AoEMP-treated and miRNA-3148 transfected HCoASMCs. Scale bar = 100 µm. B) Elution of Alizarin Red S in 10 % (v/v) formic acid confirmed that miRNA-3148 enhances calcification after 21 days. A one-way ANOVA test with Tukey correction was used. Error bars represent ± SEM. Black arrows highlight the calcified nodules. n = 3 independent transfections; *p < 0.05.

4.3. Key findings

The key findings of experiments described in this chapter show:

1. Fluorescence microscopy of AoEMPs showed that are internalised by HCoASMCs, enhance matrix mineralisation and calcium deposition *in vitro* compared to untreated cells as shown by Alizarin Red S staining and calcium deposition assays.

2. A bone-panel multiplex array found that the secretome of calcifying HCoASMCs is modulated by AoEMPs compared to untreated cells: IL-6, TNFα and OCN are increased, while OPG are decreased, during the first week of treatment with AoEMPs. SOST and OPN remain unaffected.

3. Proteomic screening of AoEMPs found that they carry HGF and other proteins involved in vascular calcification, as well as Ca^{2+}.

4. This is the first study to describe the role of miRNA-3148, which a microRNA screening found that is carried by AoEMPs and we have shown that selectively targets OPG mRNA, is partially responsible for AoEMP-enhanced calcification.

4.4. Summary

We have found that AoEMPs are not only up-taken by their targets, but that they increase the secretion of the inflammatory molecules IL-6 and TNFα, as well as the calcification promoter OCN, suggesting an active role in enhancing calcification *in vitro*. Calcification is a complicated process involving many molecules (159, 169, 201) but to our knowledge, this is the first study to describe that AoEMPs enhancing vascular calcification *in vitro* partially via the transmission of miRNA-3148, which we have found selectively targets the calcification inhibitor OPG. These findings suggest that, upon EC damage and EMP release, there could potentially be cross-talk within the vessel wall between ECs and VSMCs via EMPs. The next chapter will describe the significance of these findings and their contribution to the existing knowledge in the link between CVD and vascular calcification.

CHAPTER 5:
DISCUSSION, CONCLUSIONS AND FUTURE WORK

CHAPTER 5: DISCUSSION, CONCLUSIONS AND FUTURE WORK

5.1. Discussion

Inflammatory disorders such as SLE are associated with elevated endothelial dysfunction and accelerated vascular ageing, which lead to increased risk of CVD. Circulating EMP levels are increased in these disorders, but their role on the vessel wall is unclear. This study shows that EMP treatment of endothelial cells (HUVECs) and coronary artery smooth muscle cells (HCoASMCs) results in a modulation of endothelial function and in enhanced osteogenic differentiation of HCoASMCs respectively. HUVECs stimulated with sEMPs showed elevated EMP release compared to those treated with uEMPs, which could support the *in vivo* findings that patients with rheumatoid arthritis and SLE have elevated levels of EMPs (33, 202).

Both sEMPs and uEMPs seem to have similar effects on endothelial cell migration, proliferation and adhesion molecule (VCAM-1 and ICAM-1) levels, which may reflect specific effects on the particular vascular beds and the fact that vein endothelial cells do not respond to the microenvironment in the same way as aortic cells, which form atherosclerotic plaques while vein cells do not. On the other hand, sEMPs activate the NFκB pathway whereas uEMPs do not. Finally, AoEMPs were able to induce osteogenic differentiation and calcification of HCoASMCs after 3 weeks, and we have described for the first time a link between miRNA-3148 and deposition of a mineralised matrix. These findings suggest that endothelial dysfunction induced by inflammation in SLE may further promote the generation of EMPs, further contributing to endothelial damage and ultimately, promote vascular calcification. A more detailed discussion of the study is outlined below.

5.1.1. EMPs as indicators of endothelial function and disease activity

CVD is the largest cause of death in systemic inflammatory diseases such as SLE. As reviewed by Chironi and Boulanger *et al*., several studies have attempted to link the elevated circulating EMP levels observed in CVD patients with a potential key role in the regulation of inflammation, angiogenesis and thrombosis (140). Other studies in which circulating MPs from healthy individuals have been quantified have found that the majority of MPs are platelet-derived rather than of endothelial origin, and that the former are usually more abundant than the latter (39, 145). Given the

fact that endothelial dysfunction is apparent in patients with SLE which is an inflammatory disorder, and that reports suggest elevated EMPs in disease compared to healthy subjects, we focused our attention on understanding the role of EMPs in inflammation and endothelial function.

In addition to being associated with endothelial dysfunction, EMPs may contribute directly to the development of certain inflammatory conditions and vascular ageing. In patients with active inflammation, EMP numbers correlate with decreased endothelial function as measured by flow mediated dilation (FMD) (33). Parker *et al.* demonstrated that anti-inflammatory treatment reduces circulating EMP levels in SLE patients, and that such a reduction correlates with an improvement in endothelial function (33). In this study, we investigated the role of two EMP populations, uEMPs and sEMPs, generated by different mechanisms, in order to compare their content and effects on endothelial cell function *in vitro*. Our results suggest that uEMPs and sEMPs not only carry different proteins and microRNAs, but also have different roles on endothelial function and activate different pathways. These observations, together with the observations of other researchers in the literature, reinforce the idea that EMPs may serve as indicators of endothelial function and disease activity.

5.1.1.1. EMP content depends on the mode of EMP generation

Not only can EMP levels be altered in disease, but the phenotype of the EMPs has also been demonstrated to be altered depending on the disease and other underlying environmental conditions. In a series of studies, Berezin *et al*. showed that the expression of surface markers on circulating EMPs CD31, AnnexinV and CD62E differ between pathologies, and that body mass index is a predictor of this in patients with chronic heart failure (203). Similarly, patients suffering metabolic syndrome and developing CVD have been shown to have an immunogenic MP phenotype with an altered ratio between circulating EMPs and apoptotic bodies (204). In the current study, small phenotypical differences between uEMPs and sEMPs were detected; sEMPs may not be fully encapsulated microvesicles as their membrane in some cases did not appear to be fully enclosed, whereas this is not the case for uEMPs (Figure 18). This phenomenon could be explained by the difference in the mode of generation, in that TNFα is a stressful stimuli that leads to a rapid and more abundant sEMP generation, leading to generation of “incomplete”,

open vesicles, compared to generation under standard conditions, which requires further investigation. This possibility, which has already been explored in apoptotic bodies (42, 205), means that the chance for multiple mechanisms of interaction between EMPs and target cells is real and would explain how encapsulated molecules in the EMPs interact with membrane receptors in their target cells, allowing for a more direct interaction.

EMPs are vehicles of biological information, as they carry proteins and miRNAs from their cell of origin (10, 73, 92, 124), which also means that they are a good reflection of the status or health of the cell from which they originate. Techniques including western blotting and/or RT-qPCR have been used in the past to investigate MP content with flow cytometry to determine surface antigens. In this study, a proteomic screen and an angiogenic bioplex suspension array analysis of uEMPs and sEMPs to investigate the differences between both sets were performed (Figure 19 and Figure 20). Among proteins of the CXC chemokine family, other signalling molecules such as TNFα, IL-8 or VEGF-A were detected. CCL20, a protein involved in macrophage recruitment to sites of injury was found to be more abundant in sEMPs than in uEMPs in the proteomic screen and confirmed using flow cytometry (Figure 22). CCL20 expression is mediated by TNFα and therefore, its abundance in the cytoplasm of the TNFα-stimulated HUVECs would have been high at the time of sEMP generation and thus reflects the status of the cell of origin.

A review by Lee *et al.* summarised the importance of CCR6 and CCL20 in rheumatoid arthritis and other connective tissue diseases, and suggested that they are involved in disease progression (206). A parallel study in our laboratory (personal communication, unpublished) found a correlation between circulating EMPs and CCL20 levels in SLE patients. Koga *et al.* used a calcium/calmodulin-dependent kinase IV knockout mouse model to demonstrate the importance of CCL20 in lymphocyte Th17-mediated inflammation, and found that the expression of CCR6 (the receptor of CCL20) in peripheral blood, positively correlates with the severity of organ damage in SLE patients (207). Similarly, an investigation by Manthey *et al*. highlighted the role of CCR6 as a promoter of monocyte-mediated inflammation in CCR6 and low-density lipoprotein receptor-deficient (CCR6-/- LDL-/-) mice, and concluded that targeting CCR6 or its ligand CCL20 could be a promising therapeutic strategy to alleviate vascular damage (208). Another study by Calvayrac *et al.* showed an elevation of circulating CCL20 levels in

hypercholesterolemic individuals, as well as elevated levels in atherosclerotic plaques, and identified LDL as a mediator of such inflammation using a hVSMCs model *in vitro* (209). In this study, a microRNA screen identified miRNA-129-5p, to be more abundant in uEMPs than in sEMPs, and a bioinformatic analysis predicted its target to be CCL20. A review by Nakashima *et al.* describes the role of miRNA-129-5p in other autoimmune disorders (210) lending credence to the idea that miRNA-129-5p could be responsible for the reduced CCL20 levels in uEMPs *vs* sEMPs and in uEMP-treated cells in comparison to sEMP-treated cells (Figure 24). However, following transfection studies over-expressing miRNA-129-5p, no decrease in mRNA abundance was detected suggesting that miRNA-129-5p does not target CCL20 mRNA in our *in vitro* model (Figure 26). It is possible that the bioinformatic alignment is not strong enough and therefore the prediction is inaccurate, but it is also possible that miRNA-129-5p has an unknown target that upregulates CCL20 expression. Alternatively, it would have been interesting to generate sEMPs enriched with miRNA-129-5p and quantify their CCL20 levels, very much like the work carried out by Jansen *et al*, in which they showed that EMPs reduced ICAM-1 expression via microRNA-222 transfer (211).

5.1.1.2. EMPs effects on endothelial cell function

This study confirms that TNFα enhances EMP release *in vitro*, as shown previously (21, 28, 41); however, whether these EMPs are the result of the beginning of an apoptotic process is debatable. In this study, complete media (with serum) with the addition of 10 ng/mL of TNFα, to stimulate EMP release from HUVECs was used. After 24 hours of TNFα treatment, no phenotypical differences between the untreated and TNFα-stimulated HUVECs were observed, although elevated EMP release was observed in the TNFα-treated cells (Figure 17). Our laboratory published a study on the effects of the anti-TNFα drug Certolizumab on endothelial cell function *in vitro*, and it was found that 10 ng/mL TNFα under these conditions did not adversely affect cell viability as shown by MTT and apoptosis assays (21). Additionally, a recently published study by Teasdale e*t al.* demonstrated that 10 ng/mL TNFα is not a high enough concentration to induce apoptosis in cells, as shown by no change in cleaved Poly (ADP-ribose) polymerase (PARP) or cell viability (212). Finally, it is generally accepted that TNFα is an inflammatory stimulant but, in the absence of mRNA or protein synthesis inhibition, does not directly promote cell death (213). As such, 10 ng/mL of TNFα was used to stimulate

HUVECs for 24 hours to model an inflammatory environment and to promote EMP generation (sEMPs).

EMPs were also collected from healthy, non-stimulated HUVECs (uEMPs) in order to compare the content of the two populations. In order to generate EMPs *in vitro*, commercially available HUVECs (pooled donors) were used instead of isolating endothelial cells in our laboratory. The reasoning behind this is that EMPs can be widely heterogeneous and minimal differences in their mode of generation are expected to have a huge impact in their proteomic and nucleic acid content, and for the purposes of this study, minimal differences between uEMP and sEMP batches were sought in order to improve reproducibility.

EMPs are thought to be paracrine and autocrine mediators of intracellular signalling due to their capacity to transfer a number of molecules to target/recipient cells and as such, have an effect in the vasculature (214). Lacroix *et al.* reported that HUVEC-derived EMPs promoted angiogenesis at low concentrations, whereas they had an inhibitory effect at high concentrations, and that these effects are urokinase-type plasminogen activator (uPA) dependant (123), therefore, it was acknowledged that such effects may be concentration dependent. In this study, EMP concentrations used (10^6 EMPs/mL) were based on previously published EMP levels detected in patients. Previous findings from our laboratory demonstrated that EMP levels are elevated in inflammatory diseases compared to healthy controls, and that these levels are reduced following anti-inflammatory treatment (33). In such study, it was found that the highest concentration of EMP levels measured in plasma from SLE patients was in the magnitude order of 10^6 EMPs/mL, whereas the levels following treatment were 10-fold lower at 10^5 EMPs/mL. In light of these findings and reflect inflammation associated with SLE *in vitro,* 10^6 EMPs/mL was used in all experiments. However, it is acknowledged that EMP levels are highly variable and clearly depend on many underlying clinical parameters.

Another study from our laboratory, investigating the levels of EMPs in patients with carotid artery disease, found that median EMP levels could be as high as 10^6 EMPs/mL in asymptomatic patients with unstable plaques (similar to SLE), whereas symptomatic patients with stable plaques had significantly lower circulating EMP numbers (145). As such, it is challenging to scale down EMP concentrations *in vitro* and still resemble the *in vivo* situation in SLE. Nevertheless, in a recent study also

from our laboratory investigating the role of EMPs in lipid-induced endothelial damage (unpublished), 10^5 and 10^6 sEMPs/mL were used in the experiments and there was very little difference between the two EMP concentrations on a number of parameters tested (nitric oxide release, reactive oxygen species production and NADPH oxidase activity among others).

In this study, it was found that treatment of HUVECs with sEMPs elevated EMP release compared to untreated or uEMP-treated cells, to almost TNFα levels. However, the combination of sEMPs and TNFα did not exert a synergistic nor additive effect on EMP release, suggesting that sEMPs may enhance EMP release via a similar mechanism to that of TNFα and that a threshold level of release exists. uEMPs not only did not enhance EMP release, but they attenuated TNFα-mediated EMP release (Figure 27). As far as we are aware, this is the first study to suggest that, EMP release may be governed by EMPs themselves in a self-regulating manner, possibly contributing to the maintenance of endothelial homeostasis. The incapacity of sEMPs to reduce TNFα-mediated EMP release, as well as their ability to actually enhance EMP release could explain the observation of higher circulating EMP levels in patients with systemic inflammatory conditions compared to healthy individuals.

EMPs were initially characterised as being pro-inflammatory, with the potential to prevent vascular repair and exacerbate endothelial damage (36, 141, 144); however, findings from this study indicate a potential dual role, depending on whether they are released from healthy or activated cells. For example, endothelial cell migration is a tightly regulated process that plays a key role in a variety of physiological processes. The endothelial layer regulates the exchange of molecules and cells between the lumen and tissues, and as explained above, endothelial dysfunction is the first stage to the development of vascular complications often as a result of damage caused by sustained inflammatory stimuli. Therefore, when the endothelial layer is damaged, cells migrate to the sites of injury, a process regulated by a myriad of growth factors and cytokines such as fibroblast growth factor-2, hepatocyte growth factor, platelet-derived growth factor, epidermal growth factor, transforming growth factor-β, interleukins and TNFα among others (215-217), for endothelial repair.

It is well stablished that TNFα is a key player in the regulation of endothelial cell responses (218); Chaudhuri *et al.* demonstrated that TNFα contributes to tissue remodelling and fibrosis using human epithelioid dermal microvascular endothelial cells treated with 50 ng/mL TNFα (219). Cell migration and scratch assays are often used as *in vitro* models of endothelial repair. A study by Kanaji *et al.* using human pulmonary artery endothelial cells treated with low concentrations of TNFα (2 ng/mL) described its role on endothelial cell migration and survival via the NFκB pathway (220). As such, in this study TNFα was used as a positive control for endothelial cell migration. While sEMPs enhanced EMP release and uEMPs attenuated TNFα-driven EMP release, both populations of EMPs enhanced endothelial cell migration to similar levels (Figure 28). Although there appears to be a trend towards inhibition of TNFα-mediated endothelial cell migration, this was not statistically significant.

To ensure that closure of the wound was due to migrating cells and not due to endothelial cell proliferation, the proliferative capacity of the cells was also measured following treatment with EMPs. Neither uEMPs nor sEMPs had any effect on cell proliferation compared to untreated and TNFα-treated cells, which supports the data obtained from the uEMP and sEMP-induced endothelial cell migration.

Jansen *et al.* have reported that EMPs generated from serum starved human coronary artery endothelial cells enhanced endothelial cell migration *in vitro* via sprouty-related enabled/VASP homology 1 domain-containing protein-1 (SPRED1) and miRNA-126, an effect not observed in EMPs generated in hyperglycaemic conditions (81). Our results are interesting since they raise the point to the functional role of EMPs being dependent upon their origin. However, no differences in the induced migration capacity of uEMPs and sEMPs nor a statistically significant reduction in TNFα-mediated migration or effects on cell proliferation when using 10^6 EMPs/mL was observed. It is possible that these effects are concentration dependent and therefore, either the concentration of uEMPs was too high or the concentration of sEMPs too low. Since the objective was to investigate the differences between uEMPs and sEMPs, these effects were not investigated on a dose response manner.

VCAM-1 and ICAM-1 are two important adhesion molecules involved in the progression of inflammation by regulating inflammatory cell adhesion, which ultimately leads to inflammatory cell infiltration in the vessel wall and vascular

damage (20, 221). It is well established that TNFα increases VCAM-1 and ICAM-1 expression on endothelial cells *in vitro* (185, 222). The expression of VCAM-1, which is found mostly to be present just in endothelial cells and is known to play a key role in endothelial cell:T-cell interaction (223), and ICAM-1, which has differential spatial expression depending on cell type and vascular bed, plays a key role in leukocyte adhesion and migration (224), were investigated in this study.

RT-qPCR of transcripts harvested from uEMP and sEMP treated HUVECs demonstrated that sEMPs and uEMPs increase mRNA abundance of VCAM-1 and ICAM-1 compared to untreated cells, and that sEMPs increased mRNA levels to a greater extent than uEMPs (Figure 29). sEMPs appeared to reduce TNFα-mediated VCAM-1 and ICAM-1 mRNA levels, an effect not observed with uEMPs in combination with TNFα. This is in contrast to our previous findings that uEMPs (but not sEMPs) attenuated TNFα-driven EMP release, highlighting the heterogeneity of EMP population effects during different pathological processes. However, an increase in mRNA abundance need not necessarily indicate altered protein levels, nor an enhancement of endothelial cell adhesion. Indeed, western blot analysis showed that sEMPs and uEMPs did not elevate VCAM-1 and ICAM-1 levels above the untreated controls, in contrast to published work (Figure 30); e.g. a study by Fink *et al*. showed an EMP-mediated modulation of VCAM-1 and ICAM-1 protein levels in HUVECs in an *in vitro* comparative study between EMPs isolated from healthy and from resuscitated patients and using lower EMP concentrations (225). We are inclined to suggest that either the endothelial cells are protecting themselves from activation, or that the diverse content of the uEMPs or sEMPs is regulating VCAM-1 and ICAM-1 at the protein level.

In addition to the effects of TNFα on EMP release and endothelial cell function discussed, it is well established that TNFα induces nuclear translocation of NFκB, a common pathway that also regulates cell migration, proliferation, adhesion molecules (226, 227), and that Sapet *et al*. showed that is involved in ROCK II mediated EMP release in human mammary epithelial cells *in vitro* (46). In the NFκB pathway, TNFα can either bind the TNFR1 or TNFR2, which leads to the phosphorylation and degradation of the inhibitory protein IκBα, releasing NFκB which is then free to translocate to the nucleus, where it will act as a transcription factor of several proteins involved in inflammation, cell survival and cell proliferation

(56, 227).Therefore, TNFα was used both as a positive control and to simulate an inflammatory microenvironment for co-treatment with uEMPs and sEMPs.

Immunofluorescence microscopy demonstrated that cells treated with sEMPs, with or without TNFα, showed NFκB translocation to the nucleus, at both time points tested; 30 minutes and 16 hours. Such translocation was not observed in the untreated cells or uEMP-treated cells, suggesting that only TNFα is responsible for NFκB translocation in the uEMP-treated cells and that sEMPs are responsible for the translocation of NFκB (Figures 31 & 32).

To further validate these findings, western blot analysis of NFκB in the nuclear fraction of these cells was performed. Residual NFκB was found in untreated and uEMP-treated cells (possibly from contamination from the cytoplasmic fraction), and as expected, TNFα increased nuclear NFκB in all cells. Our data also showed that NFκB was elevated in sEMP-treated cells compared to uEMP-treated and untreated cells (Figure 33).

As a final probe into this pathway, RT-qPCR was used to measure mRNA abundance of IκB (an inhibitor protein of the NFκB complex). It was found that IκB mRNA was more abundant in sEMP-treated cells, as well as when TNFα was present, compared to uEMP and untreated cells. Taken together, it can be concluded that sEMPs act via NFκB, whereas uEMPs do not. This finding suggests that the difference in the content between sEMPs and uEMPs reflects the nature of the stimulus by which they were generated originally. sEMPs originate from TNFα-stimulated HUVECs and therefore, they are expected to carry inflammatory-like proteins and nucleic acids (228), whilst uEMPs, generated under standard conditions, may be harbouring pro-homeostatic molecules. Of note, it may be possible that nucleic acid content of EMPs (such as microRNAs) exerts a greater effect on gene regulation once delivered into the cell (as they can regulate the expression of diverse genes) by the EMPs than proteins, whose effect may be greater via interaction with cell surface receptors. However, most of the recent literature around EMPs content points to their diverse microRNA content (229, 230), possibly because microRNAs are easier to detect and amplify compared with proteins, which are more difficult to detect at the low levels observed in EMPs and therefore, explaining the reduced number of investigations in their proteomic content compared to their microRNA content. The observations from this study, together

with data reported in the literature, confirms that MPs, their mode of generation, phenotype, composition and role strongly depends on different factors. These include the presence of other inflammatory molecules, the cell of origin and stimuli of generation. A summary of the suggested role and mechanism of action of EMPs in health and disease is illustrated in Figure 45.

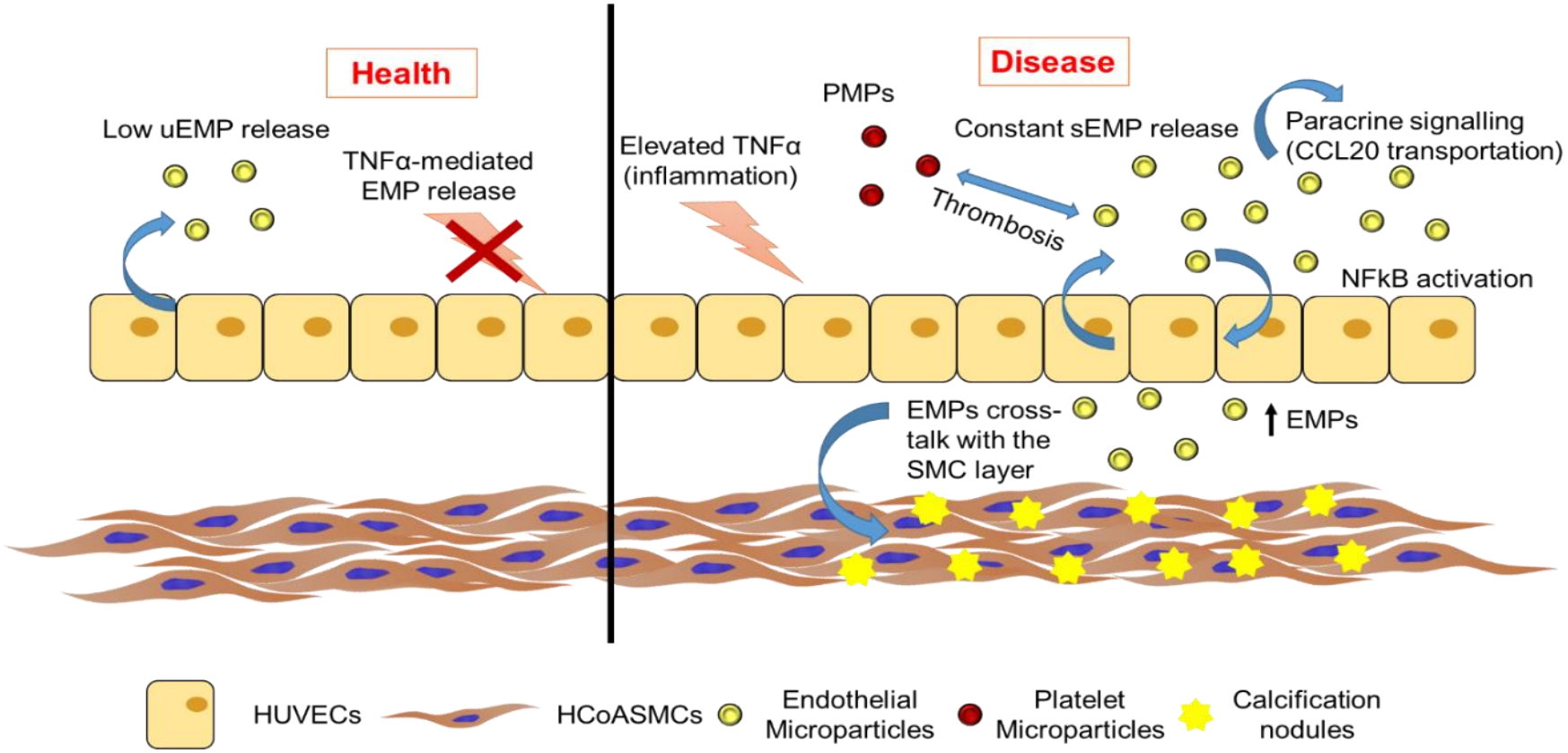

Figure 45. Proposed effects of uEMPs and sEMPs in the vasculature. In health, uEMPs show a baseline level of EMP release, which appears to reduce TNFα-mediated EMP generation. In contrast, in disease, TNFα gives rise to EMP release, which we term sEMPs, which in turn elevate EMP release compared to release from untreated cells (uEMPs). sEMPs appear to activate NFκB signalling in endothelial cells. Finally, EMPs participate in paracrine CCL20 transport, acting as signalling molecules and participating in the cross-talk with the smooth muscle layer. PMPs: platelet microparticles; EMPs: endothelial microparticles; SMC: smooth muscle cell; CCL20: chemokine (C-C motif) ligand 20.

5.1.1.3. Study limitations

1. Although we have used the nomenclature of microparticles MPs in this study, there is a growing recognition to use the word term microvesicles to describe biological microparticles, since there is growing interest in the organ damage due to chemical air pollutants, which are also being described as microparticles. It is likely this thesis is the last of the documents from our group to use microparticles and the group will adopt the use of the term extracellular vesicles.

2. EMP isolation techniques can vary from laboratory to laboratory with the recognition for the need for consistency if the field is to develop with accuracy. Thus the isolation procedure has become more refined to separate apoptotic bodies, MPs and exosomes. However, for consistency with previous work in our laboratory, ultracentrifugation at 100,000 x g for 2 hours at 4 ºC to isolate EMPs was used. Although this short, high-speed ultracentrifugation was efficient at producing MPs, it is unlikely to be long enough to extract exosomes as well, although it is possible that the preparations used in this study contain a small amount of exosomes.

3. EMP levels vary between patients with different diseases, and are modulated to a different extent under distinct micro-environment conditions. Therefore, it is difficult to elucidate the appropriate concentration of EMPs/mL that should be used in *in vitro* assays. As such, effects may be EMP concentration dependent, but this was not investigated in this work.

4. Generating EMPs *in vitro* is a common practice in many laboratories, however by doing so, all the complexity from an *in vivo* system is removed. The *in vitro* system is designed so that the specific effects of a single stimuli can be determined more easily.

5. Despite the challenges in isolating microparticle populations from different cellular origins within patients, pursuing this MP isolation procedure from patients would allow for an in-depth analysis of the differences in proteomic and nucleic acid content of microparticles and their function in different patient and disease conditions.

5.1.2. EMPs as a potential link between endothelial dysfunction and vascular calcification

Given the prevalence and implications of vascular calcification in patients with SLE (231-233), and the fact that matrix vesicles have long been associated with the deposition of a mineralised matrix within the vessel wall as discussed in the insightful review by Aikawa and colleagues (234), it was of interest to establish whether EMPs could play a role in the cross-talk between the endothelium and smooth muscle cells. The results from this study suggest that AoEMPs are internalised by HCoASMCs and that they enhance calcification, partially via miRNA-3148, which is discussed in detail in the next sections.

5.1.2.1. AoEMPs as specific regulators of vascular calcification

Tracking EMPs from the extracellular space through the cell membrane to the cytoplasm has proven to be challenging. In an elegant study by Jansen *et al.*, Calcein-AM was used to track EMP internalisation by human coronary artery endothelial cells, where they described for the first time an AnnexinI/Phosphatidylserine receptor dependent uptake mechanism and a p38 dependant EMP-mediated protection against apoptosis (235). A second study, which used a similar technique for EMP tracking, found that ROCK-dependent, miRNA-rich MPs were effectively transferring their contents to HAoECs *in vitro* (85). In a third study in which the interactions between Calcein-AM-labelled PMPs and human brain endothelial cells *in vitro* were investigated, cytochalasin D was used to inhibit the microfilament formation involved in endocytosis, confirming that PMPs are taken up via mechanisms involving phagocytosis or macropinocytosis (236). Finally, Buendia *et al.* demonstrated that Calcein-AM-labelled TNFα-derived EMPs carry a high content of calcium and BMP-2, thereby inducing calcification of hVSMCs *in vitro* (188).

In this study, fluorescent microscopy was used to track Calcein-AM labelled AoEMPs and found that they are internalised by HCoASMCs (Figure 35). Our controls included Calcium-AM without AoEMPs, which showed no cellular uptake, thus indicating that the detected fluorescence was due to AoEMP uptake. Furthermore, the AoEMP uptake experiments were performed in pre-conditioned HCoASMCs in osteogenic media to ensure that EMP uptake was viable under these high calcium and phosphate conditions, since the vascular calcification experiments

were performed under these conditions. In this regard, an important limitation to our study and those performed by other groups, is the difficulty in demonstrating that AoEMPs are not increasing membrane permeabilisation and that the observed effects are due to the interaction between EMPs and HCoASMCs and the subsequent internalisation of bio-reactive molecules. Several authors have attempted to shed some light on this topic during the past five years using different techniques from tracking MPs (37, 237-240), but there is still no consensus and, as reviewed by Mulcahy *et al*. the mechanisms appear to be very diverse (130). For example, a study by Povero *et al*. used Calcein-AM labelled hepatocyte-derived MPs to track their uptake by HUVECs and concluded that this process is Vanin-1 dependant (240), whereas Lopez-Vilchez *et al.* used electron microscopy to describe the uptake of Tissue Factor rich MPs by platelets via CD36 receptor and serotonin transporter (239, 241). Recent work by Andrews and Rizo also used Calcein-AM labelled EMPs generated from TNFα-stimulated mouse lung endothelial cells on EMP-driven endothelial activation in caveolin-1 knockout endothelial cells, and concluded that such activation requires caveolin-1/caveolae (136). However, the question of how EMPs interact with target cells is beyond the scope of this study and time restraints did not permit this line of study, but will be investigated in the future.

SLE patients have increased risk of developing CVD and many studies have shown clear links between vascular calcification and SLE (232, 242, 243), however the mechanisms underpinning their relation are still unclear. A number of studies have established that inflammatory cytokines including IL-6, IL-8 and TNFα, which are also elevated in SLE, induce osteogenic differentiation and mineralisation of vascular cells *in vitro* and *in vivo*, suggesting this could be a possible mechanism for vascular calcification in SLE (244-246). In addition, circulating EMP levels are significantly higher in conditions where TNFα is elevated, such as in SLE patients compared to healthy controls, and may be a reflection of endothelial dysfunction, a key initiating factor in vessel disease. Therefore, we used an *in vitro* model of calcification to investigate the link between EMPs and vascular calcification using AoEMPs generated under inflammatory conditions. It was found that AoEMPs enhanced matrix mineralisation and calcium deposition of HCoASMCs after 3 weeks in osteogenic media (Figure 36), with a trend towards an increase in not only bone-related proteins, but the pro-inflammatory molecules, TNFα and IL-6 (Figure 37).

These findings are supported by a recent study by Buendia *et al.* who found that HUVEC-derived EMPs promoted calcification and mineralisation in hVSMCs (188). In this study, EMPs derived from HAoECs were used to investigate their effects on HCoASMCs. We acknowledge that it may have been of some advantage to carry out the same set of experiments using human coronary artery endothelial cells (HCoAECs) derived EMPs or HAoSMCs for EMP treatment, which would allow to study the effects EMPs have on calcification in different vascular beds, a concept that has been investigated and discussed in the literature. For example, Kang *et al.* used adipose tissue-derived MPs to study their effects on HUVECs, concluding that they have angiogenic properties mediated by miRNA-31 (247), or another study by Jansen *et al.*, in which the role of HCoAEC-derived MPs in atherosclerosis prone ApoE-/- mice was studied, concluding that hypoglycaemia increased EMP-mediated NADPH oxidase activity, thereby activating endothelial cells and promoting inflammation (248).

Osteogenesis and vascular calcification are highly regulated processes involving a myriad of transcription factors, proteins and secreted molecules, and it is often the balance between these molecules that determines cell fate (168, 169). As well as a range of promoters of vascular calcification, such as OCN, ALP, BMP-2 and BMP-4, there are a number of inhibitors, including OPG, OPN and MGP (167, 177). As extensively reviewed, overexpression of vascular calcification promoters is often accompanied by elevated levels of calcification inhibitors in calcified vessels, thus the balance between the two dictates whether calcification occurs (201, 249-251).

In this study, the effects of AoEMP treatment on the secretome of HCoASMCs was investigated using Bioplex suspension array analysis of conditioned media sampled throughout the 21-day experiment (Figure 37). IL-6 and TNFα were elevated throughout the 3-week duration of the experiments, which suggests that AoEMPs may be implicated in IL-6 and TNFα mediated osteoblastic differentiation. Although not significantly, secreted OPG levels are slightly reduced during the first week of treatment in AoEMP-treated cells compared to untreated cells. Such a prompt reduction in OPG levels would support an enhanced calcification at the end of the 3 weeks, despite elevated levels are detected towards the end of the experiment. Additionally, Maetzler *et al.* showed elevated microcalcification in an OPN knock-out mouse model, demonstrating the inhibitory effects of OPN in vascular calcification (174), and similar results were found by Speer *et al.* hVSMCs isolated

from aortas of OPN knock-out mice and showing that retroviral transduction of mouse OPN cDNA into OPN-/- hVSMCs reversed the calcifying phenotype (252). In the current study, OPN is mildly affected throughout the 3 weeks of the experiment in the AoEMP-treated cells compared to untreated controls. Finally, OCN, a well-known calcification promoter, is elevated at the early stages of the treatments. In combination, these observations suggest that AoEMPs reduce the secretion of the calcification inhibitor OPG, whereas they increase inflammatory molecules IL-6 and TNFα, as well as the calcification promoter OCN, thereby creating an imbalance between calcification inhibitors and promoters, ultimately leading to vascular calcification. The molecular mechanism underlying AoEMP-induced calcification was further investigated by analysis of the content of the EMPs and determining their function in SMC vascular calcification, an idea that is discussed in the next section, which provides a suggested mechanism of action of AoEMPs on HCoASMCs.

5.1.2.2. OPG as a suggested player in the mechanism of action underlying AoEMP-mediated calcification

In order to determine how AoEMPs enhanced smooth muscle cell calcification, the molecular components of AoEMPs were analysed since they could be responsible for the observed effects (Figures 38 – 40). Previous studies have demonstrated that EMPs carry proteins and miRNAs that contribute towards the calcification of smooth muscle cells (188, 253), but little is known about the mechanisms of action by which EMPs mediate their effects. As discussed previously, Buendia *et al.* found that BMP-2-rich HUVEC-derived EMPs were up-regulating the osteoblast transcription factor Cbfa1 and decreasing the hVSMC-specific protein SM22α, thereby enhancing smooth muscle cell calcification *in vitro*, and that knocking down BMP-2 in HUVECs produced non-mineralizing TNFα-derived EMPs (188). Recent studies using murine models of calcification showed that vascular calcification involves bone remodelling and the activation of both osteoclastic and osteoblastic differentiation, with OPG attenuating osteoclastic differentiation (167, 254, 255). Additionally, Panizo *et al.* demonstrated that cells lacking RANK showed no increase in vascular calcification when incubated with RANKL, suggesting that it enhances mineralisation and that such effects are attenuated by OPG, which acts as a decoy receptor for RANKL, thereby confirming the inhibitory role of OPG in the vascular calcification process (177, 249, 256).

Potentially AoEMP-driven mineralisation could be due to the Phosphatidylserine:Annexin complex acting as a nidus for mineralisation, or to the calcium being internalised by the cells in the form of EMPs. Buendia *et al.* reported that TNFα-derived EMPs (equivalent to sEMPs used in this study) carry elevated calcium in comparison to EMPs derived from untreated cells (unstimulated EMPs (uEMPs) (188). However, we found that both sEMPs and AoEMPs carry significantly less calcium than uEMPs (Figure 40). A possible reason for the discrepancy could be that Buendia *et al*. used 20 ng/mL of TNFα for EMP generation, whereas 10 ng/mL was used in this study. *In vitro* calcification models have been extensively used by various research groups to investigate vascular calcification, with most using high calcium (> 2.6 mM $CaCl^{2+}$) and phosphate conditions to investigate the molecular mechanisms underlying osteogenic differentiation of smooth muscle cells. Therefore, the contribution of EMPs to total Ca^{2+} levels is negligible in comparison to the high calcium levels in the media, and as such their uptake by the HCoASMCs and the subsequent release of such calcium intracellularly may be key in the EMP-enhanced calcification process. Further investigation could utilise chelation techniques on AoEMPs to assess the effects of calcium free EMPs.

It is currently accepted that EMPs carry not only nucleic acids such as miRNAs, but also functional proteins (42). In our proteomic study of AoEMP content, HGF previously described by our laboratory as an inducer of smooth muscle cell osteogenic differentiation (166), was found to be of high abundance. In such study, Liu *et al.* used adenoviral transfection techniques to overexpress HGF in hVSMCs isolated from limb amputations cultured in osteogenic media, and found that HGF enhances calcification via c-Met/Akt/Notch3 signalling (166). Additionally, matrix metalloproteinases MMP-1 and MMP-10, which have been associated with the degradation of the tunica intima, were also found in this proteomic screen. Previous studies have shown that MMP-1 plays an important role in cleaving fibrillar collagen type I, II and III, leading to the instability of the collagen fibres and its degradation by other members of the MMP family. In contrast, MMP-10 digests a number of extracellular matrix molecules and actively participates in MMP (including MMP-1) activation (257). Therefore, it could be suggested that MMP activity executed within the EMPs is a potential mechanism driving the cross-talk between the endothelial and the smooth muscle cell layer.

miRNAs are key regulators of diverse biological processes, and it is known that their dysregulation often results in impaired cell function and disease progression, and in some cases, vascular calcification (258, 259). A study by Balderman *et al.* reported that miRNA-30b/c, which targets and reduces the expression of the transcription factor Runx2, is downregulated via BMP-2 in HCoASMCs *in vitro*, thus inhibition of miRNA-30b/c led to matrix mineralisation (260). Another study by Raitoharju *et al.* found that, just like calcification promoters and inhibitors, miRNA expression of miRNA-21, miRNA-34a, miRNA-146a and miRNA-210 in calcified vessels is elevated in patients with coronary artery disease (261). As reviewed by Goettsch et al., MPs can often participate in the transport of miRNAs, thus participating in the regulation of calcification (200).

miRNA-3148, which was identified in our miRNA screen and was predicted to target OPG in a bioinformatic analysis and was validated using transfection studies, has also been associated with SLE (262) and heart failure patients (263). Our data also suggests that miRNA-3148 selectively targets OPG and in turn, enhances vascular calcification (Figures 43). HCoASMCs transfected with a miRNA precursor of miRNA-3148 showed reduced OPG mRNA levels compared to both untreated cells and scrambled control cells after 4 days. A reduction in OPG mRNA abundance can also be observed in AoEMP-treated cells, although the difference compared to untreated cells was not statistically significant. This may due to the fact that a longer and more frequent exposure to AoEMPs is needed in order to observe a statistically significant reduction in OPG mRNA in AoEMP-treated cells, and in this study, RNA was extracted after 4 days of AoEMP treatment, which was only carried out once at the beginning of the experiments.

The mRNA abundance of OPN (another calcification inhibitor) was significantly reduced in AoEMP-treated cells, suggesting that AoEMPs could have direct effects on OPN expression. A bioinformatic alignment discarded the possibility of miRNA-3148 targeting OPN, suggesting that AoEMPs enhance vascular calcification via a different miRNA to miRNA-3148. However, a reduction in OPN mRNA abundance levels was not observed in the miRNA-3148 transfected cells, suggesting the selective targeting of OPG. In addition, our data suggest that AoEMPs enhance the calcification promoter OCN mRNA abundance compared to untreated and scrambled control-transfected cells. Since secreted OCN is also elevated in conditioned media of AoEMP-treated cells after 4 and 7 days, it is likely that elevated

mRNA reflects the higher protein levels detected, and plays a key role in the mechanism of action in our model. On the other hand, mRNA abundance levels of C-met, which is the receptor of HGF and has been shown to be involved in HGF-accelerated hVSMC mineralisation *in vitro* (166), were found to be decreased both in AoEMP-treated and in miRNA-3148-transfected compared to untreated and scrambled control respectively. A bioinformatic alignment of miRNA-3148 and C-met discarded the possibility of miRNA-3148 also targeting C-met, thus suggesting that the regulation of C-met in AoEMPs is due to a different miRNA.

Finally, Alizarin Red S and calcium deposition assays were also performed 3 weeks after transfection with miRNA-3148 to determine whether its early effects on OPG mRNA abundance affect calcification. miRNA-3148 transfected cells showed enhanced calcification when compared to either untreated or scrambled control-transfected cells, which is comparable to the data observed in AoEMP-treated cells (Figure 44). Despite no statistically significant differences between AoEMP-treated and miRNA-3148-transfected cells, there appears to be a trend towards lower calcification in the miRNA-3148-transfected cells in comparison to the AoEMP-treated cells. This suggests that the AoEMPs could be carrying additional miRNAs or proteins that are regulating and enhancing their effects on calcification, and/or that there is an excess of AoEMPs, thus they act as a nidus for vascular calcification, as suggested in the past by Leopold *et al.* (159). The effect of miRNA-3148 could be further validated by transfecting the HCoASMCs with an inhibitor of miRNA-3148 in addition to treatment with AoEMPs, or by producing miRNA-3148-poor AoEMPs and determine their effects on vascular calcification, but due to time constraints this assay was unable to be performed.

As reviewed by Duncan and Richardson, exosomes, alongside EMPs, are active signalling molecules that participate in cell:cell communication (119). As such, a study by Kapustin *et al.* found that smooth muscle cell calcification is mediated by exosomes (264), and we acknowledge the possibility that our AoEMP preparations may also contain exosome-like particles. Moreover, other researchers have used RNAse treatments to investigate the relevance of the nucleic acid content on the final role of EMPs on their targets (265-267), which in combination with chelation techniques, should provide further information as to which one of the 3 main components of AoEMPs (proteins, calcium and nucleic acids) is the major regulator of the calcification process.

Vascular calcification is the consequence of a combination of several molecular factors and this study has shown that EMPs also play a regulatory role in such process. A summary of the findings from this study and the suggested mechanism of action is illustrated in Figure 46.

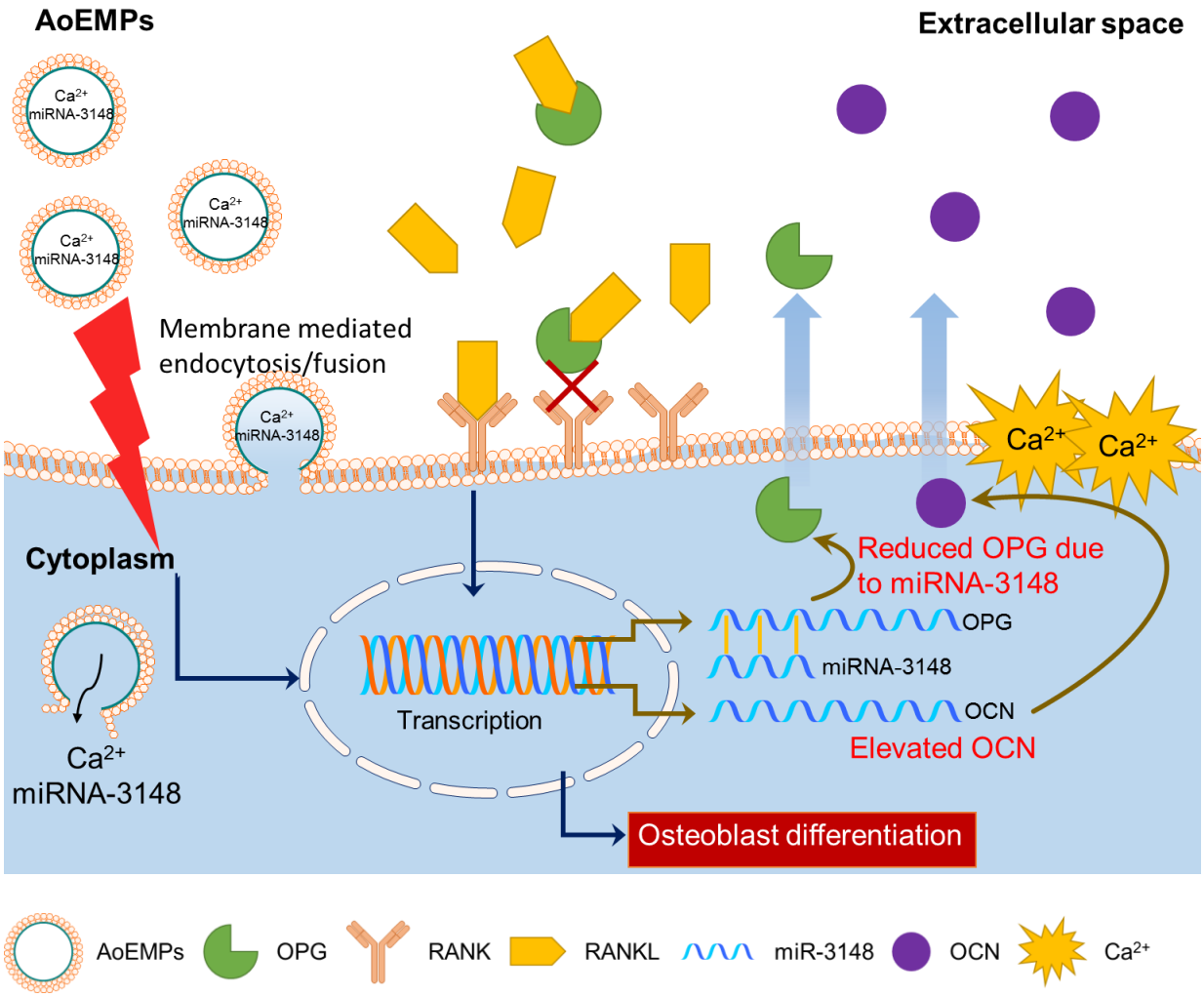

Figure 46. Proposed dual mechanism of action in AoEMP-enhanced smooth muscle cell calcification. AoEMPs are internalised by HCoASMCs and their content is released in the cytoplasm. AoEMPs carry Ca^{2+} and miRNA-3148, which targets and reduces translation of the vascular calcification inhibitor protein, OPG, during the first stages of calcification, thereby contributing to enhanced vascular calcification. Additionally, AoEMPs elevate the calcification promoter OCN mRNA and protein levels. OPG: osteoprotegerin; OCN: osteocalcin; RANK: receptor activator of nuclear factor kappa-B; RANKL: receptor activator of nuclear factor kappa-B ligand.

5.1.2.3. Study limitations

1. This study used an *in vitro* model of calcification which gives no distinctive findings for the spatial distribution which occurs *in vivo*, with regard to intimal calcification that occurs within atherosclerotic plaques nor medial calcification, which is more prevalent in the renal clinic, an area reviewed elsewhere (268, 269).
2. The *in vitro* calcification model involves 3 week long experiments and calcification in patients is predominantly associated with the ageing population and occurs over a longer period of time. Therefore, whether the *in vitro* model truly reflects what is happening physiologically is a challenge.
3. EMP production *in vitro* is a time and labour intensive process, requiring the growth and maintenance of primary human vascular cells, so the generation of this molecular tool for experimentation needed to be carried out with extreme care and precision to remove any heterogeneity that may have been introduced artefactually.
4. Despite confirming that miRNA-3148 selectively targets OPG, it is possible that this miRNA has differential effects on other cell types/targets. Therefore, further characterisation of its effects is needed before its therapeutic value can be carefully assessed.
5. Mechanistic conclusions involving OPG and OCN regulation were only performed in HCoASMC cells after 4 days in culture. Similarly, secretome analysis only reported elevated OCN levels after 4 and 7 days. A more detailed time-course should have been carried out should more time have been available.
6. Calcium scores in SLE patients are not measured as a routine clinical measure. However, the link between SLE and vascular calcification is becoming more apparent and this work would suggest that it is of potential interest to investigate further in the future.
7. The use of isolated smooth muscle cells from patients with and without calcification would be of extreme interest. However, given that this study focused on patients with SLE with no tissue available from these patients, this avenue was not pursued. However, future work will identify SLE patients with and without calcification using imaging techniques and establish their systemic secretome and effects of serum on SMCs from different vascular beds.

5.2. Conclusions

Endothelial dysfunction refers to the inability of the endothelium to vasodilate and contract, as well as to its incapacity to control inflammation, cell proliferation and thrombosis. SLE is associated with accelerated vascular ageing and endothelial dysfunction. Several studies have investigated the role of EMPs in a range of disease contexts, including SLE, in which they are found to be reduced following treatment (27, 33). In contrast, vascular calcification refers to mineral deposition in the vascular system, leading to reduced elasticity and increased vascular stiffness. Accelerated vascular ageing and calcification are present in a number of diseases and a positive correlation with CVD is well established (270, 271). This study has used an *in vitro* model of inflammation and vascular calcification to investigate the role of EMPs on endothelial function and vascular calcification, and the mechanisms/molecular components whereby they exert their effects. The results demonstrate an association between the distinct role of EMPs and their different origin and mechanism of generation, which has an important impact on their molecular components, as well as a role in the regulation of endothelial function and vascular calcification. Therefore, the original objectives of this project have been met and the main findings are as follows:

1. sEMPs enhance EMP release, whereas uEMPs do not. However, uEMPs attenuate TNFα-driven EMP release (Figure 27), suggesting that EMPs in SLE could partially be responsible for the elevated circulating EMP levels, as they may be governing EMP generation.

2. sEMPs and uEMPs enhance cell migration, but not proliferation (Figure 28). Also, uEMPs and sEMPs modulate VCAM-1 and ICAM-1 mRNA abundance on HUVECs, but such effects are not found at a protein level (Figures 29 & 30), suggesting that the diverse content of the uEMPs and sEMPs is regulating VCAM-1 and ICAM-1 at the protein level or that HUVECs protect themselves from EMP-mediated VCAM-1 and ICAM-1 expression.

3. The NFκB pathway is activated by sEMPs, but not uEMPs (Figures 31 – 34), suggesting that EMPs generated from different stimuli mediate their effects via different mechanisms of action.

4. sEMPs carry elevated CCL20 and reduced miRNA-129-5p compared to uEMPs (Figures 19 – 22). Despite a bioinformatic prediction, transfection

studies confirmed that miRNA-129-5p does not target CCL20 mRNA (Figures 23 – 26), suggesting that a different mechanism is responsible for reduced CCL20 levels in TNFα + uEMP-treated HUVECs.

5. Fluorescent microscopy confirmed that Calcein-AM-labelled AoEMPs are internalised (Figure 35). Alizarin Red S staining showed that AoEMPs enhance HCoASMCs calcification (matrix mineralisation), and Bioplex suspension arrays demonstrated that they also modulate their secretome during the process (Figures 35 – 37), potentially via miRNA-3148.

6. Transfection studies based on a bioinformatic prediction confirmed that miRNA-3148 targets OPG and is partially responsible for AoEMP-driven calcification (Figures 41 – 44)

5.3. Future work

This study has shown that EMPs contribute to both endothelial function and vascular calcification and have differential effects on endothelial function depending on their origin. Clearly, some interesting questions have arisen from this study and will form the basis of future hypothesis-driven investigations regarding the underlying molecular mechanism of action of EMPs in endothelial dysfunction and vascular calcification. For example:

- **Why do uEMPs attenuate TNFα-mediated EMP production?**

Our results suggest that sEMPs, but not uEMPs, have a direct self-feedback effect and are responsible for the elevated EMP levels observed in inflammatory diseases, as they appear to enhance EMP generation. Of note, uEMPs attenuate TNFα-driven EMP release, which raises questions underlying the mechanisms leading to EMP release and the molecular components responsible for such a response. Future work will investigate the outside-in effects of uEMPs and sEMPs through to the NFκB pathway, as a potential means to explain these observations (46). For example, it has been suggested that EMPs may activate the p38 mitogen-activated protein kinase pathway which is cytoplasmic and could in turn, be involved in both EMP release (47) and NFκB trafficking to the nucleus.

- **What other key miRNAs/proteins in uEMPs/sEMPs are responsible for their functional effects?**

This study demonstrates that EMPs from different origin and generated via different stimuli carry distinct molecular components (miRNAs and proteins). A future study could investigate the effects of a distinct miRNA of choice. For example, miRNA-129-5p was identified in a miRNA screening and a analysis bioinformatic analysis predicted that it could target CCL20, which was elevated in sEMPs compared to uEMPs and in sEMP-treated HUVECs compared to uEMP-treated cells; therefore, this and other miRNAs may also be playing a role in regulating CCL20 expression and in turn influence pathological processes, such as the enhanced cell migration capacity or activation of the NFκB pathway.

- **Do EMPs carry active/functional matrix metalloproteinases that activate the pathological cross-talk between the endothelium and the smooth muscle layer?**

This study is one of the first studies investigating the effects of EMPs on both endothelial function and vascular calcification and the cross-talk in the vessel wall. Our proteomic screening identified MMP-1 and MMP-10 in the AoEMPs. The results from our MMP activity assays are not conclusive and are not presented in this thesis. However, other authors have identified MMP activity in EMPs (123, 272). We suggest performing Gel Zymography studies of different EMP populations/subsets in order to determine their ability to degrade the intimal layer.

- **Does miRNA-3148 decrease OPG protein levels?**

OPG is a negative regulator of vascular calcification that plays a key role in osteoblast differentiation. This study described for the first time the role of miRNA-3148 in vascular calcification, and confirmed a bioinformatic prediction on its target OPG. Due to time constraints, we were unable to investigate whether miRNA-3148 had effects on OPG protein levels, and ultimately in the RANKL pathway, to confirm a mechanistic link with OPG and calcification. Additionally, and to further validate the role of miRNA-3148 in enhancing calcification, we suggest either transfecting HCoASMCs with anti-miRNA-3148 and co-treat with AoEMPs, or using a viral vector to knockdown miRNA-3148 in HAoECs and produce miRNA-3148 poor AoEMPs.

- **Which other molecular components of AoEMPs contribute towards a calcification phenotype?**

It is well established that a myriad of promoters and inhibitors regulate vascular calcification. Previous studies in our laboratory described the role of HGF/C-met in increased microvessel density within plaques and vascular calcification, and concluded that HGF could play a role as a promoter of this pathology (166, 273). In the current study, it would appear that AoEMPs contain HGF among other proteins, therefore it would be interesting to further investigate the effects of HGF-containing EMPs in vascular calcification using a pharmacological inhibitor of the C-met receptor or a genetic approach using siRNA against the C-met receptor. This study also found that AoEMPs reduce mRNA abundance of the calcification inhibitor OPN. Therefore, it would be of interest to carry out bioinformatic analysis of the other miRNAs identified in this study in order to investigate their role in the regulation of OPN. Finally, the effects of the Ca^{2+} carried by AoEMPs could be further explored by using a chelation technique to remove calcium in order to describe its relevance in the SMC phenotypic switching.

These studies would add to our understanding and provide valuable information on the role of EMPs on endothelial function and vascular calcification both in health and disease, and would contribute towards understanding the value of EMPs as biomarkers of disease or therapeutic targets in the near future.

CHAPTER 6:
REFERENCES

CHAPTER 6: REFERENCES

1. Manzi S, Meilahn EN, Rairie JE, Conte CG, Medsger TA, Jr., Jansen-McWilliams L, et al. Age-specific incidence rates of myocardial infarction and angina in women with systemic lupus erythematosus: comparison with the Framingham Study. Am J Epidemiol. 1997;145(5):408-15.
2. Gaubitz M. Epidemiology of connective tissue disorders. Rheumatology (Oxford). 2006;45 Suppl 3:iii3-4.
3. Font J, Cervera R. 1982 revised criteria for classification of systemic lupus erythematosus--ten years later. Lupus. 1993;2(5):339-41; discussion 43.
4. Bruce IN. Re-evaluation of biologic therapies in systemic lupus erythematosus. Curr Opin Rheumatol. 2010;22(3):273-7.
5. Behrendt D, Ganz P. Endothelial function. From vascular biology to clinical applications. Am J Cardiol. 2002;90(10C):40L-8L.
6. El-Magadmi M, Bodill H, Ahmad Y, Durrington PN, Mackness M, Walker M, et al. Systemic lupus erythematosus: an independent risk factor for endothelial dysfunction in women. Circulation. 2004;110(4):399-404.
7. Blausen.com staff. Medical gallery of Blausen Medical 2014. Wikijournal of Medicine. 2014;1(2).
8. Skamra C, Ramsey-Goldman R. Management of cardiovascular complications in systemic lupus erythematosus. Int J Clin Rheumtol. 2010;5(1):75-100.
9. Kerekes G, Szekanecz Z, Der H, Sandor Z, Lakos G, Muszbek L, et al. Endothelial dysfunction and atherosclerosis in rheumatoid arthritis: a multiparametric analysis using imaging techniques and laboratory markers of inflammation and autoimmunity. J Rheumatol. 2008;35(3):398-406.
10. Schiro A, Wilkinson FL, Weston R, Smyth JV, Serracino-Inglott F, Alexander MY. Endothelial microparticles as conveyors of information in atherosclerotic disease. Atherosclerosis. 2014;234(2):295-302.
11. Aringer M, Smolen JS. The role of tumor necrosis factor-alpha in systemic lupus erythematosus. Arthritis Res Ther. 2008;10(1):202.
12. Chatzidakis I, Mamalaki C. T cells as sources and targets of TNF: implications for immunity and autoimmunity. Curr Dir Autoimmun. 2010;11:105-18.

13. Zucali JR, Elfenbein GJ, Barth KC, Dinarello CA. Effects of human interleukin 1 and human tumor necrosis factor on human T lymphocyte colony formation. J Clin Invest. 1987;80(3):772-7.
14. Aringer M, Smolen JS. SLE - Complex cytokine effects in a complex autoimmune disease: tumor necrosis factor in systemic lupus erythematosus. Arthritis Res Ther. 2003;5(4):172-7.
15. Ronnblom L, Elkon KB. Cytokines as therapeutic targets in SLE. Nat Rev Rheumatol. 2010;6(6):339-47.
16. Postal M, Appenzeller S. The role of Tumor Necrosis Factor-alpha (TNF-alpha) in the pathogenesis of systemic lupus erythematosus. Cytokine. 2011;56(3):537-43.
17. Gabay C, Cakir N, Moral F, Roux-Lombard P, Meyer O, Dayer JM, et al. Circulating levels of tumor necrosis factor soluble receptors in systemic lupus erythematosus are significantly higher than in other rheumatic diseases and correlate with disease activity. J Rheumatol. 1997;24(2):303-8.
18. Kontoyiannis D, Kollias G. Accelerated autoimmunity and lupus nephritis in NZB mice with an engineered heterozygous deficiency in tumor necrosis factor. Eur J Immunol. 2000;30(7):2038-47.
19. Sterner-Kock A, Braun RK, Schrenzel MD, Hyde DM. Recombinant tumour necrosis factor-alpha and platelet-activating factor synergistically increase intercellular adhesion molecule-1 and E-selectin-dependent neutrophil adherence to endothelium in vitro. Immunology. 1996;87(3):454-60.
20. Bradley JR. TNF-mediated inflammatory disease. J Pathol. 2008;214(2):149-60.
21. Heathfield SK, Parker B, Zeef LA, Bruce IN, Alexander MY. Certolizumab pegol attenuates the pro-inflammatory state in endothelial cells in a manner that is atheroprotective. Clin Exp Rheumatol. 2013;31(2):225-33.
22. McCarthy EM, Smith S, Lee RZ, Cunnane G, Doran MF, Donnelly S, et al. The association of cytokines with disease activity and damage scores in systemic lupus erythematosus patients. Rheumatology (Oxford). 2014;53(9):1586-94.
23. Raposo G, Stoorvogel W. Extracellular vesicles: exosomes, microvesicles, and friends. J Cell Biol. 2013;200(4):373-83.

24. Zaborowski MP, Balaj L, Breakefield XO, Lai CP. Extracellular Vesicles: Composition, Biological Relevance, and Methods of Study. Bioscience. 2015;65(8):783-97.
25. S ELA, Mager I, Breakefield XO, Wood MJ. Extracellular vesicles: biology and emerging therapeutic opportunities. Nat Rev Drug Discov. 2013;12(5):347-57.
26. Sellam J, Proulle V, Jungel A, Ittah M, Miceli Richard C, Gottenberg JE, et al. Increased levels of circulating microparticles in primary Sjogren's syndrome, systemic lupus erythematosus and rheumatoid arthritis and relation with disease activity. Arthritis Res Ther. 2009;11(5):R156.
27. McCarthy EM, Wilkinson FL, Parker B, Alexander MY. Endothelial microparticles: Pathogenic or passive players in endothelial dysfunction in autoimmune rheumatic diseases? Vascul Pharmacol. 2016.
28. Boulanger CM, Amabile N, Tedgui A. Circulating microparticles: a potential prognostic marker for atherosclerotic vascular disease. Hypertension. 2006;48(2):180-6.
29. Hugel B, Martinez MC, Kunzelmann C, Freyssinet JM. Membrane microparticles: two sides of the coin. Physiology (Bethesda). 2005;20:22-7.
30. Baron M, Boulanger CM, Staels B, Tailleux A. Cell-derived microparticles in atherosclerosis: biomarkers and targets for pharmacological modulation? Journal of cellular and molecular medicine. 2012;16(7):1365-76.
31. Lacroix R, Judicone C, Mooberry M, Boucekine M, Key NS, Dignat-George F. Standardization of pre-analytical variables in plasma microparticle determination: results of the International Society on Thrombosis and Haemostasis SSC Collaborative workshop. Journal of thrombosis and haemostasis : JTH. 2013:1190-3.
32. van Ierssel SH, Van Craenenbroeck EM, Conraads VM, Van Tendeloo VF, Vrints CJ, Jorens PG, et al. Flow cytometric detection of endothelial microparticles (EMP): effects of centrifugation and storage alter with the phenotype studied. Thrombosis research. 2010;125(4):332-9.
33. Parker B, Al-Husain A, Pemberton P, Yates AP, Ho P, Gorodkin R, et al. Suppression of inflammation reduces endothelial microparticles in active systemic lupus erythematosus. Ann Rheum Dis. 2014;73(6):1144-50.
34. Nomura S, Shouzu A, Taomoto K, Togane Y, Goto S, Ozaki Y, et al. Assessment of an ELISA kit for platelet-derived microparticles by joint

research at many institutes in Japan. J Atheroscler Thromb. 2009;16(6):878-87.

35. Nomura S, Shimizu M. Clinical significance of procoagulant microparticles. J Intensive Care. 2015;3(1):2.
36. Paudel KR, Panth N, Kim DW. Circulating Endothelial Microparticles: A Key Hallmark of Atherosclerosis Progression. Scientifica (Cairo). 2016;2016:8514056.
37. Barteneva NS, Fasler-Kan E, Bernimoulin M, Stern JN, Ponomarev ED, Duckett L, et al. Circulating microparticles: square the circle. BMC Cell Biol. 2013;14:23.
38. Berckmans RJ, Nieuwland R, Boing AN, Romijn FP, Hack CE, Sturk A. Cell-derived microparticles circulate in healthy humans and support low grade thrombin generation. Thromb Haemost. 2001;85(4):639-46.
39. Flaumenhaft R, Dilks JR, Richardson J, Alden E, Patel-Hett SR, Battinelli E, et al. Megakaryocyte-derived microparticles: direct visualization and distinction from platelet-derived microparticles. Blood. 2009;113(5):1112-21.
40. Marchini JF, Miyakawa AA, Tarasoutchi F, Krieger JE, Lemos P, Croce K. Endothelial, platelet, and macrophage microparticle levels do not change acutely following transcatheter aortic valve replacement. J Negat Results Biomed. 2016;15:7.
41. Combes V, Simon aC, Grau GE, Arnoux D, Camoin L, Sabatier F, et al. In vitro generation of endothelial microparticles and possible prothrombotic activity in patients with lupus anticoagulant. The Journal of clinical investigation. 1999;104(1):93-102.
42. Dignat-George F, Boulanger CM. The many faces of endothelial microparticles. Arteriosclerosis, thrombosis, and vascular biology. 2011;31(1):27-33.
43. Morel O, Morel N, Jesel L, Freyssinet JM, Toti F. Microparticles: a critical component in the nexus between inflammation, immunity, and thrombosis. Semin Immunopathol. 2011;33(5):469-86.
44. Lee SK, Yang SH, Kwon I, Lee OH, Heo JH. Role of tumour necrosis factor receptor-1 and nuclear factor-kappaB in production of TNF-alpha-induced pro-inflammatory microparticles in endothelial cells. Thromb Haemost. 2014;112(3):580-8.

45. Pasquet JM, Dachary-Prigent J, Nurden AT. Calcium influx is a determining factor of calpain activation and microparticle formation in platelets. Eur J Biochem. 1996;239(3):647-54.
46. Sapet C, Simoncini S, Loriod B, Puthier D, Sampol J, Nguyen C, et al. Thrombin-induced endothelial microparticle generation: identification of a novel pathway involving ROCK-II activation by caspase-2. Blood. 2006;108(6):1868-76.
47. Curtis AM, Wilkinson PF, Gui M, Gales TL, Hu E, Edelberg JM. p38 mitogen-activated protein kinase targets the production of proinflammatory endothelial microparticles. J Thromb Haemost. 2009;7(4):701-9.
48. Brodsky SV, Zhang F, Nasjletti A, Goligorsky MS. Endothelium-derived microparticles impair endothelial function in vitro. Am J Physiol Heart Circ Physiol. 2004;286(5):H1910-5.
49. Mostefai HA, Agouni A, Carusio N, Mastronardi ML, Heymes C, Henrion D, et al. Phosphatidylinositol 3-kinase and xanthine oxidase regulate nitric oxide and reactive oxygen species productions by apoptotic lymphocyte microparticles in endothelial cells. J Immunol. 2008;180(7):5028-35.
50. Mezentsev A, Merks RMH, O'Riordan E, Chen J, Mendelev N, Goligorsky MS, et al. Endothelial microparticles affect angiogenesis in vitro: role of oxidative stress. Am J Physiol Heart Circ Physiol. 2005;289(3):H1106-14.
51. Kim HK, Song KS, Chung JH, Lee KR, Lee SN. Platelet microparticles induce angiogenesis in vitro. Br J Haematol. 2004;124(3):376-84.
52. Distler JH, Huber LC, Hueber AJ, Reich CF, 3rd, Gay S, Distler O, et al. The release of microparticles by apoptotic cells and their effects on macrophages. Apoptosis. 2005;10(4):731-41.
53. Curtis AM, Edelberg J, Jonas R, Rogers WT, Moore JS, Syed W, et al. Endothelial microparticles: sophisticated vesicles modulating vascular function. Vasc Med. 2013;18(4):204-14.
54. Wajant H, Pfizenmaier K, Scheurich P. Tumor necrosis factor signaling. Cell Death Differ. 2003;10(1):45-65.
55. Chen G, Goeddel DV. TNF-R1 signaling: a beautiful pathway. Science. 2002;296(5573):1634-5.
56. Hoesel B, Schmid JA. The complexity of NF-kappaB signaling in inflammation and cancer. Mol Cancer. 2013;12:86.

57. Bernimoulin M, Waters EK, Foy M, Steele BM, Sullivan M, Falet H, et al. Differential stimulation of monocytic cells results in distinct populations of microparticles. J Thromb Haemost. 2009;7(6):1019-28.
58. Cerri C, Chimenti D, Conti I, Neri T, Paggiaro P, Celi A. Monocyte/macrophage-derived microparticles up-regulate inflammatory mediator synthesis by human airway epithelial cells. J Immunol. 2006;177(3):1975-80.
59. Enjeti AK, Lincz L, Seldon M. Bio-maleimide as a generic stain for detection and quantitation of microparticles. Int J Lab Hematol. 2008;30(3):196-9.
60. Jimenez JJ, Jy W, Mauro LM, Soderland C, Horstman LL, Ahn YS. Endothelial cells release phenotypically and quantitatively distinct microparticles in activation and apoptosis. Thromb Res. 2003;109(4):175-80.
61. MacKenzie A, Wilson HL, Kiss-Toth E, Dower SK, North RA, Surprenant A. Rapid secretion of interleukin-1beta by microvesicle shedding. Immunity. 2001;15(5):825-35.
62. Pizzirani C, Ferrari D, Chiozzi P, Adinolfi E, Sandona D, Savaglio E, et al. Stimulation of P2 receptors causes release of IL-1beta-loaded microvesicles from human dendritic cells. Blood. 2007;109(9):3856-64.
63. Berda-Haddad Y, Robert S, Salers P, Zekraoui L, Farnarier C, Dinarello CA, et al. Sterile inflammation of endothelial cell-derived apoptotic bodies is mediated by interleukin-1alpha. Proc Natl Acad Sci U S A. 2011;108(51):20684-9.
64. Gulinelli S, Salaro E, Vuerich M, Bozzato D, Pizzirani C, Bolognesi G, et al. IL-18 associates to microvesicles shed from human macrophages by a LPS/TLR-4 independent mechanism in response to P2X receptor stimulation. Eur J Immunol. 2012;42(12):3334-45.
65. Hasegawa H, Thomas HJ, Schooley K, Born TL. Native IL-32 is released from intestinal epithelial cells via a non-classical secretory pathway as a membrane-associated protein. Cytokine. 2011;53(1):74-83.
66. Zhang HG, Liu C, Su K, Yu S, Zhang L, Zhang S, et al. A membrane form of TNF-alpha presented by exosomes delays T cell activation-induced cell death. J Immunol. 2006;176(12):7385-93.
67. Kandere-Grzybowska K, Letourneau R, Kempuraj D, Donelan J, Poplawski S, Boucher W, et al. IL-1 induces vesicular secretion of IL-6 without degranulation from human mast cells. J Immunol. 2003;171(9):4830-6.

68. Taraboletti G, D'Ascenzo S, Giusti I, Marchetti D, Borsotti P, Millimaggi D, et al. Bioavailability of VEGF in tumor-shed vesicles depends on vesicle burst induced by acidic pH. Neoplasia. 2006;8(2):96-103.
69. Baj-Krzyworzeka M, Weglarczyk K, Mytar B, Szatanek R, Baran J, Zembala M. Tumour-derived microvesicles contain interleukin-8 and modulate production of chemokines by human monocytes. Anticancer Res. 2011;31(4):1329-35.
70. Chen T, Guo J, Yang M, Zhu X, Cao X. Chemokine-containing exosomes are released from heat-stressed tumor cells via lipid raft-dependent pathway and act as efficient tumor vaccine. J Immunol. 2011;186(4):2219-28.
71. Valadi H, Ekstrom K, Bossios A, Sjostrand M, Lee JJ, Lotvall JO. Exosome-mediated transfer of mRNAs and microRNAs is a novel mechanism of genetic exchange between cells. Nat Cell Biol. 2007;9(6):654-9.
72. Georgantas RW, 3rd, Hildreth R, Morisot S, Alder J, Liu CG, Heimfeld S, et al. CD34+ hematopoietic stem-progenitor cell microRNA expression and function: a circuit diagram of differentiation control. Proc Natl Acad Sci U S A. 2007;104(8):2750-5.
73. Camaioni C, Gustapane M, Cialdella P, Della Bona R, Biasucci LM. Microparticles and microRNAs: new players in the complex field of coagulation. Internal and emergency medicine. 2013;8(4):291-6.
74. Lee Y, Kim M, Han J, Yeom KH, Lee S, Baek SH, et al. MicroRNA genes are transcribed by RNA polymerase II. EMBO J. 2004;23(20):4051-60.
75. Diederichs S, Haber DA. Dual role for argonautes in microRNA processing and posttranscriptional regulation of microRNA expression. Cell. 2007;131(6):1097-108.
76. Carthew RW, Sontheimer EJ. Origins and Mechanisms of miRNAs and siRNAs. Cell. 2009;136(4):642-55.
77. Kim VN, Han J, Siomi MC. Biogenesis of small RNAs in animals. Nat Rev Mol Cell Biol. 2009;10(2):126-39.
78. Nahid MA, Pauley KM, Satoh M, Chan EK. miR-146a is critical for endotoxin-induced tolerance: IMPLICATION IN INNATE IMMUNITY. J Biol Chem. 2009;284(50):34590-9.
79. Nahid MA, Satoh M, Chan EK. Mechanistic role of microRNA-146a in endotoxin-induced differential cross-regulation of TLR signaling. J Immunol. 2011;186(3):1723-34.

80. Boldin MP, Taganov KD, Rao DS, Yang L, Zhao JL, Kalwani M, et al. miR-146a is a significant brake on autoimmunity, myeloproliferation, and cancer in mice. J Exp Med. 2011;208(6):1189-201.
81. Jansen F, Yang X, Hoelscher M, Cattelan A, Schmitz T, Proebsting S, et al. Endothelial microparticle-mediated transfer of MicroRNA-126 promotes vascular endothelial cell repair via SPRED1 and is abrogated in glucose-damaged endothelial microparticles. Circulation. 2013;128(18):2026-38.
82. Jansen F, Wang H, Przybilla D, Franklin BS, Dolf A, Pfeifer P, et al. Vascular endothelial microparticles-incorporated microRNAs are altered in patients with diabetes mellitus. Cardiovasc Diabetol. 2016;15:49.
83. Thum T, Gross C, Fiedler J, Fischer T, Kissler S, Bussen M, et al. MicroRNA-21 contributes to myocardial disease by stimulating MAP kinase signalling in fibroblasts. Nature. 2008;456(7224):980-4.
84. Fichtlscherer S, De Rosa S, Fox H, Schwietz T, Fischer A, Liebetrau C, et al. Circulating microRNAs in patients with coronary artery disease. Circ Res. 2010;107(5):677-84.
85. Alexy T, Rooney K, Weber M, Gray WD, Searles CD. TNF-alpha alters the release and transfer of microparticle-encapsulated miRNAs from endothelial cells. Physiol Genomics. 2014;46(22):833-40.
86. Corsten MF, Dennert R, Jochems S, Kuznetsova T, Devaux Y, Hofstra L, et al. Circulating MicroRNA-208b and MicroRNA-499 reflect myocardial damage in cardiovascular disease. Circ Cardiovasc Genet. 2010;3(6):499-506.
87. Liang H, Yan X, Pan Y, Wang Y, Wang N, Li L, et al. MicroRNA-223 delivered by platelet-derived microvesicles promotes lung cancer cell invasion via targeting tumor suppressor EPB41L3. Mol Cancer. 2015;14:58.
88. Landry P, Plante I, Ouellet DL, Perron MP, Rousseau G, Provost P. Existence of a microRNA pathway in anucleate platelets. Nat Struct Mol Biol. 2009;16(9):961-6.
89. Tijsen AJ, Creemers EE, Moerland PD, de Windt LJ, van der Wal AC, Kok WE, et al. MiR423-5p as a circulating biomarker for heart failure. Circ Res. 2010;106(6):1035-9.
90. Bandres E, Bitarte N, Arias F, Agorreta J, Fortes P, Agirre X, et al. microRNA-451 regulates macrophage migration inhibitory factor production and

proliferation of gastrointestinal cancer cells. Clin Cancer Res. 2009;15(7):2281-90.

91. Ikeda S, Kong SW, Lu J, Bisping E, Zhang H, Allen PD, et al. Altered microRNA expression in human heart disease. Physiol Genomics. 2007;31(3):367-73.
92. Diehl P, Fricke A, Sander L, Stamm J, Bassler N, Htun N, et al. Microparticles: major transport vehicles for distinct microRNAs in circulation. Cardiovasc Res. 2012;93(4):633-44.
93. Li S, Ren J, Xu N, Zhang J, Geng Q, Cao C, et al. MicroRNA-19b functions as potential anti-thrombotic protector in patients with unstable angina by targeting tissue factor. J Mol Cell Cardiol. 2014;75:49-57.
94. Zhou W, Fong MY, Min Y, Somlo G, Liu L, Palomares MR, et al. Cancer-secreted miR-105 destroys vascular endothelial barriers to promote metastasis. Cancer Cell. 2014;25(4):501-15.
95. Alexander M, Hu R, Runtsch MC, Kagele DA, Mosbruger TL, Tolmachova T, et al. Exosome-delivered microRNAs modulate the inflammatory response to endotoxin. Nat Commun. 2015;6:7321.
96. Zernecke A, Bidzhekov K, Noels H, Shagdarsuren E, Gan L, Denecke B, et al. Delivery of microRNA-126 by apoptotic bodies induces CXCL12-dependent vascular protection. Sci Signal. 2009;2(100):ra81.
97. Hunter MP, Ismail N, Zhang X, Aguda BD, Lee EJ, Yu L, et al. Detection of microRNA expression in human peripheral blood microvesicles. PLoS One. 2008;3(11):e3694.
98. Fernandez-Messina L, Gutierrez-Vazquez C, Rivas-Garcia E, Sanchez-Madrid F, de la Fuente H. Immunomodulatory role of microRNAs transferred by extracellular vesicles. Biol Cell. 2015;107(3):61-77.
99. Christersson C, Johnell M, Siegbahn A. Evaluation of microparticles in whole blood by multicolour flow cytometry assay. Scand J Clin Lab Invest. 2013;73(3):229-39.
100. Connor DE, Exner T, Ma DD, Joseph JE. The majority of circulating platelet-derived microparticles fail to bind annexin V, lack phospholipid-dependent procoagulant activity and demonstrate greater expression of glycoprotein Ib. Thromb Haemost. 2010;103(5):1044-52.
101. Ayers L, Kohler M, Harrison P, Sargent I, Dragovic R, Schaap M, et al. Measurement of circulating cell-derived microparticles by flow cytometry:

sources of variability within the assay. Thrombosis research. 2011;127(4):370-7.

102. Shet AS, Aras O, Gupta K, Hass MJ, Rausch DJ, Saba N, et al. Sickle blood contains tissue factor-positive microparticles derived from endothelial cells and monocytes. Blood. 2003;102(7):2678-83.

103. Nieuwland R, Berckmans RJ, McGregor S, Boing AN, Romijn FP, Westendorp RG, et al. Cellular origin and procoagulant properties of microparticles in meningococcal sepsis. Blood. 2000;95(3):930-5.

104. Feng B, Chen Y, Luo Y, Chen M, Li X, Ni Y. Circulating level of microparticles and their correlation with arterial elasticity and endothelium-dependent dilation in patients with type 2 diabetes mellitus. Atherosclerosis. 2010;208(1):264-9.

105. Skeppholm M, Mobarrez F, Malmqvist K, Wallen H. Platelet-derived microparticles during and after acute coronary syndrome. Thromb Haemost. 2012;107(6):1122-9.

106. Bulut D, Tuns H, Mugge A. CD31+/Annexin V+ microparticles in healthy offsprings of patients with coronary artery disease. Eur J Clin Invest. 2009;39(1):17-22.

107. Joop K, Berckmans RJ, Nieuwland R, Berkhout J, Romijn FP, Hack CE, et al. Microparticles from patients with multiple organ dysfunction syndrome and sepsis support coagulation through multiple mechanisms. Thromb Haemost. 2001;85(5):810-20.

108. Leroyer AS, Ebrahimian TG, Cochain C, Recalde A, Blanc-Brude O, Mees B, et al. Microparticles from ischemic muscle promotes postnatal vasculogenesis. Circulation. 2009;119(21):2808-17.

109. Arteaga RB, Chirinos JA, Soriano AO, Jy W, Horstman L, Jimenez JJ, et al. Endothelial microparticles and platelet and leukocyte activation in patients with the metabolic syndrome. Am J Cardiol. 2006;98(1):70-4.

110. Belmont HM, Buyon J, Giorno R, Abramson S. Up-regulation of endothelial cell adhesion molecules characterizes disease activity in systemic lupus erythematosus. The Shwartzman phenomenon revisited. Arthritis Rheum. 1994;37(3):376-83.

111. Simak J, Holada K, Risitano AM, Zivny JH, Young NS, Vostal JG. Elevated circulating endothelial membrane microparticles in paroxysmal nocturnal haemoglobinuria. Br J Haematol. 2004;125(6):804-13.

112. Mallat Z, Benamer H, Hugel B, Benessiano J, Steg PG, Freyssinet JM, et al. Elevated levels of shed membrane microparticles with procoagulant potential in the peripheral circulating blood of patients with acute coronary syndromes. Circulation. 2000;101(8):841-3.
113. Yoshioka Y, Konishi Y, Kosaka N, Katsuda T, Kato T, Ochiya T. Comparative marker analysis of extracellular vesicles in different human cancer types. J Extracell Vesicles. 2013;2.
114. Bobrie A, Colombo M, Krumeich S, Raposo G, Thery C. Diverse subpopulations of vesicles secreted by different intracellular mechanisms are present in exosome preparations obtained by differential ultracentrifugation. J Extracell Vesicles. 2012;1.
115. Crescitelli R, Lasser C, Szabo TG, Kittel A, Eldh M, Dianzani I, et al. Distinct RNA profiles in subpopulations of extracellular vesicles: apoptotic bodies, microvesicles and exosomes. J Extracell Vesicles. 2013;2.
116. Burger D, Schock S, Thompson CS, Montezano AC, Hakim AM, Touyz RM. Microparticles: biomarkers and beyond. Clin Sci (Lond). 2013;124(7):423-41.
117. Beyer C, Pisetsky DS. The role of microparticles in the pathogenesis of rheumatic diseases. Nat Rev Rheumatol. 2010;6(1):21-9.
118. Thery C, Ostrowski M, Segura E. Membrane vesicles as conveyors of immune responses. Nat Rev Immunol. 2009;9(8):581-93.
119. Duncan R, Richardson SC. Endocytosis and intracellular trafficking as gateways for nanomedicine delivery: opportunities and challenges. Mol Pharm. 2012;9(9):2380-402.
120. Brodsky SV, Malinowski K, Golightly M, Jesty J, Goligorsky MS. Plasminogen activator inhibitor-1 promotes formation of endothelial microparticles with procoagulant potential. Circulation. 2002;106(18):2372-8.
121. Banfi C, Brioschi M, Wait R, Begum S, Gianazza E, Pirillo A, et al. Proteome of endothelial cell-derived procoagulant microparticles. Proteomics. 2005;5(17):4443-55.
122. Distler JH, Pisetsky DS, Huber LC, Kalden JR, Gay S, Distler O. Microparticles as regulators of inflammation: novel players of cellular crosstalk in the rheumatic diseases. Arthritis Rheum. 2005;52(11):3337-48.
123. Lacroix R, Sabatier F, Mialhe A, Basire A, Pannell R, Borghi H, et al. Activation of plasminogen into plasmin at the surface of endothelial

microparticles: a mechanism that modulates angiogenic properties of endothelial progenitor cells in vitro. Blood. 2007;110(7):2432-9.

124. Peterson DB, Sander T, Kaul S, Wakim BT, Halligan B, Twigger S, et al. Comparative proteomic analysis of PAI-1 and TNF-alpha-derived endothelial microparticles. Proteomics. 2008;8(12):2430-46.
125. Shefler I, Salamon P, Reshef T, Mor A, Mekori YA. T cell-induced mast cell activation: a role for microparticles released from activated T cells. J Immunol. 2010;185(7):4206-12.
126. Devaraj S, Kumaresan PR, Jialal I. C-reactive protein induces release of both endothelial microparticles and circulating endothelial cells in vitro and in vivo: further evidence of endothelial dysfunction. Clin Chem. 2011;57(12):1757-61.
127. Takahashi T, Kobayashi S, Fujino N, Suzuki T, Ota C, Tando Y, et al. Differences in the released endothelial microparticle subtypes between human pulmonary microvascular endothelial cells and aortic endothelial cells in vitro. Exp Lung Res. 2013;39(4-5):155-61.
128. Moreno-Martinez D, Wilkinson F, McCarthy E, Mahmoud A, Alexander M. 36 Endothelial microparticles: investigating their role on endothelial cells in vitro. Heart. 2015;101(Suppl 6):A12.
129. Nolan S, Dixon R, Norman K, Hellewell P, Ridger V. Nitric oxide regulates neutrophil migration through microparticle formation. Am J Pathol. 2008;172(1):265-73.
130. Mulcahy LA, Pink RC, Carter DR. Routes and mechanisms of extracellular vesicle uptake. J Extracell Vesicles. 2014;3.
131. Alvarez-Erviti L, Seow Y, Yin H, Betts C, Lakhal S, Wood MJ. Delivery of siRNA to the mouse brain by systemic injection of targeted exosomes. Nat Biotechnol. 2011;29(4):341-5.
132. Montecalvo A, Larregina AT, Shufesky WJ, Stolz DB, Sullivan ML, Karlsson JM, et al. Mechanism of transfer of functional microRNAs between mouse dendritic cells via exosomes. Blood. 2012;119(3):756-66.
133. Parolini I, Federici C, Raggi C, Lugini L, Palleschi S, De Milito A, et al. Microenvironmental pH is a key factor for exosome traffic in tumor cells. J Biol Chem. 2009;284(49):34211-22.
134. Christianson HC, Svensson KJ, van Kuppevelt TH, Li JP, Belting M. Cancer cell exosomes depend on cell-surface heparan sulfate proteoglycans for their

internalization and functional activity. Proc Natl Acad Sci U S A. 2013;110(43):17380-5.

135. Svensson KJ, Christianson HC, Wittrup A, Bourseau-Guilmain E, Lindqvist E, Svensson LM, et al. Exosome uptake depends on ERK1/2-heat shock protein 27 signaling and lipid Raft-mediated endocytosis negatively regulated by caveolin-1. J Biol Chem. 2013;288(24):17713-24.
136. Andrews AM, Rizzo V. Microparticle-Induced Activation of the Vascular Endothelium Requires Caveolin-1/Caveolae. PLoS One. 2016;11(2):e0149272.
137. Feng D, Zhao WL, Ye YY, Bai XC, Liu RQ, Chang LF, et al. Cellular internalization of exosomes occurs through phagocytosis. Traffic. 2010;11(5):675-87.
138. Zech D, Rana S, Buchler MW, Zoller M. Tumor-exosomes and leukocyte activation: an ambivalent crosstalk. Cell Commun Signal. 2012;10(1):37.
139. Lu X, Kassab GS. Assessment of endothelial function of large, medium, and small vessels: a unified myograph. Am J Physiol Heart Circ Physiol. 2011;300(1):H94-H100.
140. Chironi GN, Boulanger CM, Simon A, Dignat-George F, Freyssinet JM, Tedgui A. Endothelial microparticles in diseases. Cell Tissue Res. 2009;335(1):143-51.
141. Julich H, Willms A, Lukacs-Kornek V, Kornek M. Extracellular vesicle profiling and their use as potential disease specific biomarker. Front Immunol. 2014;5:413.
142. Abid Hussein MN, Boing AN, Biro E, Hoek FJ, Vogel GM, Meuleman DG, et al. Phospholipid composition of in vitro endothelial microparticles and their in vivo thrombogenic properties. Thromb Res. 2008;121(6):865-71.
143. Leroyer AS, Isobe H, Leseche G, Castier Y, Wassef M, Mallat Z, et al. Cellular origins and thrombogenic activity of microparticles isolated from human atherosclerotic plaques. J Am Coll Cardiol. 2007;49(7):772-7.
144. Perez-Casal M, Downey C, Cutillas-Moreno B, Zuzel M, Fukudome K, Toh CH. Microparticle-associated endothelial protein C receptor and the induction of cytoprotective and anti-inflammatory effects. Haematologica. 2009;94(3):387-94.
145. Schiro A, Wilkinson FL, Weston R, Smyth JV, Serracino-Inglott F, Alexander MY. Elevated levels of endothelial-derived microparticles, and serum CXCL9

and SCGF-beta are associated with unstable asymptomatic carotid plaques. Sci Rep. 2015;5:16658.

146. Mahmoud AM, Wilkinson FL, Moreno-Martinez D, Jiménez R, Duarte J, Alexander MY. 180 Endothelial microparticles prevent lipid-induced endothelial dysfunction through activation of AKT/ENOS signalling pathway and attenuation of oxidative stress. Heart. 2015;101(Suppl 4):A102.
147. Abid Hussein MN, Boing AN, Sturk A, Hau CM, Nieuwland R. Inhibition of microparticle release triggers endothelial cell apoptosis and detachment. Thromb Haemost. 2007;98(5):1096-107.
148. Maria Pieri BP, M. Yvonne Alexander,. Endothelial microparticles (EMPs) as biomarkers of endothelial dysfunction and atherosclerosis: Focus on autoimmune disorders. BSCR bulletin. 2012.
149. Loyer X, Vion AC, Tedgui A, Boulanger CM. Microvesicles as cell-cell messengers in cardiovascular diseases. Circ Res. 2014;114(2):345-53.
150. Murdaca G, Colombo BM, Cagnati P, Gulli R, Spano F, Puppo F. Endothelial dysfunction in rheumatic autoimmune diseases. Atherosclerosis. 2012;224(2):309-17.
151. Martinez MC, Tesse A, Zobairi F, Andriantsitohaina R. Shed membrane microparticles from circulating and vascular cells in regulating vascular function. Am J Physiol Heart Circ Physiol. 2005;288(3):H1004-9.
152. Singh RB, Mengi SA, Xu YJ, Arneja AS, Dhalla NS. Pathogenesis of atherosclerosis: A multifactorial process. Exp Clin Cardiol. 2002;7(1):40-53.
153. Iyemere VP, Proudfoot D, Weissberg PL, Shanahan CM. Vascular smooth muscle cell phenotypic plasticity and the regulation of vascular calcification. J Intern Med. 2006;260(3):192-210.
154. Shanahan CM, Weissberg PL, Metcalfe JC. Isolation of gene markers of differentiated and proliferating vascular smooth muscle cells. Circ Res. 1993;73(1):193-204.
155. Alexander MY. RANKL links arterial calcification with osteolysis. Circ Res. 2009;104(9):1032-4.
156. Shanahan CM, Cary NR, Salisbury JR, Proudfoot D, Weissberg PL, Edmonds ME. Medial localization of mineralization-regulating proteins in association with Monckeberg's sclerosis: evidence for smooth muscle cell-mediated vascular calcification. Circulation. 1999;100(21):2168-76.

157. Speer MY, Giachelli CM. Regulation of cardiovascular calcification. Cardiovasc Pathol. 2004;13(2):63-70.
158. Burger D, Kwart DG, Montezano AC, Read NC, Kennedy CR, Thompson CS, et al. Microparticles induce cell cycle arrest through redox-sensitive processes in endothelial cells: implications in vascular senescence. J Am Heart Assoc. 2012;1(3):e001842.
159. Leopold JA. Vascular calcification: Mechanisms of vascular smooth muscle cell calcification. Trends Cardiovasc Med. 2015;25(4):267-74.
160. Kapustin AN, Shanahan CM. Calcium regulation of vascular smooth muscle cell-derived matrix vesicles. Trends Cardiovasc Med. 2012;22(5):133-7.
161. Straub AC, Zeigler AC, Isakson BE. The myoendothelial junction: connections that deliver the message. Physiology (Bethesda). 2014;29(4):242-9.
162. Heberlein KR, Straub AC, Isakson BE. The myoendothelial junction: breaking through the matrix? Microcirculation. 2009;16(4):307-22.
163. Mugge A, Lopez JA, Piegors DJ, Breese KR, Heistad DD. Acetylcholine-induced vasodilatation in rabbit hindlimb in vivo is not inhibited by analogues of L-arginine. Am J Physiol. 1991;260(1 Pt 2):H242-7.
164. Garland CJ, Hiley CR, Dora KA. EDHF: spreading the influence of the endothelium. Br J Pharmacol. 2011;164(3):839-52.
165. Gladwin MT, Kim-Shapiro DB. Vascular biology: Nitric oxide caught in traffic. Nature. 2012;491(7424):344-5.
166. Liu Y, Wang T, Yan J, Jiagbogu N, Heideman DA, Canfield AE, et al. HGF/c-Met signalling promotes Notch3 activation and human vascular smooth muscle cell osteogenic differentiation in vitro. Atherosclerosis. 2011;219(2):440-7.
167. Ndip A, Williams A, Jude EB, Serracino-Inglott F, Richardson S, Smyth JV, et al. The RANKL/RANK/OPG signaling pathway mediates medial arterial calcification in diabetic Charcot neuroarthropathy. Diabetes. 2011;60(8):2187-96.
168. Cannata-Andia JB, Roman-Garcia P, Hruska K. The connections between vascular calcification and bone health. Nephrology Dialysis Transplantation. 2011;26(11):3429-36.
169. Johnson RC, Leopold JA, Loscalzo J. Vascular calcification: pathobiological mechanisms and clinical implications. Circ Res. 2006;99(10):1044-59.

170. Murshed M, Schinke T, McKee MD, Karsenty G. Extracellular matrix mineralization is regulated locally; different roles of two gla-containing proteins. J Cell Biol. 2004;165(5):625-30.
171. Schafer C, Heiss A, Schwarz A, Westenfeld R, Ketteler M, Floege J, et al. The serum protein alpha 2-Heremans-Schmid glycoprotein/fetuin-A is a systemically acting inhibitor of ectopic calcification. J Clin Invest. 2003;112(3):357-66.
172. Tyson KL, Reynolds JL, McNair R, Zhang Q, Weissberg PL, Shanahan CM. Osteo/chondrocytic transcription factors and their target genes exhibit distinct patterns of expression in human arterial calcification. Arterioscler Thromb Vasc Biol. 2003;23(3):489-94.
173. Kapustin AN, Shanahan CM. Osteocalcin: a novel vascular metabolic and osteoinductive factor? Arterioscler Thromb Vasc Biol. 2011;31(10):2169-71.
174. Maetzler W, Berg D, Funke C, Sandmann F, Stunitz H, Maetzler C, et al. Progressive secondary neurodegeneration and microcalcification co-occur in osteopontin-deficient mice. Am J Pathol. 2010;177(2):829-39.
175. Karsenty G. Update on the transcriptional control of osteoblast differentiation. IBMS BoneKEy. 2007;4(6):164-70.
176. Shimizu T, Tanaka T, Iso T, Matsui H, Ooyama Y, Kawai-Kowase K, et al. Notch signaling pathway enhances bone morphogenetic protein 2 (BMP2) responsiveness of Msx2 gene to induce osteogenic differentiation and mineralization of vascular smooth muscle cells. J Biol Chem. 2011;286(21):19138-48.
177. Panizo S, Cardus A, Encinas M, Parisi E, Valcheva P, Lopez-Ongil S, et al. RANKL increases vascular smooth muscle cell calcification through a RANK-BMP4-dependent pathway. Circ Res. 2009;104(9):1041-8.
178. Karwowski W, Naumnik B, Szczepanski M, Mysliwiec M. The mechanism of vascular calcification - a systematic review. Med Sci Monit. 2012;18(1):RA1-11.
179. Tanimura A, McGregor DH, Anderson HC. Matrix vesicles in atherosclerotic calcification. Proc Soc Exp Biol Med. 1983;172(2):173-7.
180. Haque S, Alexander MY, Bruce IN. Endothelial progenitor cells: a new player in lupus? Arthritis Res Ther. 2012;14(1):203.
181. Modur V, Zimmerman GA, Prescott SM, McIntyre TM. Endothelial cell inflammatory responses to tumor necrosis factor alpha. Ceramide-dependent

and -independent mitogen-activated protein kinase cascades. J Biol Chem. 1996;271(22):13094-102.

182. Burke-Gaffney A, Hellewell PG. Tumour necrosis factor-alpha-induced ICAM-1 expression in human vascular endothelial and lung epithelial cells: modulation by tyrosine kinase inhibitors. Br J Pharmacol. 1996;119(6):1149-58.

183. Pugin J, Ulevitch RJ, Tobias PS. Tumor necrosis factor-alpha and interleukin-1 beta mediate human endothelial cell activation in blood at low endotoxin concentrations. J Inflamm. 1995;45(1):49-55.

184. Wong D, Dorovini-Zis K. Expression of vascular cell adhesion molecule-1 (VCAM-1) by human brain microvessel endothelial cells in primary culture. Microvasc Res. 1995;49(3):325-39.

185. Lin CC, Pan CS, Wang CY, Liu SW, Hsiao LD, Yang CM. Tumor necrosis factor-alpha induces VCAM-1-mediated inflammation via c-Src-dependent transactivation of EGF receptors in human cardiac fibroblasts. J Biomed Sci. 2015;22:53.

186. Zhao X, Bausano B, Pike BR, Newcomb-Fernandez JK, Wang KK, Shohami E, et al. TNF-alpha stimulates caspase-3 activation and apoptotic cell death in primary septo-hippocampal cultures. J Neurosci Res. 2001;64(2):121-31.

187. Martinez DM, Wilkinson F, McCarthy E, Mahmoud A, Parker B, Alexander Y. 177 Endothelial Microparticles: Novel Regulators of Vascular Calcification in vitro. Heart. 2016;102(Suppl 6):A122-A3.

188. Buendía P, Montes de Oca A, Madueño JA, Merino A, Martín-Malo A, Aljama P, et al. Endothelial microparticles mediate inflammation-induced vascular calcification. FASEB journal : official publication of the Federation of American Societies for Experimental Biology. 2015;29(1):173-81.

189. Yang Y, Yu F, Li JX, Tang CS, Li CY. [Promoting effect of hyperhomocysteinemia on vascular calcification in rats]. Zhongguo Ying Yong Sheng Li Xue Za Zhi. 2004;20(4):333-6.

190. Steitz SA, Speer MY, Curinga G, Yang HY, Haynes P, Aebersold R, et al. Smooth muscle cell phenotypic transition associated with calcification: upregulation of Cbfa1 and downregulation of smooth muscle lineage markers. Circ Res. 2001;89(12):1147-54.

191. Olink. Proximity Extension Assay (PEA) technology 2007 [cited 2017 2017]. Available from: http://www.olink.com/data-you-can-trust/technology/.

192. Sugita S, Kohno T, Yamamoto K, Imaizumi Y, Nakajima H, Ishimaru T, et al. Induction of macrophage-inflammatory protein-3alpha gene expression by TNF-dependent NF-kappaB activation. J Immunol. 2002;168(11):5621-8.
193. Mayr M, Grainger D, Mayr U, Leroyer AS, Leseche G, Sidibe A, et al. Proteomics, metabolomics, and immunomics on microparticles derived from human atherosclerotic plaques. Circ Cardiovasc Genet. 2009;2(4):379-88.
194. Rinnerthaler G, Hackl H, Gampenrieder SP, Hamacher F, Hufnagl C, Hauser-Kronberger C, et al. miR-16-5p Is a Stably-Expressed Housekeeping MicroRNA in Breast Cancer Tissues from Primary Tumors and from Metastatic Sites. Int J Mol Sci. 2016;17(2).
195. Poliseno L, Tuccoli A, Mariani L, Evangelista M, Citti L, Woods K, et al. MicroRNAs modulate the angiogenic properties of HUVECs. Blood. 2006;108(9):3068-71.
196. Savoia C, Sada L, Zezza L, Pucci L, Lauri FM, Befani A, et al. Vascular inflammation and endothelial dysfunction in experimental hypertension. Int J Hypertens. 2011;2011:281240.
197. Rudijanto A. The role of vascular smooth muscle cells on the pathogenesis of atherosclerosis. Acta Med Indones. 2007;39(2):86-93.
198. Romero-Diaz J, Vargas-Vorackova F, Kimura-Hayama E, Cortazar-Benitez LF, Gijon-Mitre R, Criales S, et al. Systemic lupus erythematosus risk factors for coronary artery calcifications. Rheumatology (Oxford). 2012;51(1):110-9.
199. Kiani AN, Fishman EK, Petri M. Aortic valve calcification in systemic lupus erythematosus. Lupus. 2006;15(12):873-6.
200. Goettsch C, Hutcheson JD, Aikawa E. MicroRNA in cardiovascular calcification: focus on targets and extracellular vesicle delivery mechanisms. Circ Res. 2013;112(7):1073-84.
201. Liu Y, Shanahan CM. Signalling pathways and vascular calcification. Front Biosci (Landmark Ed). 2011;16:1302-14.
202. Rodriguez-Carrio J, Alperi-Lopez M, Lopez P, Alonso-Castro S, Carro-Esteban SR, Ballina-Garcia FJ, et al. Altered profile of circulating microparticles in rheumatoid arthritis patients. Clin Sci (Lond). 2015;128(7):437-48.
203. Berezin AE, Kremzer AA. Impaired phenotype of circulating endothelial microparticles in chronic heart failure patients: Relevance to body mass index. Diabetes Metab Syndr. 2015;9(4):230-6.

204. Berezin AE, Kremzer AA, Samura TA, Berezina TA, Kruzliak P. Impaired immune phenotype of circulating endothelial-derived microparticles in patients with metabolic syndrome and diabetes mellitus. J Endocrinol Invest. 2015;38(8):865-74.
205. Hristov M, Erl W, Linder S, Weber PC. Apoptotic bodies from endothelial cells enhance the number and initiate the differentiation of human endothelial progenitor cells in vitro. Blood. 2004;104(9):2761-6.
206. Lee AY, Korner H. CCR6 and CCL20: emerging players in the pathogenesis of rheumatoid arthritis. Immunol Cell Biol. 2014;92(4):354-8.
207. Koga T, Otomo K, Mizui M, Yoshida N, Umeda M, Ichinose K, et al. Calcium/Calmodulin-Dependent Kinase IV Facilitates the Recruitment of Interleukin-17-Producing Cells to Target Organs Through the CCR6/CCL20 Axis in Th17 Cell-Driven Inflammatory Diseases. Arthritis Rheumatol. 2016;68(8):1981-8.
208. Manthey HD, Cochain C, Barnsteiner S, Karshovska E, Pelisek J, Koch M, et al. CCR6 selectively promotes monocyte mediated inflammation and atherogenesis in mice. Thromb Haemost. 2013;110(6):1267-77.
209. Calvayrac O, Rodriguez-Calvo R, Alonso J, Orbe J, Martin-Ventura JL, Guadall A, et al. CCL20 is increased in hypercholesterolemic subjects and is upregulated by LDL in vascular smooth muscle cells: role of NF-kappaB. Arterioscler Thromb Vasc Biol. 2011;31(11):2733-41.
210. Nakashima T, Jinnin M, Yamane K, Honda N, Kajihara I, Makino T, et al. Impaired IL-17 signaling pathway contributes to the increased collagen expression in scleroderma fibroblasts. J Immunol. 2012;188(8):3573-83.
211. Jansen F, Yang X, Baumann K, Przybilla D, Schmitz T, Flender A, et al. Endothelial microparticles reduce ICAM-1 expression in a microRNA-222-dependent mechanism. J Cell Mol Med. 2015;19(9):2202-14.
212. Teasdale JE, Hazell GG, Peachey AM, Sala-Newby GB, Hindmarch CC, McKay TR, et al. Cigarette smoke extract profoundly suppresses TNFalpha-mediated proinflammatory gene expression through upregulation of ATF3 in human coronary artery endothelial cells. Sci Rep. 2017;7:39945.
213. Madge LA, Pober JS. TNF signaling in vascular endothelial cells. Exp Mol Pathol. 2001;70(3):317-25.
214. Leroyer AS, Tedgui A, Boulanger CM. Role of microparticles in atherothrombosis. J Intern Med. 2008;263(5):528-37.

215. Vitorino P, Meyer T. Modular control of endothelial sheet migration. Genes Dev. 2008;22(23):3268-81.
216. Michaelis UR. Mechanisms of endothelial cell migration. Cell Mol Life Sci. 2014;71(21):4131-48.
217. Lamalice L, Le Boeuf F, Huot J. Endothelial cell migration during angiogenesis. Circ Res. 2007;100(6):782-94.
218. Saklatvala J, Davis W, Guesdon F. Interleukin 1 (IL1) and tumour necrosis factor (TNF) signal transduction. Philos Trans R Soc Lond B Biol Sci. 1996;351(1336):151-7.
219. Chaudhuri V, Zhou L, Karasek M. Inflammatory cytokines induce the transformation of human dermal microvascular endothelial cells into myofibroblasts: a potential role in skin fibrogenesis. J Cutan Pathol. 2007;34(2):146-53.
220. Kanaji N, Sato T, Nelson A, Wang X, Li Y, Kim M, et al. Inflammatory cytokines regulate endothelial cell survival and tissue repair functions via NF-kappaB signaling. J Inflamm Res. 2011;4:127-38.
221. Sprent J, Tough DF, Sun S. Factors controlling the turnover of T memory cells. Immunol Rev. 1997;156:79-85.
222. Zhang F, Yu W, Hargrove JL, Greenspan P, Dean RG, Taylor EW, et al. Inhibition of TNF-alpha induced ICAM-1, VCAM-1 and E-selectin expression by selenium. Atherosclerosis. 2002;161(2):381-6.
223. Shimizu Y, Newman W, Tanaka Y, Shaw S. Lymphocyte interactions with endothelial cells. Immunol Today. 1992;13(3):106-12.
224. Martin S, Lampeter EF, Kolb H. A physiological role for circulating adhesion molecules? Immunol Today. 1994;15(3):141.
225. Fink K, Moebes M, Vetter C, Bourgeois N, Schmid B, Bode C, et al. Selenium prevents microparticle-induced endothelial inflammation in patients after cardiopulmonary resuscitation. Crit Care. 2015;19:58.
226. Manna SK, Aggarwal BB. Vesnarinone suppresses TNF-induced activation of NF-kappa B, c-Jun kinase, and apoptosis. J Immunol. 2000;164(11):5815-25.
227. Schutze S, Wiegmann K, Machleidt T, Kronke M. TNF-induced activation of NF-kappa B. Immunobiology. 1995;193(2-4):193-203.

228. Mause SF, Weber C. Microparticles: protagonists of a novel communication network for intercellular information exchange. Circ Res. 2010;107(9):1047-57.
229. Flamant S, Tamarat R. Extracellular Vesicles and Vascular Injury: New Insights for Radiation Exposure. Radiat Res. 2016;186(2):203-18.
230. de Gonzalo-Calvo D, Cenarro A, Civeira F, Llorente-Cortes V. microRNA expression profile in human coronary smooth muscle cell-derived microparticles is a source of biomarkers. Clin Investig Arterioscler. 2016;28(4):167-77.
231. Shields KJ, Barinas-Mitchell E, Gingo MR, Tepper P, Goodpaster BH, Kao AH, et al. Perivascular adipose tissue of the descending thoracic aorta is associated with systemic lupus erythematosus and vascular calcification in women. Atherosclerosis. 2013;231(1):129-35.
232. Plazak W, Pasowicz M, Kostkiewicz M, Podolec J, Tomkiewicz-Pajak L, Musial J, et al. Influence of chronic inflammation and autoimmunity on coronary calcifications and myocardial perfusion defects in systemic lupus erythematosus patients. Inflamm Res. 2011;60(10):973-80.
233. Yiu KH, Wang S, Mok MY, Ooi GC, Khong PL, Mak KF, et al. Pattern of arterial calcification in patients with systemic lupus erythematosus. J Rheumatol. 2009;36(10):2212-7.
234. Krohn JB, Hutcheson JD, Martinez-Martinez E, Aikawa E. Extracellular vesicles in cardiovascular calcification: expanding current paradigms. J Physiol. 2016;594(11):2895-903.
235. Jansen F, Yang X, Hoyer FF, Paul K, Heiermann N, Becher MU, et al. Endothelial microparticle uptake in target cells is annexin I/phosphatidylserine receptor dependent and prevents apoptosis. Arterioscler Thromb Vasc Biol. 2012;32(8):1925-35.
236. Faille D, El-Assaad F, Mitchell AJ, Alessi MC, Chimini G, Fusai T, et al. Endocytosis and intracellular processing of platelet microparticles by brain endothelial cells. J Cell Mol Med. 2012;16(8):1731-8.
237. Sharma R, Muttil P, Yadav AB, Rath SK, Bajpai VK, Mani U, et al. Uptake of inhalable microparticles affects defence responses of macrophages infected with Mycobacterium tuberculosis H37Ra. J Antimicrob Chemother. 2007;59(3):499-506.

238. Bergsmedh A, Szeles A, Henriksson M, Bratt A, Folkman MJ, Spetz AL, et al. Horizontal transfer of oncogenes by uptake of apoptotic bodies. Proc Natl Acad Sci U S A. 2001;98(11):6407-11.
239. Lopez-Vilchez I, Diaz-Ricart M, Galan AM, Roque M, Caballo C, Molina P, et al. Internalization of Tissue Factor-Rich Microvesicles by Platelets Occurs Independently of GPIIb-IIIa, and Involves CD36 Receptor, Serotonin Transporter and Cytoskeletal Assembly. J Cell Biochem. 2016;117(2):448-57.
240. Povero D, Eguchi A, Niesman IR, Andronikou N, de Mollerat du Jeu X, Mulya A, et al. Lipid-induced toxicity stimulates hepatocytes to release angiogenic microparticles that require Vanin-1 for uptake by endothelial cells. Sci Signal. 2013;6(296).
241. Lopez-Vilchez I, Diaz-Ricart M, White JG, Escolar G, Galan AM. Serotonin enhances platelet procoagulant properties and their activation induced during platelet tissue factor uptake. Cardiovasc Res. 2009;84(2):309-16.
242. Yildiz F, Kelle B, Tas DA, Kaya B, Altun E, Erken E. Diffuse soft tissue and vascular calcification in systemic lupus erythematosus with chronic kidney disease. Z Rheumatol. 2014;73(8):754-7.
243. Yiu KH, Wang S, Mok MY, Ooi GC, Khong PL, Lau CS, et al. Relationship between cardiac valvular and arterial calcification in patients with rheumatoid arthritis and systemic lupus erythematosus. J Rheumatol. 2011;38(4):621-7.
244. Demer LL, Tintut Y. Vascular calcification: pathobiology of a multifaceted disease. Circulation. 2008;117(22):2938-48.
245. Al-Aly Z. Arterial calcification: a tumor necrosis factor-alpha mediated vascular Wnt-opathy. Transl Res. 2008;151(5):233-9.
246. Aikawa E, Nahrendorf M, Figueiredo JL, Swirski FK, Shtatland T, Kohler RH, et al. Osteogenesis associates with inflammation in early-stage atherosclerosis evaluated by molecular imaging in vivo. Circulation. 2007;116(24):2841-50.
247. Kang T, Jones TM, Naddell C, Bacanamwo M, Calvert JW, Thompson WE, et al. Adipose-Derived Stem Cells Induce Angiogenesis via Microvesicle Transport of miRNA-31. Stem Cells Transl Med. 2016;5(4):440-50.
248. Jansen F, Yang X, Franklin BS, Hoelscher M, Schmitz T, Bedorf J, et al. High glucose condition increases NADPH oxidase activity in endothelial

microparticles that promote vascular inflammation. Cardiovasc Res. 2013;98(1):94-106.

249. Ndip A, Wilkinson FL, Jude EB, Boulton AJ, Alexander MY. RANKL-OPG and RAGE modulation in vascular calcification and diabetes: novel targets for therapy. Diabetologia. 2014.

250. Bostrom KI, Rajamannan NM, Towler DA. The regulation of valvular and vascular sclerosis by osteogenic morphogens. Circ Res. 2011;109(5):564-77.

251. Sage AP, Tintut Y, Demer LL. Regulatory mechanisms in vascular calcification. Nat Rev Cardiol. 2010;7(9):528-36.

252. Speer MY, Chien YC, Quan M, Yang HY, Vali H, McKee MD, et al. Smooth muscle cells deficient in osteopontin have enhanced susceptibility to calcification in vitro. Cardiovasc Res. 2005;66(2):324-33.

253. Rautou PE, Vion AC, Amabile N, Chironi G, Simon A, Tedgui A, et al. Microparticles, vascular function, and atherothrombosis. Circ Res. 2011;109(5):593-606.

254. Mabilleau G, Petrova NL, Edmonds ME, Sabokbar A. Increased osteoclastic activity in acute Charcot's osteoarthropathy: the role of receptor activator of nuclear factor-kappaB ligand. Diabetologia. 2008;51(6):1035-40.

255. Tseng W, Graham LS, Geng Y, Reddy A, Lu J, Effros RB, et al. PKA-induced Receptor Activator of NF-κB Ligand (RANKL) Expression in Vascular Cells Mediates Osteoclastogenesis but Not Matrix Calcification. J Biol Chem. 2010;285(39):29925-31.

256. Simonet WS, Lacey DL, Dunstan CR, Kelley M, Chang MS, Luthy R, et al. Osteoprotegerin: a novel secreted protein involved in the regulation of bone density. Cell. 1997;89(2):309-19.

257. Benjamin MM, Khalil RA. Matrix Metalloproteinase Inhibitors as Investigative Tools in the Pathogenesis and Management of Vascular Disease. Exs. 2012;103:209-79.

258. Bartel DP. MicroRNAs: target recognition and regulatory functions. Cell. 2009;136(2):215-33.

259. Small EM, Olson EN. Pervasive roles of microRNAs in cardiovascular biology. Nature. 2011;469(7330):336-42.

260. Balderman JA, Lee HY, Mahoney CE, Handy DE, White K, Annis S, et al. Bone morphogenetic protein-2 decreases microRNA-30b and microRNA-30c

to promote vascular smooth muscle cell calcification. J Am Heart Assoc. 2012;1(6):e003905.

261. Raitoharju E, Lyytikainen LP, Levula M, Oksala N, Mennander A, Tarkka M, et al. miR-21, miR-210, miR-34a, and miR-146a/b are up-regulated in human atherosclerotic plaques in the Tampere Vascular Study. Atherosclerosis. 2011;219(1):211-7.

262. Deng Y, Zhao J, Sakurai D, Kaufman KM, Edberg JC, Kimberly RP, et al. MicroRNA-3148 modulates allelic expression of toll-like receptor 7 variant associated with systemic lupus erythematosus. PLoS Genet. 2013;9(2):e1003336.

263. Cakmak HA, Coskunpinar E, Ikitimur B, Barman HA, Karadag B, Tiryakioglu NO, et al. The prognostic value of circulating microRNAs in heart failure: preliminary results from a genome-wide expression study. J Cardiovasc Med (Hagerstown). 2015;16(6):431-7.

264. Kapustin AN, Chatrou ML, Drozdov I, Zheng Y, Davidson SM, Soong D, et al. Vascular smooth muscle cell calcification is mediated by regulated exosome secretion. Circ Res. 2015;116(8):1312-23.

265. Cantaluppi V, Gatti S, Medica D, Figliolini F, Bruno S, Deregibus MC, et al. Microvesicles derived from endothelial progenitor cells protect the kidney from ischemia-reperfusion injury by microRNA-dependent reprogramming of resident renal cells. Kidney Int. 2012;82(4):412-27.

266. Ullal AJ, Pisetsky DS, Reich CF, 3rd. Use of SYTO 13, a fluorescent dye binding nucleic acids, for the detection of microparticles in in vitro systems. Cytometry A. 2010;77(3):294-301.

267. Ju GQ, Cheng J, Zhong L, Wu S, Zou XY, Zhang GY, et al. Microvesicles derived from human umbilical cord mesenchymal stem cells facilitate tubular epithelial cell dedifferentiation and growth via hepatocyte growth factor induction. PLoS One. 2015;10(3):e0121534.

268. Kockelkoren R, Vos A, Van Hecke W, Vink A, Bleys RL, Verdoorn D, et al. Computed Tomographic Distinction of Intimal and Medial Calcification in the Intracranial Internal Carotid Artery. PLoS One. 2017;12(1):e0168360.

269. Vattikuti R, Towler DA. Osteogenic regulation of vascular calcification: an early perspective. Am J Physiol Endocrinol Metab. 2004;286(5):E686-96.

270. Liu W, Zhang Y, Yu CM, Ji QW, Cai M, Zhao YX, et al. Current understanding of coronary artery calcification. J Geriatr Cardiol. 2015;12(6):668-75.

271. Alexander MY, Wilkinson FL, Kirton JP, Rock CF, Collett GD, Jeziorska M, et al. Identification and characterization of vascular calcification-associated factor, a novel gene upregulated during vascular calcification in vitro and in vivo. Arterioscler Thromb Vasc Biol. 2005;25(9):1851-7.
272. Lozito TP, Tuan RS. Endothelial cell microparticles act as centers of matrix metalloproteinsase-2 (MMP-2) activation and vascular matrix remodeling. J Cell Physiol. 2012;227(2):534-49.
273. Chowdhury M, Ghosh J, Slevin M, Smyth JV, Alexander MY, Serracino-Inglott F. A comparative study of carotid atherosclerotic plaque microvessel density and angiogenic growth factor expression in symptomatic versus asymptomatic patients. European journal of vascular and endovascular surgery : the official journal of the European Society for Vascular Surgery. 2010;39(4):388-95.